FHWA/ NJ-99-013-7630

RECYCLED PLASTICS FOR HIGHWAY APPURTENANCES

Final Report

JULY 1999

BY

M. ALA SAADEGHVAZIRI, and
KEITH M. MACBAIN

Prepared By
New Jersey Institute of Technology
Department of Civil and Environmental Engineering
In Cooperation With
New Jersey Department of Transportation
Division of Research and Technology,
U.S. Department of Transportation
Federal Highway Administration

DISCLAIMER STATEMENT
(USDOT)

The contents of this report reflect the views of the authors, who are responsible for the facts and the accuracy of the information presented herein. This document is disseminated under sponsorship of the Department of Transportation, University Transportation Centers Program, in the interest of information exchange. The U.S. Government assumes no liability for the contents or use thereof.

DISCLAIMER STATEMENT
(NJDOT)

The contents of this report reflect the views of the authors who are responsible for the facts and the accuracy of the data presented herein. The contents do not necessarily reflect the views or policies of New Jersey Institute of Technology, the New Jersey Department of Transportation, or the Federal Highway Administration. This report does not constitute a standard, specification or regulation.

NOTICE

Neither New Jersey Institute of Technology, the New Jersey Department of Transportation, nor the Federal Highway Administration endorse products or manufacturers. Trade or Manufacturers' names appear herein solely because they are considered essential to the object of this report.

TECHNICAL REPORT STANDARD TITLE PAGE

1. Report No.	2. Government Accession No.	3. Recipient's Catalog No.
FHWA/NJ-99-013-7630		

4. Title and Subtitle	5. Report Date
RECYCLED PLASTICS FOR HIGHWAY APPURTENANCES	July 1999
	6. Performing Organization Code

7. Author(s)	8. Performing Organization Report No.
M. Ala Saadeghvaziri and Keith M. MacBain	FHWA/NJ-99-013-7630

9. Performing Organization Name and Address	10. Work Unit No.
New Jersey Department of Transportation CN 600 Trenton, NJ 08625	11. Contract or Grant No.
	13. Type of Report and Period Covered Final Report May 1995 – April 1998
12. Sponsoring Agency Name and Address Federal Highway Administration U.S. Department of Transportation Washington, D.C.	14. Sponsoring Agency Code

15. Supplementary Notes

16. Abstract

This report presents the results of a comprehensive experimental and analytical study on the use of recycled plastic for highway appurtenances. The study included material tests (including creep and freeze / thaw tests) to determine mechanical properties of various recycled plastics, development of an analytical model to define stress-strain relationship, member tests, finite element analysis, crash analysis, wind tests, and sound tests. Performance evaluation of a noise wall manufactured from recycled plastics indicates that the proposed design is as effective as traditional designs. Analytical analyses and experimental tests indicate that a noise wall made of recycled plastics can easily withstand typical design wind load. Sound tests have also shown that the prototype panels, which are multi-layered, are very effective acoustically. Due to lightweight of recycled plastics the proposed design allows for greater panel length, thus, making more economical designs by reducing the number of posts. Due to high strength and durability of the material, it is also expected that the life-cycle cost of the proposed noise wall is less than that of current designs. Evaluation of the use of the material as guardrail posts is not conclusive due to lack of adequate performance requirements. In general, the material is viable and has merit for use in the design of other highway devices such as culverts and glare screens. To this end, preliminary results on its application in the development of a dual-purpose glare screen pedestrian fence are very satisfactory and encouraging. Future work must consider manufacturing, development of appropriate design criteria, and long term performance.

17. Key Words	18. Distribution Statement
Recycled Plastics, Noise Wall, Guardrail Recycled Plastics Characteristics	No Restrictions

19. Security Classif (of this report)	20. Security Classif. (of this page)	21. No of Pages	22. Price
Unclassified	Unclassified	151	

Form DOT F 1700.7 (8-69)

Table of Contents

1.0 Executive Summary

This report presents the results of an experimental and analytical study on recycled plastics that can be used in the design of highway appurtenances. Performance evaluation of a noise wall manufactured from recycled plastics indicates that the proposed design is as effective as traditional designs. The life-cycle cost of the proposed design is expected to be less than that of traditional designs. Evaluation of the use of recycled plastics as guardrail posts is not conclusive due to lack of adequate performance requirements. In general, the material is viable and has merit for use in the design of other highway devices, such as culverts and glarescreens. Future work must consider manufacturing, development of appropriate design criteria, and long term performance.

2.0 Background

2.1 General

Recycling is an environmentally acceptable means of reducing solid waste and conserving resources. Many federal, state and local laws, such as the "Intermodal Surface Transportation Efficiency Act," emphasize the importance of recycled materials in construction, more specifically in highway construction. The overall objective of this research and development study is to develop highway applications for recycled plastics that will have performance characteristics that are similar to, if not superior than, traditional designs. The primary applications are the use of recycled plastics for noise walls and guardrail posts. However, due to lack of knowledge about the material, especially the long term performance, a significant portion of the effort was devoted toward material testing and evaluation of mechanical and structural properties. Acoustical and wind tests of the noise walls and analytical crash tests of the guardrail posts are among other objectives of this study. Detailed interim reports are attached as appendices. However, a brief summary of these reports and findings from the initial phases of this work follows.

2.2 Summary of Interim Reports

The widespread use of recycled plastics has been restricted in part, because of the limited state of knowledge about the behavior of this material and the lack of unified design procedures. The material behaves differently in tension and compression and the nonlinear nature of recycled plastic makes traditional terminology such as modulus

of elasticity difficult to determine because generally, there is no clearly defined yield point. Furthermore, the modulus of rupture, a property determined from beam tests, can vary for different sections making these terms specific to the section rather than exclusively a material property. Phase I of the study investigated the properties of recycled plastics and methods of testing and analyzing recycled plastic members in both axial compression and flexure.

In effort to provide a more unified design procedure, uni-axial material tests of discrete sections were performed to develop a proposed constitutive material model that archetypes the stress - strain behavior. The model was used to predict member response based on section geometry alone. This enables one to predict member response of sections not yet tested or even constructed with greater accuracy than previously possible, regardless of the differences in tension - compression behavior and material nonlinearities or variations in material properties among manufacturers. The findings of this phase can be summarized as:

- Recycled plastic has a highly nonlinear stress - strain behavior.
- Stress - strain behavior is different in tension and compression.
- For thick cross - sections (such 4X4 or 6X8) stress - strain behavior for shell and core materials are significantly different.
- Stiffness ranges from 50 to 300 ksi, strength ranges from 500 to 2,500 psi thus structural applications are possible.
- Freeze / thaw appears to be a problem for recycled plastics with wood fibers.
- The proposed constitutive model can simulate member results with good accuracy for service loads and gives a fair estimate of ultimate strength.

Upon completion of the material tests, an innovative noise wall design that uses recycled plastic and takes advantage of multi-layering to increase stiffness and sound effectiveness was proposed and analyzed. During the second phase of this study, prototypes of the proposed design were constructed and tested for sound transmission to determine their effectiveness and show the desirability of a multi-layered approach. The results show that acoustically, the transmission loss of the proposed design is as effective as the traditional designs. The sound tests report is included in Phase II report as an appendix. Furthermore, finite element analyses as well as an analytical model developed specifically for recycled plastics indicate that structurally, the proposed design can increase spans between posts resulting in a design that is potentially more economical than current designs. Due to their lighter weight they are also more suitable for mounting on structures such as bridges. The Phase II report also discusses results of creep testing and simulated crash analyses of guardrail systems. Results indicate that creep is a significant problem and applications involving large sustained loads

should be avoided. Furthermore, comparison of analytical crash tests demonstrated that guardrail system with recycled plastic posts allow for greater barrier deflections but vehicle accelerations are reduced significantly, implying safer redirection and less damage to the occupants and the car. This is further discussed in this final report using the results of other studies too.

3.0 Noise Wall

Wind tests were among important objectives of the study that were addressed during the final phase of the work. In determining the wind load, NJDOT[1] uses the wind load equation given by the AASHTO's Guide Specifications for Structural Supports for Highway Signs, Luminaires and Traffic Signals. This is the same equation given by AASHTO's Guide Specifications for Structural Design of Sound Barriers (1989), which is as follows:

$$P = 0.00256\ (1.3V)^2\ C_d\ C_c$$

where P is pressure in pounds per square foot, V is design wind velocity in miles per hour and the 1.3 coefficient accounts for a 30% increase in design wind velocity due to gust. The drag coefficient, C_d, is equal to 1.2 for noise barriers. C_c is combined height, exposure and location coefficient, which for typical noise wall heights is equal to unity. In the state of New Jersey, the design wind velocity to be used in the above equation is 90 mph (145 km/hr) resulting in a pressure of 42 psf. Much of the state is in or below the 80 mph (130 km/hr) isotach however (AASHTO), resulting in a pressure of 33 psf. This value was used in early phases of this study and will be used here to allow for consistent comparison with earlier analysis. Additionally, the value of C_c can actually range from 0.59 to 1.49 depending on application thus also changing the minimum design pressure greatly. The intention here is to investigate a typical installation rather than the most critical application.

3.1 Wind Tests

The objective of the wind tests was to determine the maximum capacity, flexural stiffness and failure mode of the recycled plastics panels under wind load. The geometry of the proposed design (flat rectangular panels to be stacked on top of each other) is quite similar to the traditional precast concrete panels. Therefore, it is expected that current design equations, such as the above equation, are adequate in

1. Engineering Instruction 93-B5, June 14, 1993.

determining the pressure load for a given wind speed. Another concern would be if the flow of wind over the top of the wall shed vortices that would excite the wall and cause it to vibrate and generate low frequency sound. Again, for the same reason, this is not expected to be an issue.

The wind tests were performed at the Wind Load Testing Facility at Clemson University under the supervision of Professor Scott Schiff. A copy of the wind test report is attached (Appendix I). The tests included two 12-ft long 2-ft wide box shaped panels made up of 1/2" thick recycled plastic sheets. The overall depth of the cross section was 8" (71/2" center to center). For 1/2" thick recycled plastics sheets currently 12-ft is the longest length available. Determination of the other dimensions (width and depth) of the panels is discussed in the Phase II report.

The wind tests can be summarized as successful. The recycled plastics panels were able to withstand high pressure load (in excess of 90 psf) without any sign of damage, while mid-span deflections never exceeded 2 in as seen in the test report (Appendix I). The tests had to be stopped due to failure of the plastic sheet used to seal the pressure chamber. In the following section the wind tests results are extrapolated to evaluate performance of longer panels in terms of the maximum deflection and flexural stresses.

3.2 Parametric Study

The response of the panels under wind load can be idealized as that of a simply supported beam under distributed load. Under such an assumption the central deflection will be equal to $5wL^4/384EI$, where **w** is load per unit length along the span, **L** is the span length, **E** is Modulus of Elasticity, and **I** is the moment of inertia. Based on material tests the average modulus of elasticity for the recycled plastics used in building the panels is equal to 140 ksi. This value is obtained using results from both tension and compression tests. The moment of inertia for a boxed rectangular section made up of 1/2" thick sheets with overall depth of 8" (71/2" center to center) and a width of 2-ft (24") is 366 in^4. The load intensity, as discussed before, for New Jersey (80 mph wind speed) is 33 psf. This is equal to **w** of 5.5 lb/in. Thus, the mid-span deflection as a function of span length, **L** in inches, is equal to $1.4X10^{-9}L^4$ in. For a 12' panel this equation gives a deflection of 0.6 in. Based on the experimental wind tests the following equations are proposed for mid-span deflections at the top and middle of the cross section (section 2.4 of Appendix I):

$y = 0.0161P$	Top Center
$y = 0.0191P$	Middle Center

in these equations y is displacement in inches, and P is the pressure in pounds per square foot. Note that anywhere along the span, especially on the windward face, deflection at the middle of the cross section is different (more for windward face and less for leeward face) than that at the top or bottom of the cross section. This is due to the two way action (bending) of the flanges. Based on the above equations at mid-span this difference is about 16%. Finite element analysis of the panels gives similar value. Using these equations for 33 psf wind pressure, the mid-span deflections are 0.53" and 0.63" at the top and middle of the cross section, respectively. The value of 0.6" obtained based on the simplified analysis is in close agreement with these values. Factors that can be associated with the difference between the analytical and experimental values are: i) actual clear span is less than 12', ii) 3-D action, and iii) actual modulus of elasticity and material nonlinearity.

The maximum flexural stress at mid-span, based on the idealized assumption of a simply supported beam and assuming linear material behavior, is equal to $Mc/I = 0.0075\ L^2$, where L is in inches. Thus, the maximum stress of 155 psi for a 12' panel is well below the ultimate capacity (less than 1/20 in tension and less than 1/40 in compression) of the recycled plastics used.

Following the above procedure, the maximum mid-span deflections are estimated at 1.5" and 4.6" for 15' and 20' long panels, respectively. The maximum flexural stresses will be 243 psi and 432 psi. These values indicate that the proposed design can allow even greater panel length, conceivably making more economical designs by further reducing the number of posts. It should be noted that no deflection requirements were found in the FHWA guides[1]. The widely referenced generic deflection limits, such as L/360, were developed for less flexible materials such as concrete. More importantly, these limits have been set up based on serviceability criteria, such as limiting crack width to protect reinforcements. Thus, these limits are not appropriate for recycled plastics, especially when the loading considered corresponds to a wind speed based upon a 50-year mean recurrence interval.

It should be mentioned that the flexibility of recycled plastics (compared to precast concrete panels) will also have a beneficial effect on construction tolerances. This in

1. "Guide Specifications for Structural Design of Sound Barriers," AASHTO, 1989.

turn can result in more economical designs.

Ultimately, the proposed design would be extruded as a single unit rather than assembled from sheets, thus, reducing assembly time and allowing for easier installation. A preliminary estimate of the cost for the panels shows them to be comparable to current designs. Based on the retail cost of the materials used to construct the prototype panels, the proposed design costs $7.00 per square foot. From 1991 to 1995, reported average costs[1] for installed barriers are $14 per square foot for wood and $18 per square foot for concrete. Assuming the barrier material cost comprises one third of the total installed cost, this equates to a material cost of $4.67 for wood and $6.00 for concrete. The lifecycle cost of the recycled plastic design is expected to be significantly lower due to its inherent characteristics which is durable and recyclable.

4.0 CAD / CAA Program

With a more complete knowledge of the material behavior from Phase I, a computer program was developed to analyze and design recycled plastic sections. The program uses the nonlinear material model obtained from tests and classical beam theory to predict the response of a recycled plastic beam. Two distinct regions were noted in the cross section of thick (e.g., 4x4) recycled plastic members and the properties were found to differ in tension and compression. These regions were termed 'core' and 'shell' and thus to completely describe the behavior in flexure, four sets of material constants are needed for the material model. It was shown in Phase I and II that it is possible to predict member response with good accuracy (5 - 10%) using this method. The key advantages of this are that it incorporates the material nonlinearity into the analysis and allows for differences in tension and compression behavior. This avoids the ambiguity of selecting the 'correct' Modulus for this nonlinear material.

While this analysis can be applied to any recycled plastic beam, it will be discussed here as applied to the proposed noise wall design. The principle limitation is that because the analysis is two dimensional, the results cannot be used to determine the amount of two way action, particularly in the outer (windward) face. For the 12 ft panel above, the program anticipates a 0.55 inch (1.4 cm) deflection at the top of the cross section under the 33 psf distributed load. This compares well with the test result of 0.53 inch. It is well worth noting that the program predicts a predominantly linear response

1. "Summary of Noise Barriers Constructed by end of 1995," U. S. Department of Transportation, The Wall Journal, Issue No. 27, 1997

indicating that the material is well below the ultimate stress level at this loading and for this case, the previous linear FE analysis is valid. This conclusion can only be obtained when the material nonlinearities are taken into account. As a design aid, one can use this sort of reasoning to determine qualitatively where the material is on the stress-strain diagram and determine if a linear analysis is appropriate.

The FORTRAN source code and executable file for this program are on the attached diskette. The program is also accessible via the internet where the user can directly plot the load deflection response although fewer program options are available. Figure 1 shows the input fields for the internet based version found at http://koenig.njit.edu/~ala/keith/JAVA/rp.html. The numbers entered in the fields represent the 12 ft prototype panel, the distributed load box is checked, and the ultimate load of 5.5 pounds per inch (33 psf) is entered. The 'ignore core' option is activated and suitable for analysis of this section because the prototype is entirely 'shell' material. As noted previously, the appearance of distinct core and shell regions disappears with thinner sheets and the sheets used to construct the prototype panel (0.5 inch) showed no evidence of this distinction. The internet version uses the material constants of Manufacturer B noted in Phase I because it is completely recycled plastic (i.e., no additives) and is considered a good choice of recycled plastic in terms of durability and availability.

While the FORTRAN version does not directly plot a load deflection graph, it is more flexible. If a material other than Type B is to be considered, this program will be needed along with the material constants that define that material. The appropriate constants for recycled plastic mixed with fiberglass and recycled plastic mixed with wood fibers are listed in the Phase I report. The program first develops a theoretical moment curvature array and then uses this to obtain the theoretical load deflection. The internet version operates in the same way but does not allow the user to change many of the values that effect the accuracy of the results. It has certain default values that may not be appropriate for all loads and sections considered. These include:

- material constants (properties)
- maximum strain reached
- tolerance for the force imbalance
- number of iterations
- number of subdivisions of the cross-section
- number of moment curvature points
- number of load deflection points
- step size along beam for integration

If the user requests a load beyond the maximum moment that the section can support, the load deflection data is processed up to the maximum load possible and the remainder of the array is filled with zeros. For this reason, the user should attempt to nearly realize the maximum load of the section as it will give the best representation for the default range. If more accuracy is desired, parameters such as the number of iterations, subdivisions, and points should be increased. The internet application does however, allow the designer to quickly review different configurations. Variations in shell thickness and overall depth of the cross section can be easily examined with varying lengths conceivably allowing for an optimal section size and post spacing to be determined for a particular need.

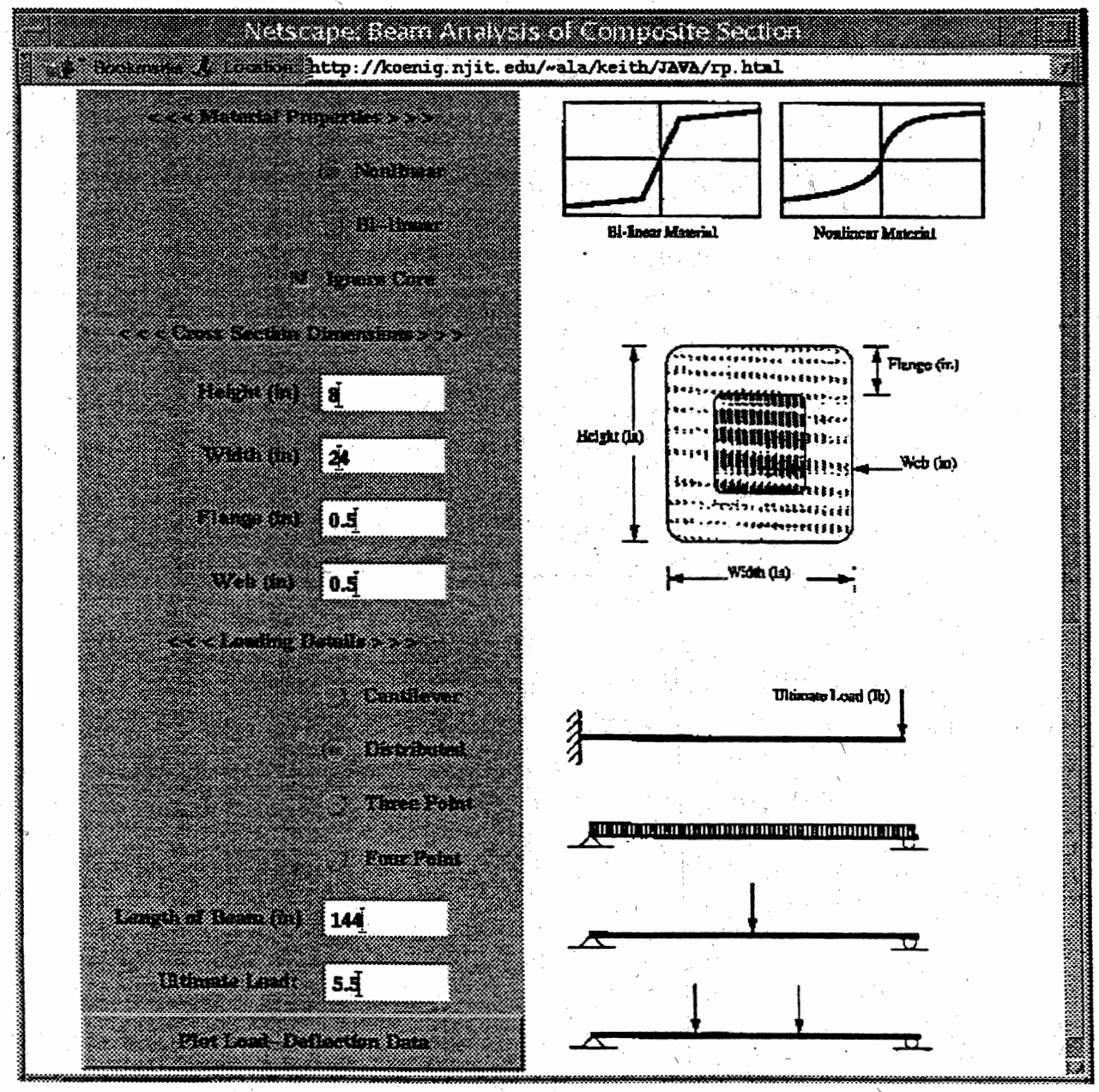

Figure 1

5.0 Guardrail System

The primary function of a guardrail system is to contain and smoothly redirect an errant vehicle. In this study a guardrail system that uses recycled plastics posts and W-beam railing was considered. The flexible nature of the posts is expected to reduce after-collision kinematics of the vehicle, thus, minimizing occupant's risk. As shown in Phase II report through crash analysis using Barrier VII, the maximum lateral and longitudinal accelerations are reduced significantly when recycled plastics posts are used instead of steel posts. However, deflection of the system using recycled posts is much higher. But, no limitation on deflection was found in the Recommended Procedures for the Safety Performance Evaluation of Highway Features (NCHRP Report 350).

In a recent report by FHWA[1] results of a full scale crash test using similar design (i.e., recycled plastic posts and W-beam railing) is reported. The conclusions of this study are that the test data complies with the requirements of NCHRP Report 230[2] but the test is considered unsuccessful because of large lateral deflection. However, the report does not provide a reference on the "established value of less than 1m (3 ft)" for lateral deflection. The impact conditions in the crash test reported were a 2129 kg (4,695 lb) sedan travelling at 93.5 km/h (58.2 mi/h) and 24.4 degrees.

In another study performed by Roschke et al.[3] a guardrail system that uses standard W-beam steel rail supported by composite commingled plastic posts was investigated. The guardrail posts are manufactured with thin-wall steel pipes encased in recycled plastics. The study included laboratory and full-scale tests to determine if commingled plastic post is an acceptable alternative to current standard wooden and steel posts. The conclusion of the full-scale crash test is that the guardrail system fulfilled its primary function. The impact conditions were a 2,043 kg (4,500 lb) sedan travelling at 99.3 km/h (61.6 mi/h) at an impact angle of 25.9 degrees. The maximum dynamic deflection of 0.8 m (2.8 ft) is reported to be comparable to that for traditional designs (i.e., strong-post guardrail systems that use wood or steel posts).

Therefore, the suitability of a guardrail system that uses recycled plastics posts is still

1. Evaluation of Recycled Materials for Roadside Safety Devices, U.S. Department of Transportation, Publication No FHWA-RD-97-XXX, March 1997
2. NCHRP Report 350 is an update to NCHRP Report 230.
3. Roschke, Paul N., R. P. Bligh, and K. R. Pruski, "Commingle Plastic Guardrail Post," ASCE, Journal of Transportation Engineering, Vol. 121, No. 2, March/April, 1995.

an open question that will require further investigation. Design requirements must consider the flexibility of the system and application of current requirements that have been developed based on rigid systems may not be appropriate.

6.0 Conclusions

The results of this study indicate that recycled plastic is a viable material that can be used in the construction of certain components of the highway system. The noise wall panels developed and investigated under this study will have structural and acoustical performance comparable to traditional designs. Furthermore, they are much lighter making them suitable for mounting on structures such as bridges. For the same reason, the design can allow for greater panel length, thus, making more economical designs by further reducing the number of posts. Weight and limit on stresses during construction and transportation are among factors limiting the length of current designs.

Therefore, it is recommended that the proposed design be installed in field in an experimental basis. This will allow evaluation of environmental effects such as long term freeze / thaw exposure, objects thrown from traffic striking the panels, and similar field conditions that were not a part of this study.

The use of recycled plastics in the design of a guardrail system as posts is questionable using current design methodology which was developed based on performance of strong-post systems. Another possible issue in application of recycled plastic as guardrail posts is constructability. Currently, steel posts are hammered in, however, placement of a recycled plastic post will require drilling a hole in advance. The cost associated with this two steps process need to be considered.

Recycled plastic lumber is a thermoplastic material and highly susceptible to temperature and the effects of creep are significant. It is recommended that sustained stress levels greater than 10% of ultimate should be avoided. Furthermore, freeze/thaw exposure indicates that recycled plastics with high percentage of additives (such as wood fibers) are not suitable for long term outdoor exposure. Quality control and development of testing standards are issues that need to be considered by manufacturers and organizations such as ASTM. Recently, ASTM approved first set of test standards. These are: D6108-97 Compression, D6109-97 Flex, D6111-97 Density, D6112-97 Creep, and D6117-97 Fasteners. Work on coefficient of thermal expansion, shear properties, coefficient of friction, and specifications of deck boards and joists are currently underway.

Future studies should investigate the use of recycled plastics in the design of other highway appurtenances such as culverts and glarescreens. Long term performance evaluation and durability, manufacturing techniques (rotational molding, heat welding, etc.) and design specs are also among areas that require further research.

7.0 Acknowledgment

This research and development study was sponsored by the New Jersey Department of Transportation (NJDOT) and the Federal Highway Administration (FHWA). The results and conclusions are those of the authors and do not necessarily reflect the views of the sponsors.

RECYCLED PLASTIC, SOUND-WALL, BOX BEAMS

Wind Load Testing Facility
Clemson University

SPECIMEN TESTING PERFORMED:
1-31-98

TENSION COUPON TESTING PERFORMED:
2-20-98

COMPRESSION COUPON TESTING PERFORMED:
3-24-98

KEVIN DAVENPORT

SCOTT SCHIFF

1.0 SET-UP

1. 1 Plastic Beam Specimens

Construction of the box beams was done a week before testing. Plastic has the tendency to creep with time and temperature variations, thus minimizing time between construction and testing reduced the possibility of any problems associated with failure of the fasteners. Two (2) 2ft x 12ft x ½ in. and two (2) 7in. x 12ft x ½ in. plastic sheets comprised a box beam. The beams were assembled screwing 2 inch #6 course drywall screws into pre-drilled holes spaced 3 in. on center for the entire 12 ft length of the beam. Temporary supports were placed inside the beam to accelerate the construction process. Two (2) beams were constructed with the material available and will from this point on be referred to as Beams A and B, respectively. A typical beam is illustrated in Figure A.1.

1.2 Testing Frame Configuration

The Wind Load Test Facility at Clemson University was utilized to perform pressure tests on the box beams. Specifically the 144 square foot vertical-testing chamber provided ample room to subject 2 x 12-ft specimens to various pressures. After discussing several testing frame designs, a final one was selected and built based on both simplicity and efficiency. Only a portion of the chamber, approximately 3 ft, was necessary for testing, so the remainder of the chamber was internally blocked off with 2x12's as shown in Figure A.2. End supports were built with the dimensions currently used in the field and are illustrated in Figure A.3. Oriented strand boards traversed the bottom of both supports and were covered with 6-mil plastic to provide a "frictionless" surface between the support and the specimen bearing down upon it. Each support was connected to the side channel of the chamber using three pipe clamps. Three (3)- 2x4 braces were then screwed to the outside edge of the supports to maintain a length of 12½ft and to prevent any possible rotation of the supports during testing. Three locations were drilled on each of the top two braces so Linear Voltage Differential Transducers (LVDT's) could later be installed. A continuous piece of 6-mil plastic was taped to the bottom 2 x 12 inside the chamber and wrapped around the inside of the end supports. Beams were then lowered into the frame, shown in Figure A.4, and enveloped with the excess plastic at the top. A seal was completed by taping all edges of the plastic to the top 2 x 12 inside the chamber. Figure A.5 shows the entire configuration, with beam in place, prior to testing. Not shown in this figure is the pipeline attached from the back of the chamber to the pump. Throughout the test, the pipeline was used to regulate the amount of suction provided by the pump and a water manometer was used to monitor the suction. In addition, Figure A.6a and b illustrates how the plastic enveloped the specimen and where the suction occurred on the beam, respectively. The plastic envelope was wrapped such that suction was applied on the inside face of the exterior panel, producing a differential pressure. The suction caused the beam to be drawn towards the chamber.

2.0 ANALYSIS PROCESS

The raw data was obtained and put into a format that is easier to understand. In order to ensure reliable results as well as ease the analysis, several steps were required to analyze the data. The following sections discuss in detail the analysis process. Data for Beams A and B are located in Appendix B and C, respectively.

2.1 LVDT Calibration

All data was obtained in the form of voltages, which were then converted to displacements through a calibration process. Each LVDT was displaced 1-½ inches while simultaneously measuring the resulting differential voltage. Calibration factors for each LVDT were obtained by dividing the displacement by the change in voltage. Both one and two inch range LVDT's were used with calibration factors of approximately 0.1in/volt and 0.2in/volt, respectively. All calibration factors are shown in Table 2.1.

TABLE 2.1 Calibration Factors for LVDT's

Top Left	Top Center	Top Right	Middle Left	Middle Center	Middle Right
0.1007	0.2040	0.1002	0.2179	0.2006	0.1984

NOTE: All factors in Inches per Volt

2.2 LVDT Locations

LVDT's were located at the coordinates listed in Table 2.2 and illustrated in Figure A.1. It should be noted that the Middle Center LVDT was located slightly off center. However, using beam theory analysis with simply supported boundary conditions, the actual center displacements can be compared with the offset location with a very high degree of accuracy. Supporting calculations can be found in Appendix H.

TABLE 2.2 LVDT Locations

		Coordinates	
LVDT location		X	Y
Top	Left	5	22.5
	Center	72	22.5
	Right	139	22.5
Middle	Left	4.75	12
	Center	69.75	12
	Right	138.75	12

NOTE: 1.) All coordinates in Inches, and
2.) The origin is located at the lower left corner of the beams.

2.3 Determining Displacements

Displacements were calculated by zeroing all voltage readings by each LVDT initial voltage reading, then multiplied by the appropriate calibration factor. These displacement readings account for the beam's position throughout the duration of the test. The readings were then adjusted for the rigid body shift (RBS) that occurred in the beginning of the tests at very low pressures. The displacements were also adjusted for the cyclic load applied to the specimens. While testing the box beams, the pump had the tendency to cut-off prematurely with the gradual restriction of air loss. Figures B.1 and C.1 show displacement time history plots for Beams A and B, respectively and indicate when the pump cut-off and was re-started. In order to achieve higher pressures "sub-tests" were performed. These subsequent tests began capturing data where the first test ended. The first sub-test ranged from zero to approximately 45 psf for both Beams A and B. Two subsequent tests on Beam A were necessary to reach pressures around 80 psf whereas only one was needed for Beam B. Re-starting the pump essentially subjected the specimen to a cyclic load and moved it to a slightly new starting position each test. Consequently, data from each "sub-test" had to be analyzed independently to determine the new starting position. For each test, LVDT displacements were plotted against pressure and fit with a line. As expected, the best-line does not intercept the displacement axis at the origin signifying the beam indeed underwent a rigid body shift prior to any relative displacements of the center with respect to the extreme ends. The intercept indicates the magnitude of the RBS and thus subtracting it from all displacements provides information pertaining to the deflections of the beam. Intercepts of each sub-test for Beam A and B are shown in Figures B.2-B.3 and C.2-C.3, respectively. Using both Top and Middle Center LVDT intercepts for determining the RBS eliminated the need for additional LVDT locations (Top Left, Top Right, Middle Left, and Middle Left), therefore they were not used in the analysis process.

2.4 Equations from Sub-Tests

Next, displacements adjusted for a RBS, for all sub-tests of both beams were plotted against pressure and fit with a line. Table G.1 lists all the deflections plotted in Figure G.1. Based on the slopes of each equation, mid-span deflections at the Top and Middle of the beam at any pressure were determined with less than 3% error. The equations are in the form of $y = -mx$, where y is displacement in inches, x is the pressure in pounds per square foot, and m is the slope in inches per pounds per sq. ft (in/psf). Slopes and corresponding coefficient of correlation values (R^2) are listed in Table 2.3. It should be noted that equations are based on all data collected in which pressures ranged from 0 to 93.6 psf.

TABLE 2.3 Slopes of Top and Middle Center LVDT's

	Slope (m)	R^2
Top Center	0.0161	0.9740
Middle Center	0.0191	0.9747

3.0 MATERIAL PROPERTIES

Coupons were made from the same sheets of plastic that the beams were made from. This ensured an accurate determination of the material properties of the beams being tested. Both the tensile and compressive Modulus of Elasticity were of interest. The following sections describe how these properties were obtained. All data from the tension and compression coupon tests are provided in Appendix D and E, respectively.

3.1 Tensile Modulus of Elasticity (TMOE)

Three (3) tension coupons were milled from the excess material. Each coupon was given a two-inch gage length and placed in a Universal Testing Machine. A tensile force was applied at a rate of 0.1 in/min and extension readings were taken every 100pounds. At first it was thought that an extensometer would disturb the coupon when attaching to the two-inch gage length, therefore, the initial attempt at measuring extension was through the use of dividers. Figure D.1 shows how this method provided data for the duration of the test. However, at the beginning of the test, extensions became difficult to read using this method so subsequent coupons were tested with an extensometer. The extensometer provided precise information in the beginning of the test but began slipping after some time. This resulted as the thickness of the necked region reduced with load, therefore, readings were discarded after slippage had occurred. Normal stress strain curves were then constructed and the MOE was calculated from the linear portion on the stress strain curves for only the coupons tested with the extensometer. As seen in Figures D.2 and D.3, neither coupon behaved linearly for the duration of the test therefore slopes were taken at the proportional limits. These limits were chosen such that the stresses at these points were slightly greater than the maximum stresses induced at the extreme fibers of the beam when tested. Calculations of maximum stresses can be found in Appendix H. The first coupon exhibited signs of "tearing" in the necked gage length region whereas the second and third appeared to have foreign contents in the failure surface. The non-uniformity experienced in the latter is to be expected when working with recycled materials. Both coupons exhibited a non-linear, ductile failure with a MOE around 215 ksi. Shown in Figure D.4 is a typical failed tension coupon.

3.2 Compressive Modulus of Elasticity (CMOE)

Compression coupons were made with the dimensions of 4 x 1.3 x 2 cm. These were placed in a Universal Testing Machine and applied a compressive load along the 2cm direction at a rate of 0.05 in/min. Extension readings were taken with the crosshead movement every 200 pounds, up to 4000 pounds. Thereafter, the load increased much slower allowing readings to be taken every 100 pounds until the coupon visibly yielded (approximately 30% strain). Stress-Strain curves of the material in compression were then constructed and analyzed. Three (3) coupons were tested and all provided similar plots. Figures E.1-E.3 show the non-linear behavior of the material. The CMOE was calculated using the linear stress strain relationship at low stresses. CMOE ranged from 62 to 75 ksi with an average approximately 65.5 ksi. Figure E.4 shows an original and the three tested compression coupons. All coupons deformed in a similar manner.

4.0 COMMENTS

4.1 Behavior of Connections

As shown in Figure F.1, some screws had the tendency to come out the side of the ½ inch thick piece they were being screwed into. However, this did not seem to effect the overall performance of the beams in that no signs of failure were evident in either the screws or plastic. In addition, no sign of slippage at the connections was observed throughout the tests suggesting the beam performed as if it were an extruded piece of plastic.

4.2 Stiffness and Flexibility of Plastic

When handling individually, the sheets of the plastic were very difficult to handle, they were very flexible and would deflect approximately 4 feet. However, when assembled into the box configuration, there was no apparent deflection whatsoever when handling. Moreover, when testing the box configuration, deflections at the mid-span never exceeded 2 inches. The flexibility of the box beam configuration can be seen in the slope of the equations in Section 2.4. The stiffness is inversely proportional to flexibility, and thus the slope, and can be expressed in units of psf/in. The stiffness of the two center LVDT locations are listed below in Table 4.1.

TABLE 4.1 Stiffness of Center LVDT Locations

	Stiffness (psf/in)
Top Center	62.1
Middle Center	52.4

4.3 Rigid Body Movements

Immediately after the pump was turned on the entire beam underwent a rigid body translation. The translation was detected by all LVDT's and is a result of the intended gap between the support and the beam, shown in Figure A.3. Also detected was the rigid rotation of the top of the beam coming into contact with the supports. This can be explained by excess plastic that built up under the inside edge of the beam when installing it. This also explains why Top Center intercepts are roughly twice as large as the Middle Center. With essentially a pivot point at the base of the beam, a rotation with respect to this point caused twice as much movement at the Top of the beam with respect to the Middle because it is twice as far away.

4.4 Beam Profile at Mid-Span

During the test, the Middle Center of the beam was observed to displace more than the Top, resulting in a concavity of the beam profile. Accordingly, this was accounted for in the LVDT displacements. In order to plot the profile at various pressures, a bottom location was assumed to act the same as the top. This allowed for a line to be connected trough three points at each pressure level. The equations from Section 2.4 were used for plotting displacements using pressures ranging from 0 to 90 psf in increments of 10psf. A mid-span profile plot can be found in Figure F.2.

4.5 Deflection of Beams

No signs of failure were evident in either beam tested. Pressures in excess of 90 psf were achieved while mid-span deflections never exceeded 2 in. As supported in Section 2.2 and shown in Figure G.1, the beams demonstrated an overall deflected shape of a simply supported beam. Using this observation, theoretical mid-span deflections for a simply supported beam were calculated, in terms of pressure, and compared to the equations given in Section 2.4. Calculations can be found in Appendix H. Slopes were calculated using three different MOE's, the TMOE, CMOE and an average of the two MOE's. The latter providing the least amount of error of 11.3 and 5.2% for Top Center and Middle Center locations, respectively. Comparisons can be found in Table G.2. Due to the concavity mentioned earlier, both Top and Middle Center displacements are listed for comparison.

Reasons why the differences between the two exist are as follows. Theoretical equations assume the beam is prismatic, monolithically extruded eliminating the use of screws. The fact that screws are holding the plastic together in the beam configuration allows for potentially small displacements between the layers of plastic, resulting in larger deflections than those obtained theoretically. Another explanation arises when examining the contact area between the beam and the end supports throughout the test. Theoretically, the tributary area for a box beam is 12ft by 2ft, providing the simple support is only in contact with the two extreme ends of the beam. However, when subjected to pressure the beams bear on the inside face of the supports thus reducing the clear span from twelve feet to something slightly less. The theoretical calculation does not compensate for the reduced length and thus computes theoretical deflections greater than those obtained experimentally. Theoretically this will result in calculating deflections larger than those obtained experimentally. This would be the case when examining the slope comparison of Top Center LVDT with that obtained using beam theory with the average MOE. The slope of the Top Center (0.0161) is indeed less than the slope obtained using beam theory (0.01815).

4.6 Relationship Between Pressure and Wind Speeds

As requested, Table 4.2 was produced to provide a relationship between the pressure induced on the plastic box beam and wind speed. Wall height was also taken into consideration when making the table. The table is in accordance with *American Society of Civil Engineers Minimum Design Loads for Buildings and Other Structures* (ASCE 7-93). Several tables and sections of the code were referred to and are noted in Sample Calculations H.4 which can be found on page H-5 in Appendix H.

TABLE 4.2 Wind Speed, Pressure and Wall Height Relationship

Height (ft)	Fastest Mile Wind Speed (mph)	Pressure (psf)
≤ 15	70	14.3
	90	23.7
	110	35.4
20	70	15.2
	90	25.2
	110	37.6
30	70	16.8
	90	27.7
	110	41.4

Wind Test Report Appendixes

A	Figures of Beam, End Support and Testing Frame
B	Beam A Data
C	Beam B Data
D	Tension Coupon Data
E	Compression Coupon Data
F	Observations
G	Deflection Comparisons
H	Sample Calculations

APPENDIX A

FIGURES OF BEAM, END SUPPORT AND TESTING FRAME

Figure A.1 LVDT Locations on Typical Beam

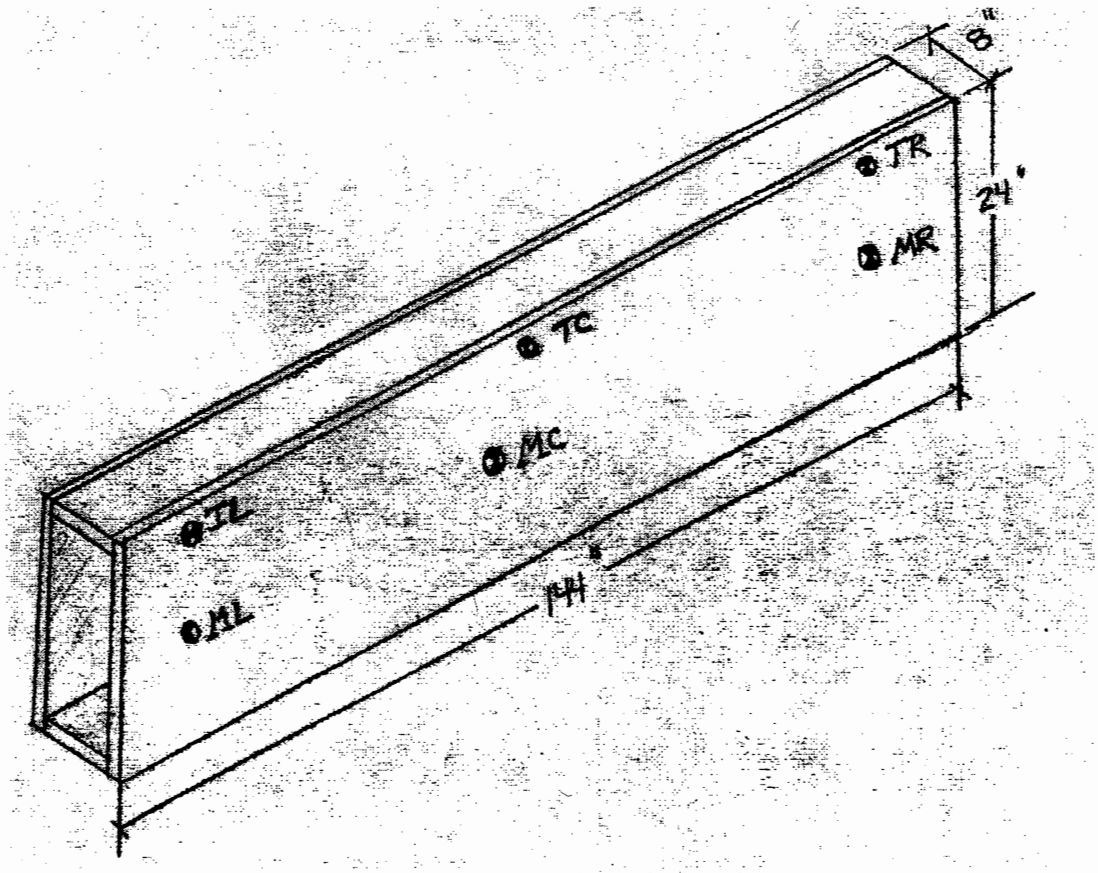

Figure A.2 Inside Framing of Chamber

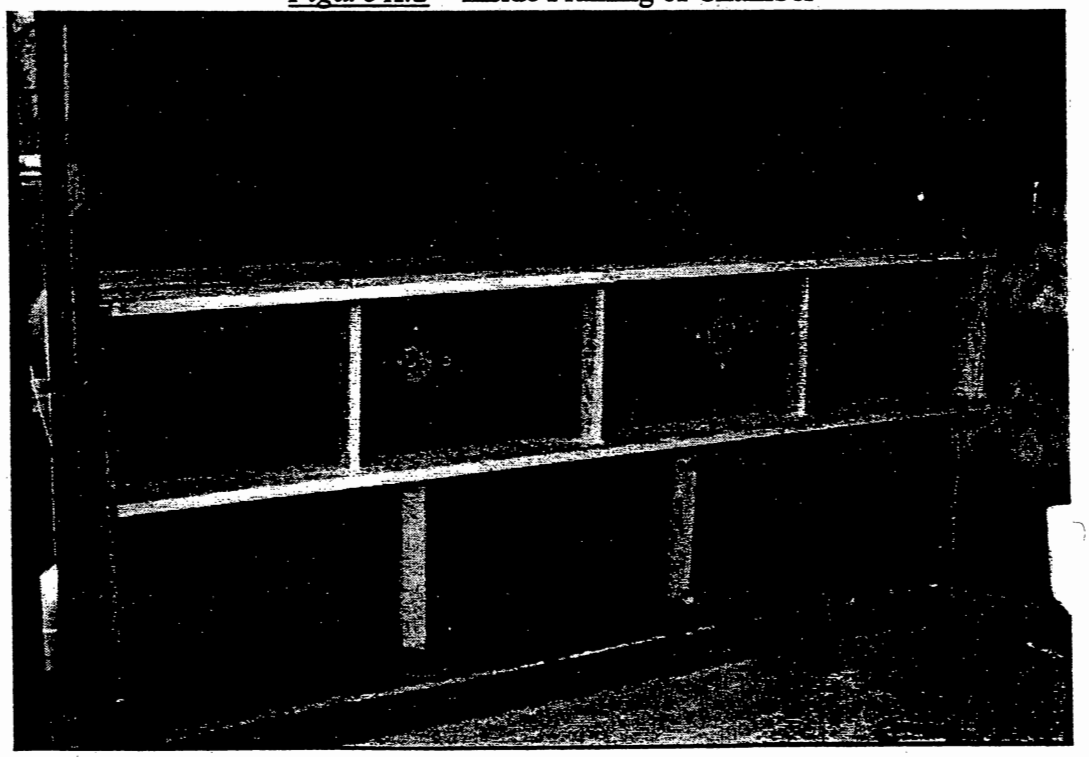

Figure A.3 Detail of Supports

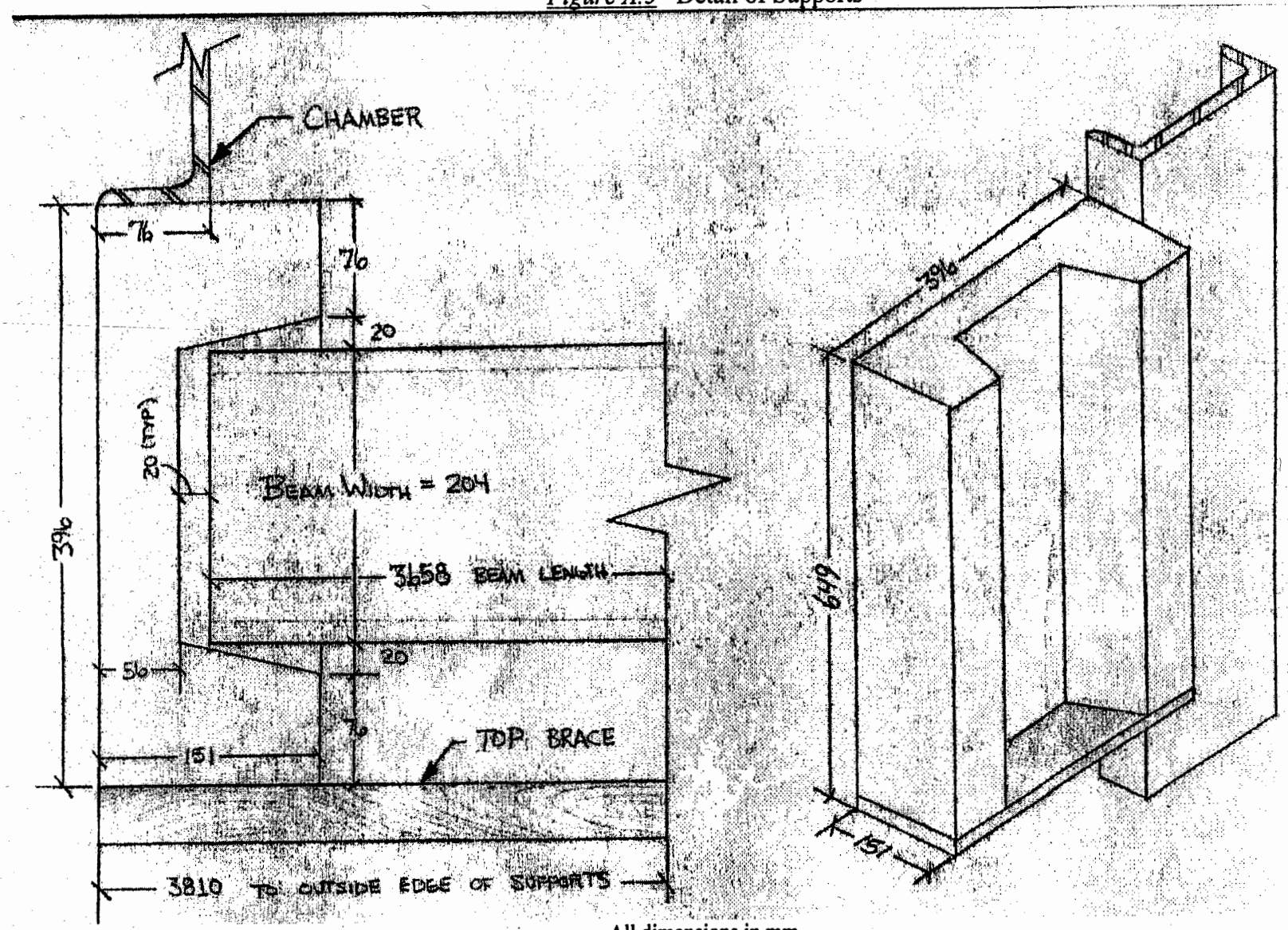

All dimensions in mm.

Figure A.4 Beam Location in Supports

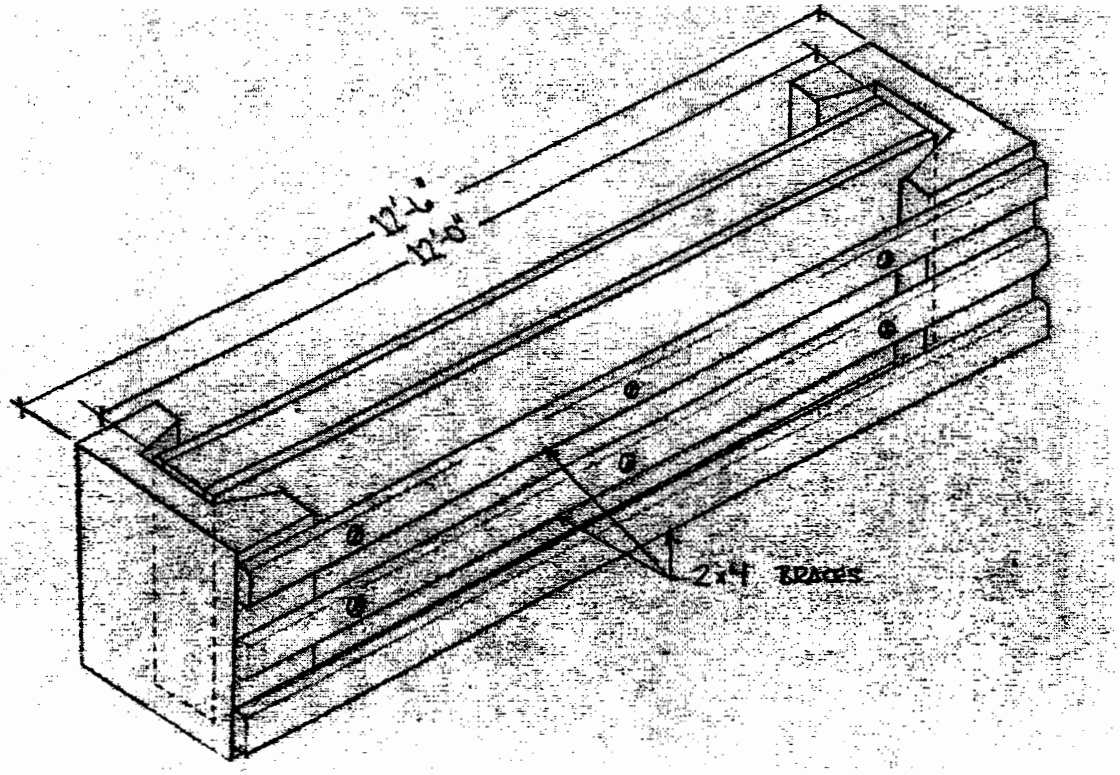

Figure A.5 Beam in Testing Position

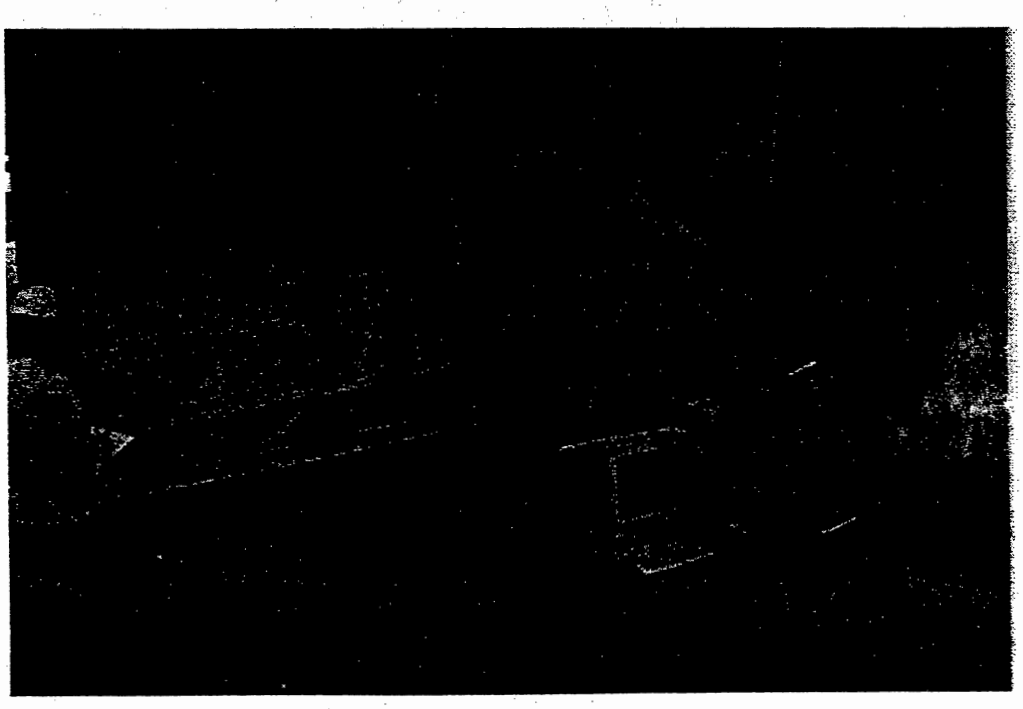

Figure A.6 **Suction from Enveloped Plastic**

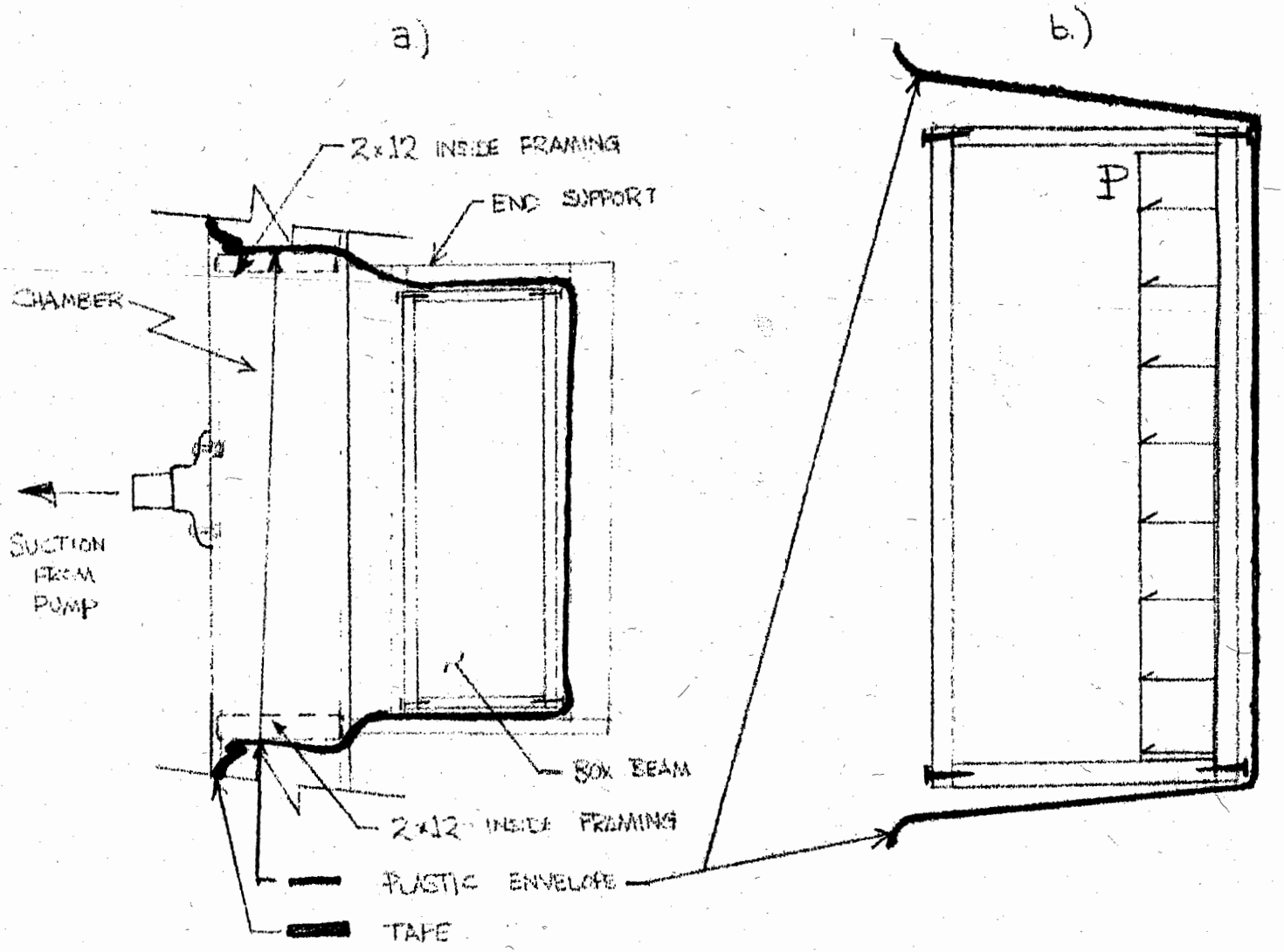

CROSS - SECTION VIEWS

APPENDIX B

BEAM A DATA

Figure B.1

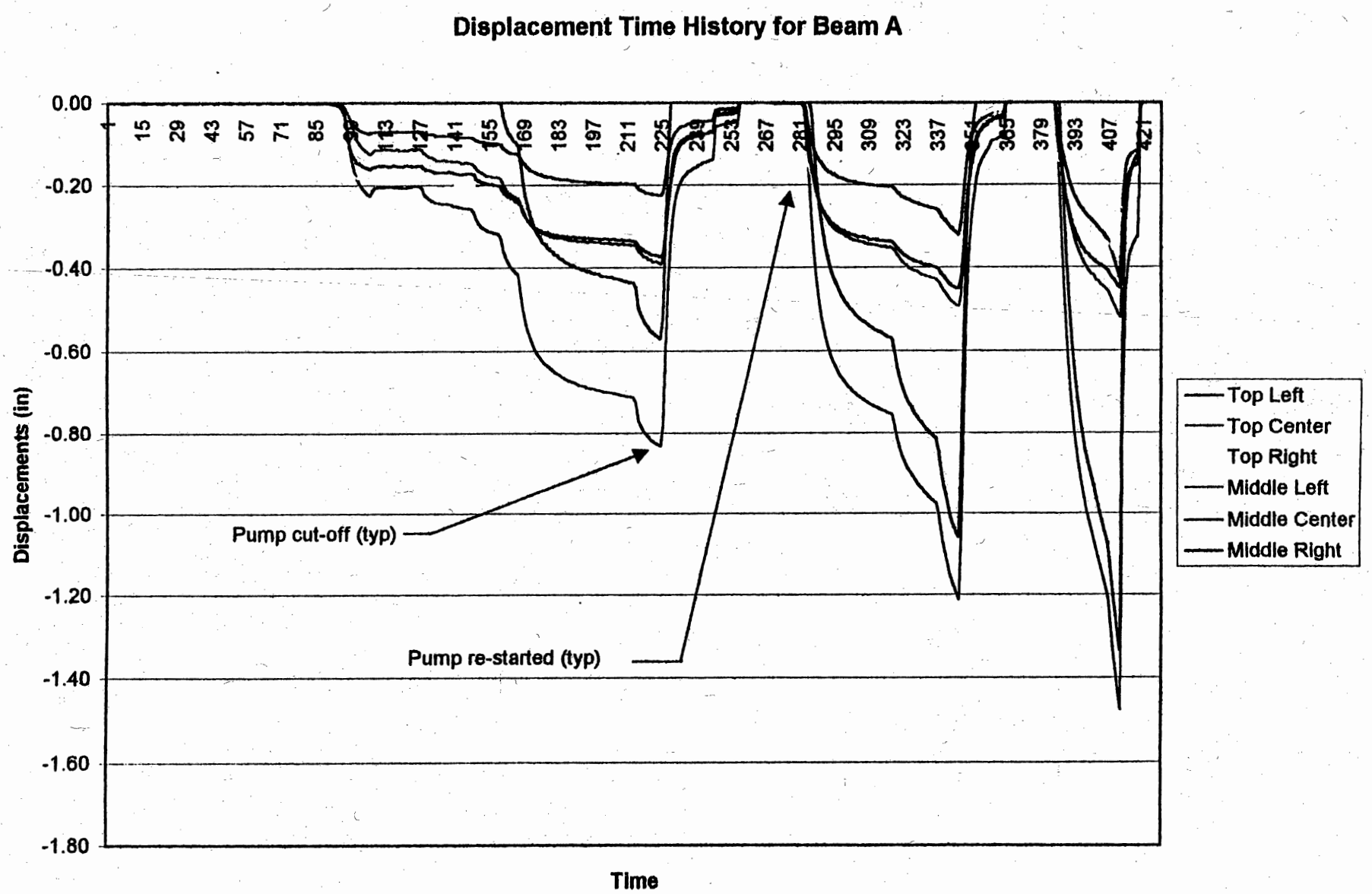
Displacement Time History for Beam A
0.00
-0.20
-0.40
-0.60
-0.80
-1.00
-1.20
-1.40
-1.60
-1.80
Displacements (in)
1
15
29
43
57
71
85
99
113
127
141
155
169
183
197
211
225
239
253
267
281
295
309
323
337
351
365
379
393
407
421
Time
Pump cut-off (typ)
Pump re-started (typ)
Top Left
Top Center
Top Right
Middle Left
Middle Center
Middle Right

Figure B.2

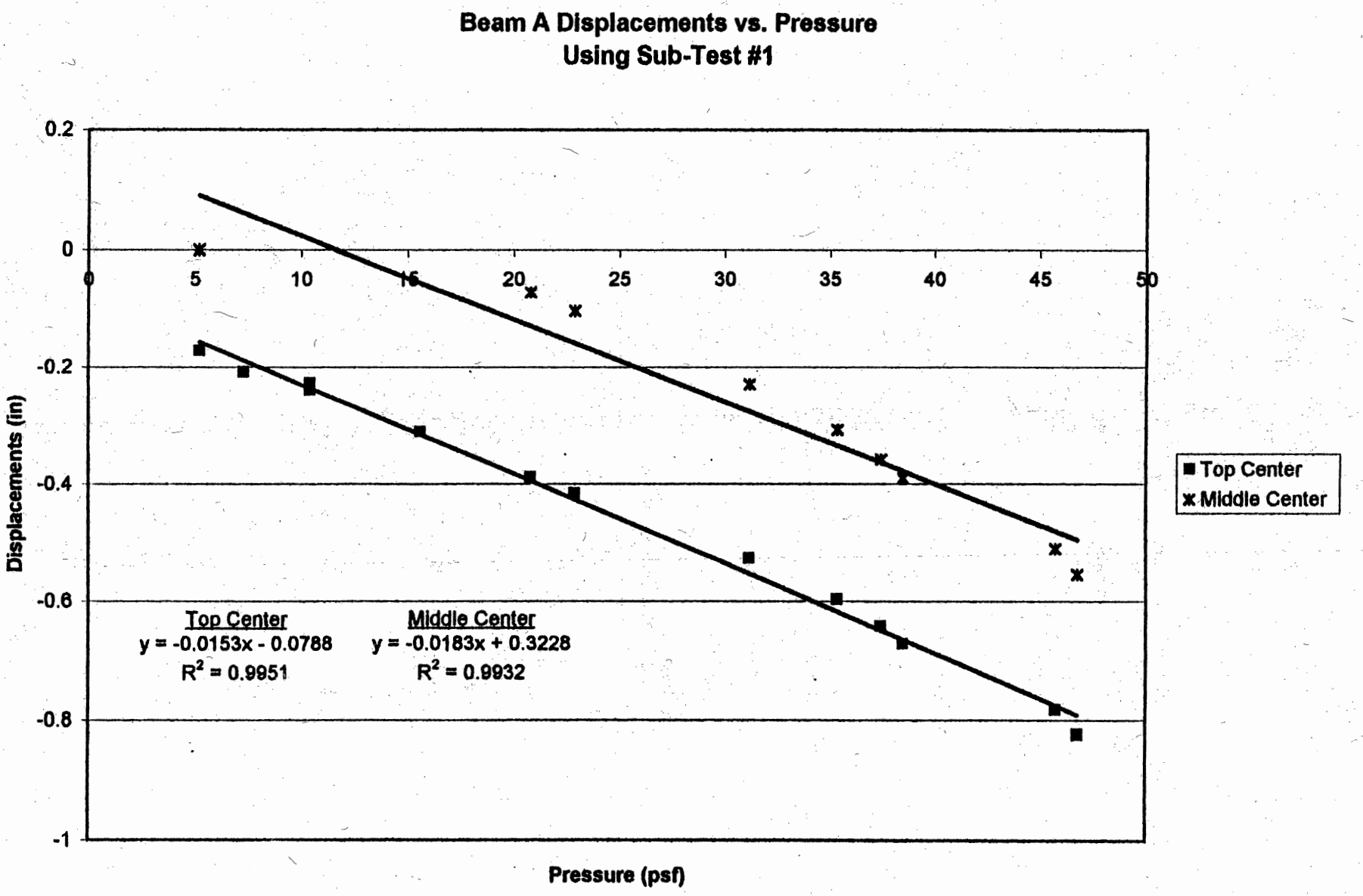
Beam A Displacements vs. Pressure
Using Sub-Test #1
0.2
0
-0.2
-0.4
-0.6
-0.8
-1
0
5
10
15
20
25
30
35
40
45
50
Displacements (in)
Pressure (psf)
Top Center
y = -0.0153x - 0.0788
R² = 0.9951
Middle Center
y = -0.0183x + 0.3228
R² = 0.9932
Top Center
Middle Center

Figure B.3

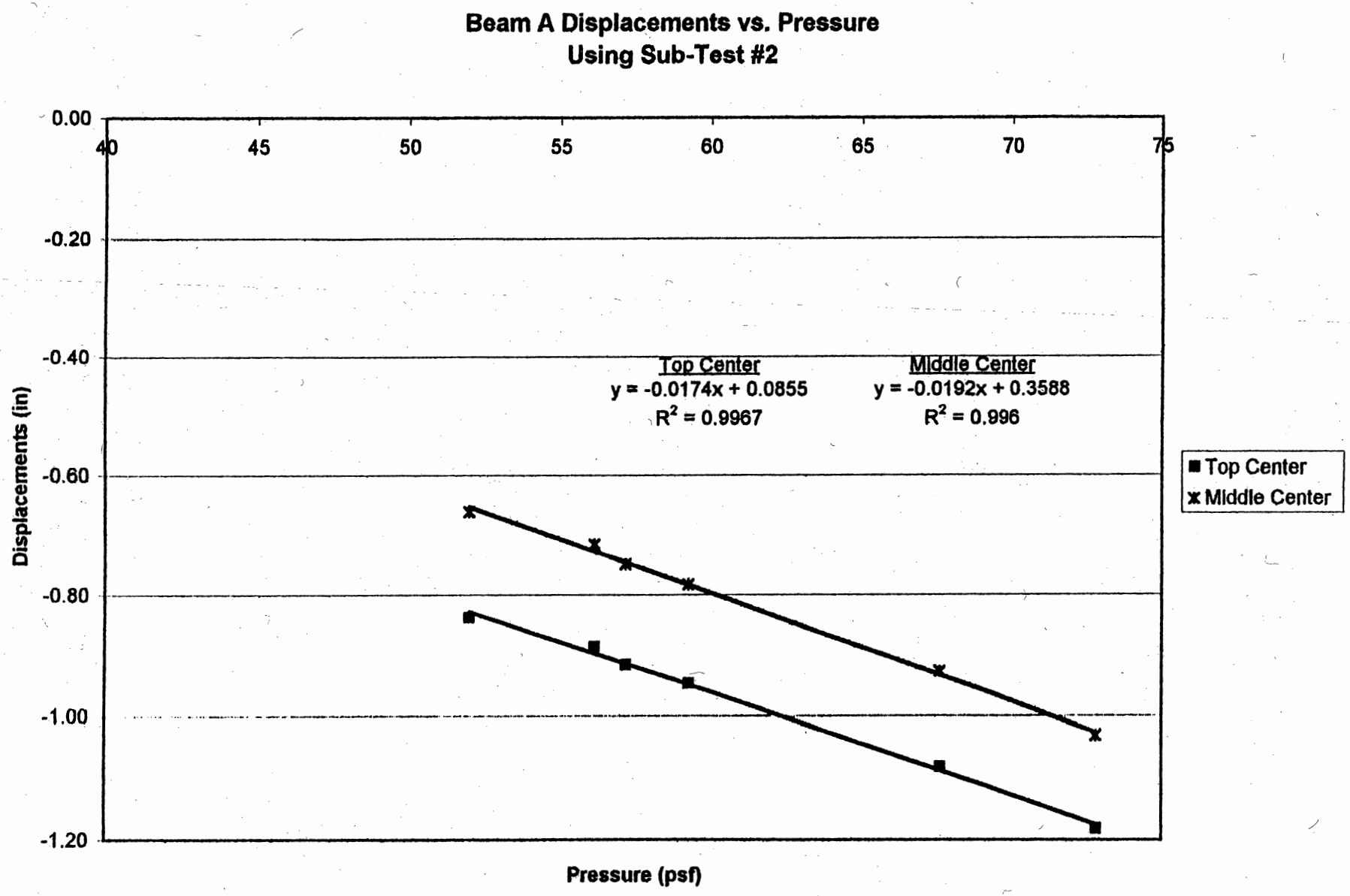
Beam A Displacements vs. Pressure
Using Sub-Test #2
0.00
-0.20
-0.40
-0.60
-0.80
-1.00
-1.20
40
45
50
55
60
65
70
75
Displacements (in)
Pressure (psf)
Top Center
y = -0.0174x + 0.0855
R2 = 0.9967
Middle Center
y = -0.0192x + 0.3588
R2 = 0.996
Top Center
Middle Center

APPENDIX C

BEAM B DATA

Figure C.1

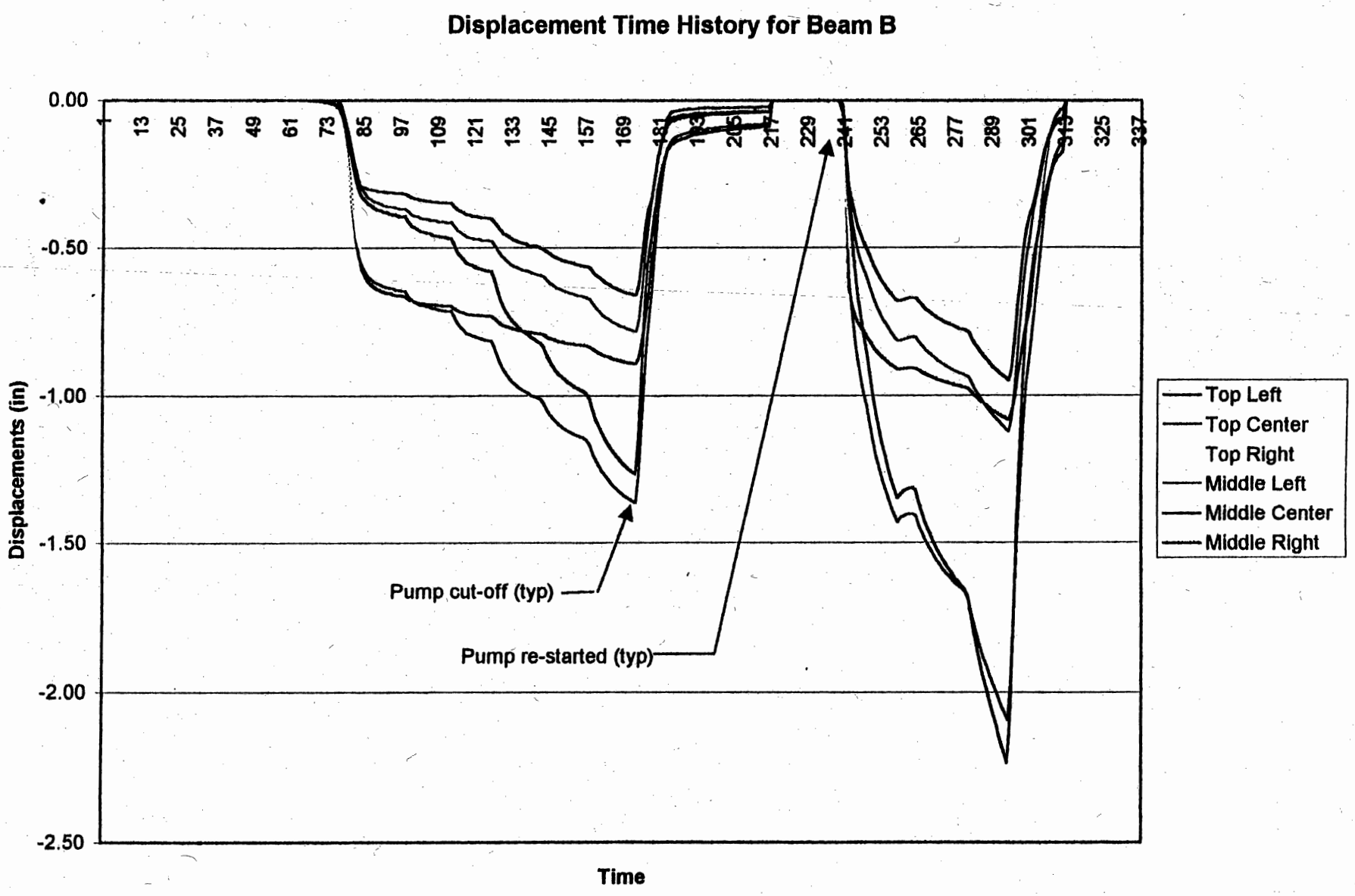
Displacement Time History for Beam B
0.00
-0.50
-1.00
-1.50
-2.00
-2.50
Displacements (in)
1
13
25
37
49
61
73
85
97
109
121
133
145
157
169
181
193
205
217
229
241
253
265
277
289
301
313
325
337
Time
Pump cut-off (typ)
Pump re-started (typ)
Top Left
Top Center
Top Right
Middle Left
Middle Center
Middle Right

Figure C.2

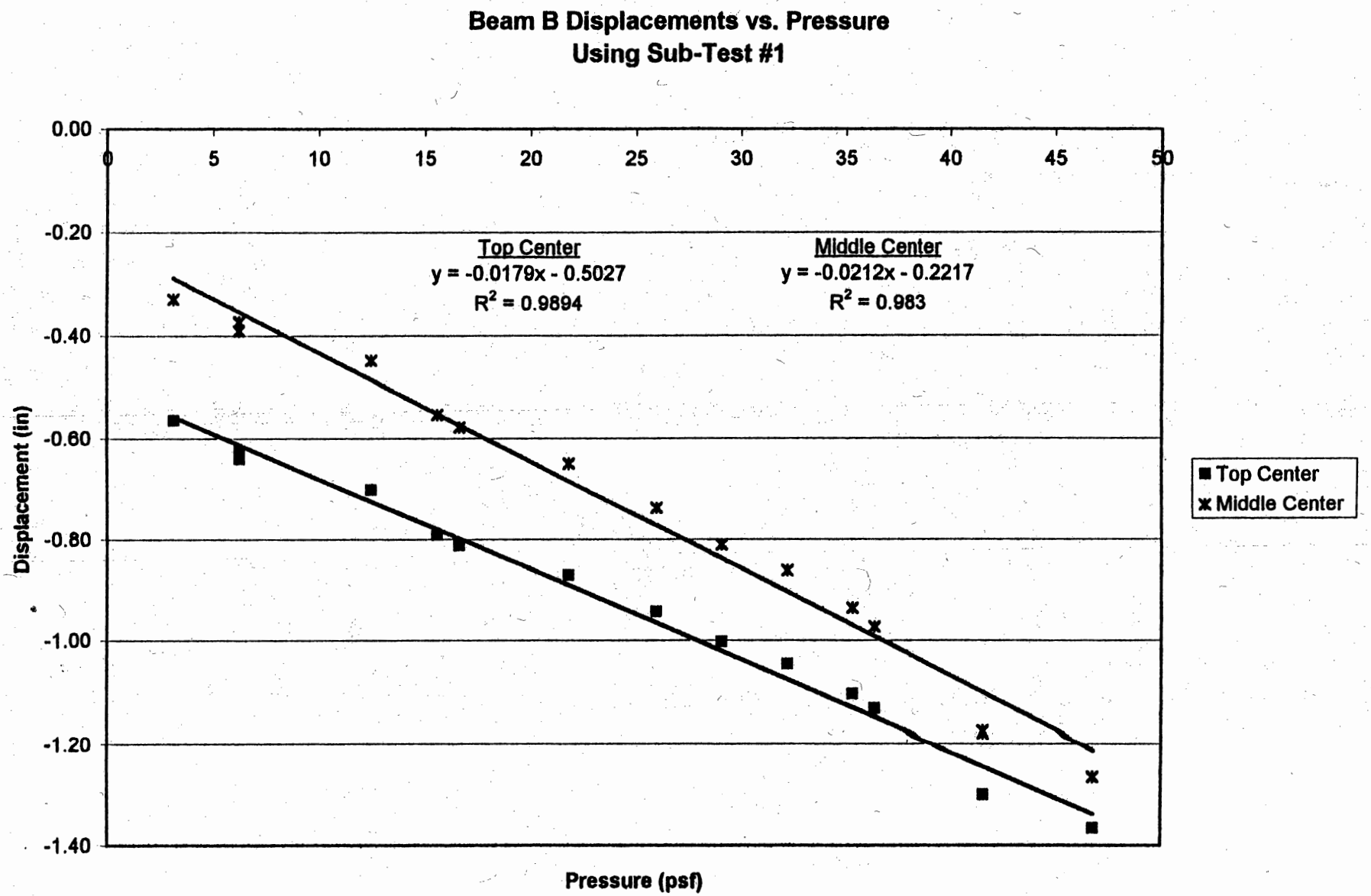
Beam B Displacements vs. Pressure
Using Sub-Test #1
0.00
-0.20
-0.40
-0.60
-0.80
-1.00
-1.20
-1.40
0
5
10
15
20
25
30
35
40
45
50
Displacement (in)
Pressure (psf)
Top Center
y = -0.0179x - 0.5027
R2 = 0.9894
Middle Center
y = -0.0212x - 0.2217
R2 = 0.983
Top Center
Middle Center

Figure C.3

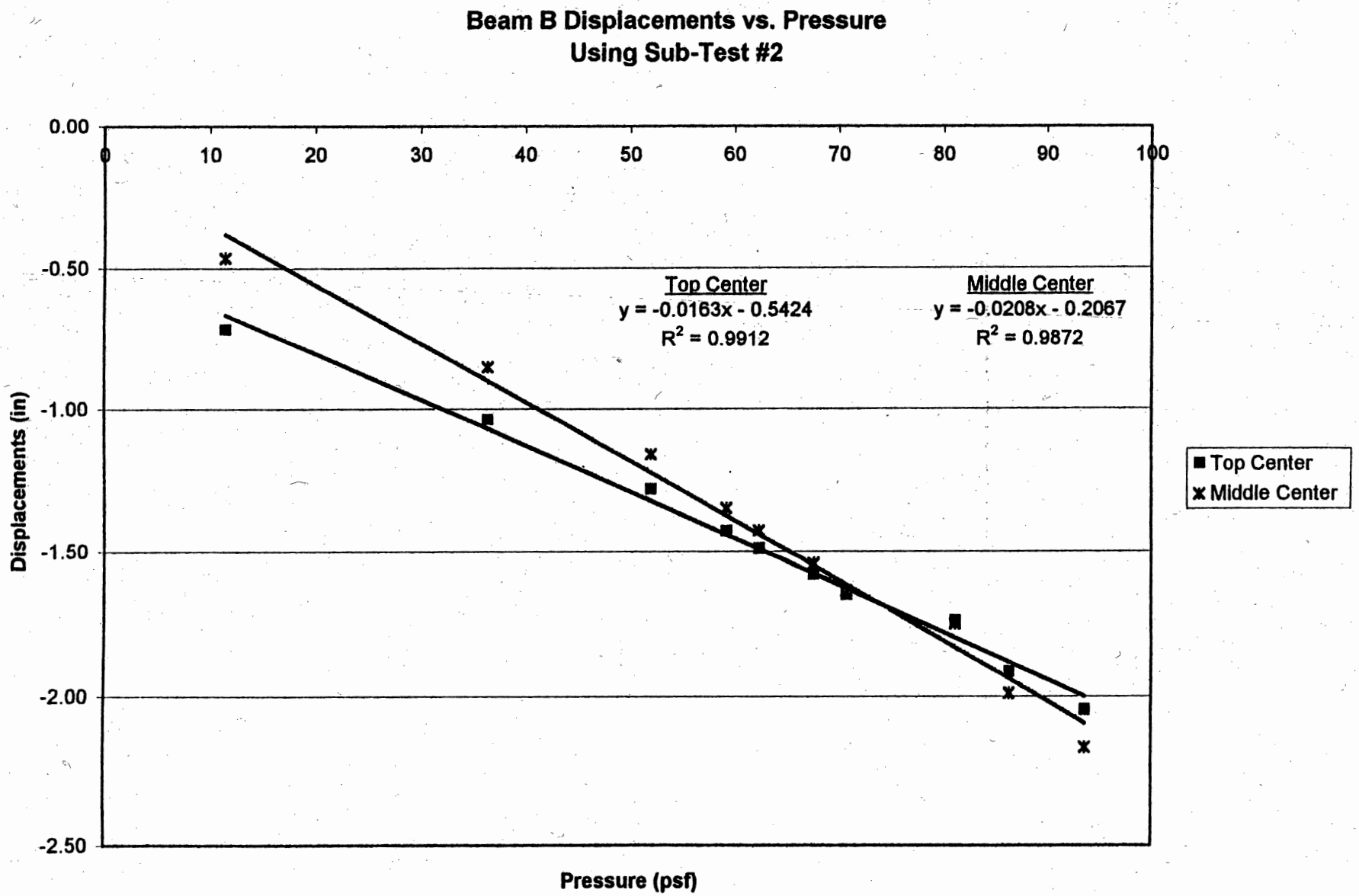
Beam B Displacements vs. Pressure
Using Sub-Test #2
0.00
-0.50
-1.00
-1.50
-2.00
-2.50
0
10
20
30
40
50
60
70
80
90
100
Displacements (in)
Pressure (psf)
Top Center
y = -0.0163x - 0.5424
R2 = 0.9912
Middle Center
y = -0.0208x - 0.2067
R2 = 0.9872
Top Center
Middle Center

APPENDIX D

TENSION COUPON DATA

Figure D.1

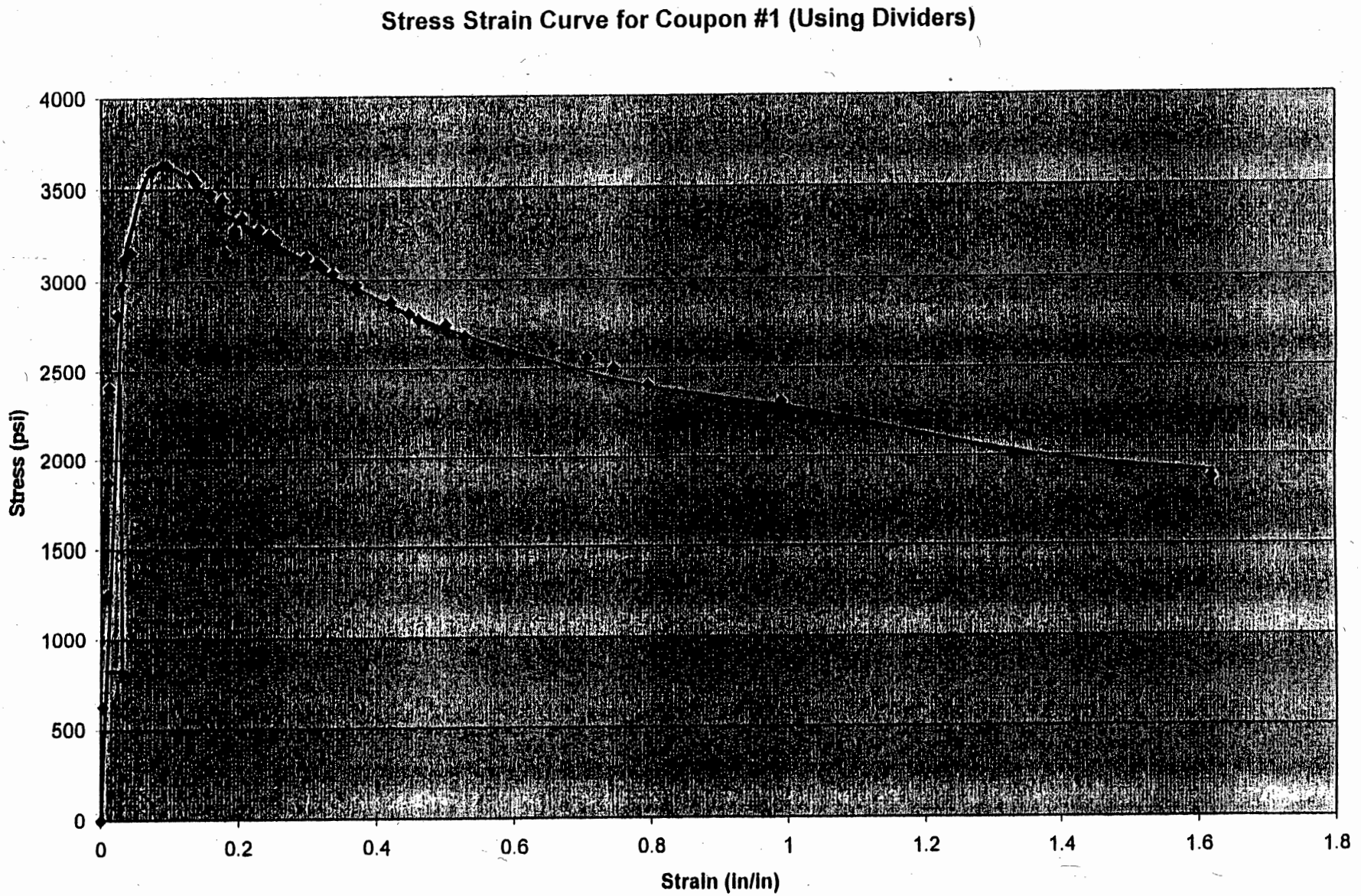
Stress Strain Curve for Coupon #1 (Using Dividers)
Stress (psi)
4000
3500
3000
2500
2000
1500
1000
500
0
0
0.2
0.4
0.6
0.8
1
1.2
1.4
1.6
1.8
Strain (in/in)

Table D.1

Determining of Modulus of Elasticity

Coupon #2
Width = 0.704 in
Thickness = 0.456 in
Area = 0.3210 in2
Gage Length = 2 in

Load Rate (in/min)	Load (#)	Extension (in)	Stress (psi)	Strain (in/in)
0.1	0	0.00000	0.0	0.0000
	50	0.00200	155.8	0.0010
	100	0.00350	311.5	0.0018
	150	0.00435	467.3	0.0022
	200	0.00580	623.0	0.0029
	250	0.00680	778.8	0.0034
	300	0.00890	934.5	0.0045
	350	0.01070	1090.3	0.0054
	400	0.01250	1246.0	0.0063
	450	0.01500	1401.8	0.0075
	500	0.01689	1557.5	0.0084
	550	0.01998	1713.3	0.0100
	600	0.02270	1869.0	0.0114
	650	0.02630	2024.8	0.0132
	700	0.02980	2180.5	0.0149
	750	0.03470	2336.3	0.0174
	800	0.03970	2492.0	0.0199
	850	0.04560	2647.8	0.0228
	900	0.05268	2803.5	0.0263
	950	0.06010	2959.3	0.0301
	1000	0.06900	3115.0	0.0345
	1050	0.07910	3270.8	0.0396

E = 214568 psi from best-fit line using
pressures from 0 to 778.8 psi
with an R^2 value = 0.9765

Figure D.2

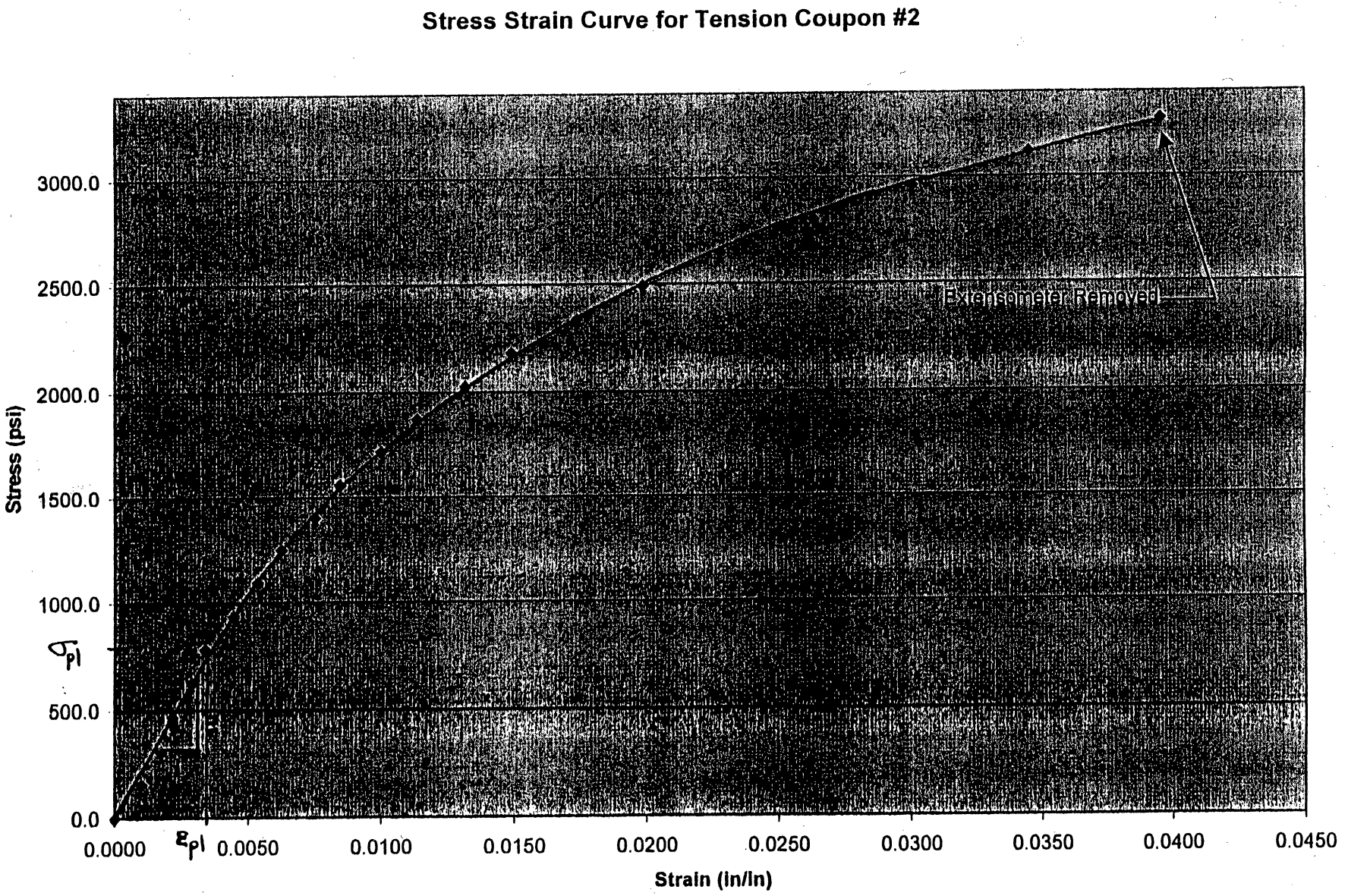
Stress Strain Curve for Tension Coupon #2
Stress (psi)
3000.0
2500.0
2000.0
1500.0
1000.0
500.0
0.0
σ_{pl}
ε_{pl}
0.0000
0.0050
0.0100
0.0150
0.0200
0.0250
0.0300
0.0350
0.0400
0.0450
Strain (in/in)
Extensometer Removed

Table D.2

Determining of Modulus of Elasticity

Coupon #3
Width = 0.685 in
Thickness = 0.454 in
Area = 0.3110 in2
Gage Length = 2 in

Load Rate (in/min)	Load (#)	Extension (in)	Stress (psi)	Strain (in/in)
0.1	0	0.00000	0.0	0.0000
	50	0.00218	160.8	0.0011
	100	0.00280	321.6	0.0014
	150	0.00430	482.3	0.0022
	200	0.00580	643.1	0.0029
	250	0.00750	803.9	0.0038
	300	0.00960	964.7	0.0048
	350	0.01150	1125.4	0.0058
	400	0.01345	1286.2	0.0067
	450	0.01530	1447.0	0.0077
	500	0.01800	1607.8	0.0090
	550	0.02190	1768.5	0.0110
	600	0.02490	1929.3	0.0125
	650	0.02930	2090.1	0.0147
	700	0.03390	2250.9	0.0170
	750	0.03860	2411.7	0.0193
	800	0.04490	2572.4	0.0225
	850	0.05260	2733.2	0.0263
	900	0.06010	2894.0	0.0301
	950	0.07130	3054.8	0.0357
	1000	0.08375	3215.5	0.0419

E = 216314 psi from best-fit line using
pressures from 0 to 803.9 psi
with an R^2 value = 0.9855

Figure D.3

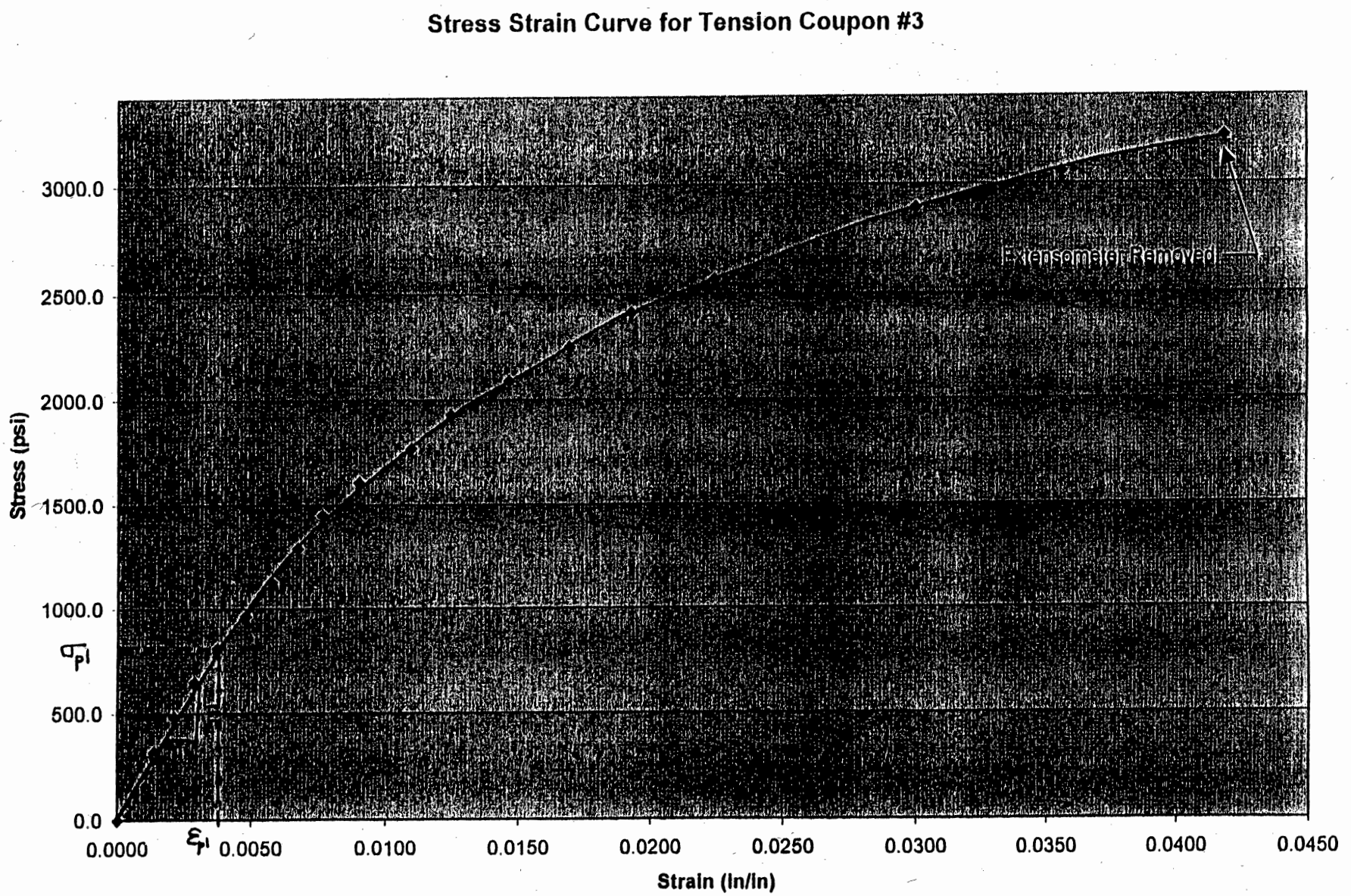
Stress Strain Curve for Tension Coupon #3
Extensometer Removed
3000.0
2500.0
2000.0
1500.0
1000.0
500.0
0.0
Stress (psi)
σ_{pl}
0.0000
ε_{pl}
0.0050
0.0100
0.0150
0.0200
0.0250
0.0300
0.0350
0.0400
0.0450
Strain (in/in)

Figure D.5 Typical Failed Tension Coupon

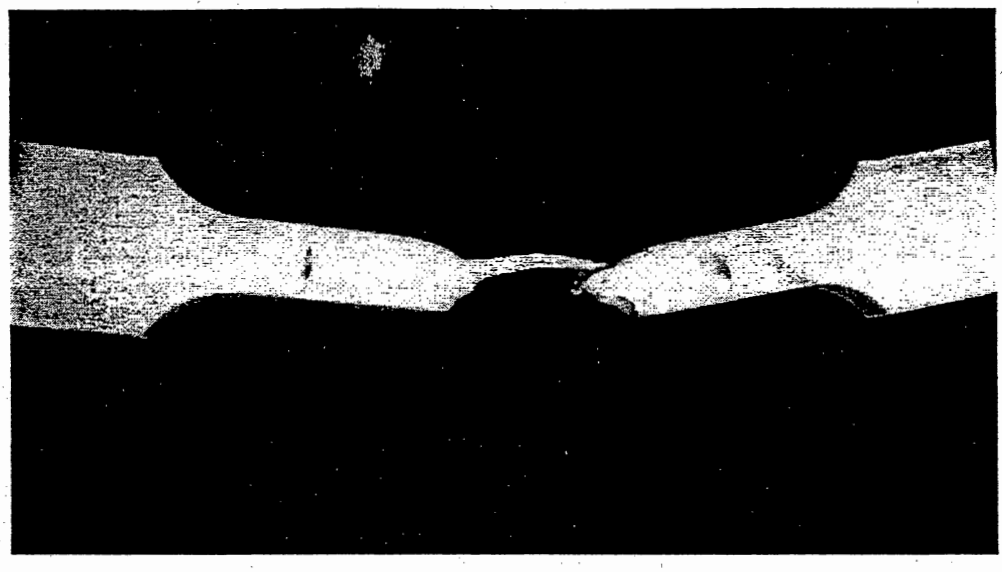

APPENDIX E

COMPRESSION COUPON DATA

Table E.1

Determining of Compressive MOE

Coupon #1			
Width =	1.573 in		
Thickness =	0.456 in		
Area =	0.7173 in2		
Original Length =	0.791 in		
Load (#)	Extension (in)	Stress (psi)	Strain (in/in)
0	0.0000	0.0	0.0000
100	0.0024	139.4	0.0030
200	0.0045	278.8	0.0057
400	0.0072	557.7	0.0091
800	0.0097	1115.3	0.0123
1000	0.0119	1394.1	0.0150
1200	0.0134	1673.0	0.0169
1400	0.0159	1951.8	0.0201
1600	0.0179	2230.6	0.0226
1800	0.0190	2509.5	0.0240
2000	0.0234	2788.3	0.0296
2200	0.0290	3067.1	0.0367
2400	0.0332	3345.9	0.0420
2600	0.0372	3624.8	0.0470
2800	0.0425	3903.6	0.0537
3000	0.0485	4182.4	0.0613
3200	0.0567	4461.2	0.0717
3400	0.0667	4740.1	0.0843
3600	0.0812	5018.9	0.1027
3800	0.0997	5297.7	0.1260
4000	0.1198	5576.6	0.1515
4100	0.1307	5716.0	0.1652
4200	0.1406	5855.4	0.1777
4300	0.1498	5994.8	0.1894
4400	0.1595	6134.2	0.2016
4600	0.1775	6413.0	0.2244
4700	0.1857	6552.5	0.2348
4800	0.1948	6691.9	0.2463
4900	0.2037	6831.3	0.2575
5200	0.2309	7249.5	0.2919
5300	0.2413	7388.9	0.3051

Compressive Modulus of Elasticity was determined to be
75553 psi using stresses from 0 to 1115.3 psi.
with a R^2 = 0.8927

Figure E.1

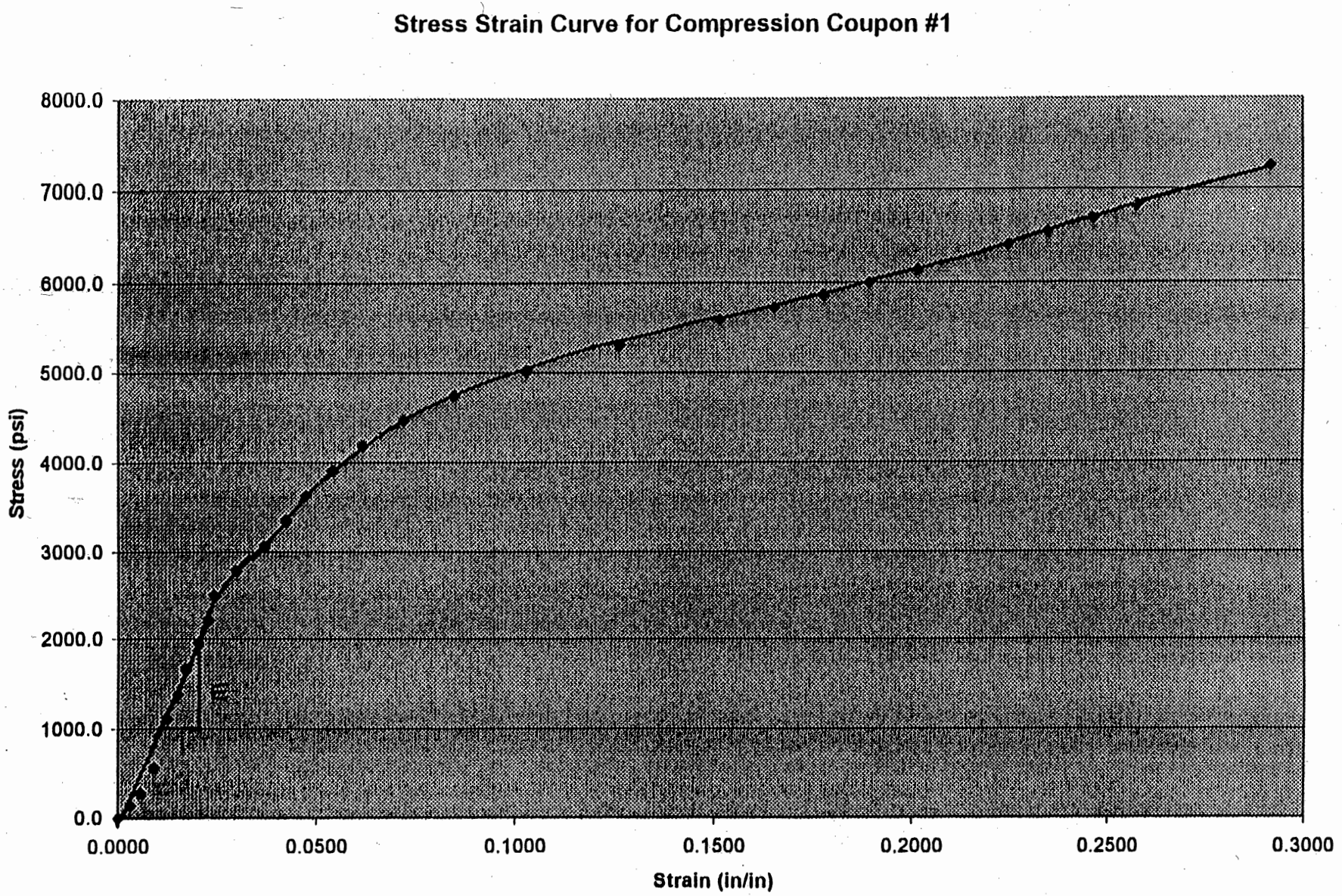
Stress Strain Curve for Compression Coupon #1
8000.0
7000.0
6000.0
5000.0
4000.0
3000.0
2000.0
1000.0
0.0
Stress (psi)
0.0000
0.0500
0.1000
0.1500
0.2000
0.2500
0.3000
Strain (in/in)

Table E.2

Determining of Compressive MOE

Coupon #2			
Width =	1.573 in		
Thickness =	0.457 in		
Area =	0.7189 in2		
Original Length =	0.791 in		
Load (#)	Extension (in)	Stress (psi)	Strain (in/in)
0	0.0000	0.0	0.0000
100	0.0037	139.1	0.0047
200	0.0057	278.2	0.0072
600	0.0107	834.7	0.0135
800	0.0125	1112.9	0.0158
1000	0.0145	1391.1	0.0183
1200	0.0163	1669.3	0.0206
1400	0.0189	1947.5	0.0239
1800	0.0237	2504.0	0.0300
2000	0.0263	2782.2	0.0332
2200	0.0302	3060.4	0.0382
2400	0.0339	3338.6	0.0429
2600	0.0392	3616.8	0.0496
2800	0.0443	3895.1	0.0560
3000	0.0514	4173.3	0.0650
3200	0.0606	4451.5	0.0766
3300	0.0662	4590.6	0.0837
3400	0.0734	4729.7	0.0928
3500	0.0800	4868.8	0.1011
3600	0.0898	5007.9	0.1135
3700	0.0990	5147.0	0.1252
3800	0.1108	5286.1	0.1401
3900	0.1215	5425.2	0.1536
4000	0.1327	5564.4	0.1678
4100	0.1437	5703.5	0.1817
4200	0.1536	5842.6	0.1942
4300	0.1638	5981.7	0.2071
4400	0.1742	6120.8	0.2202
4500	0.1833	6259.9	0.2317
4600	0.1952	6399.0	0.2468
4700	0.2028	6538.1	0.2564
4800	0.2132	6677.2	0.2695
4900	0.2361	6816.3	0.2985
5000	0.2493	6955.4	0.3152

Compressive Modulus of Elasticity was determined to be
62253 psi using stresses from 0 to 1112.9 psi.
with a R^2 = 0.9246

Figure E.2

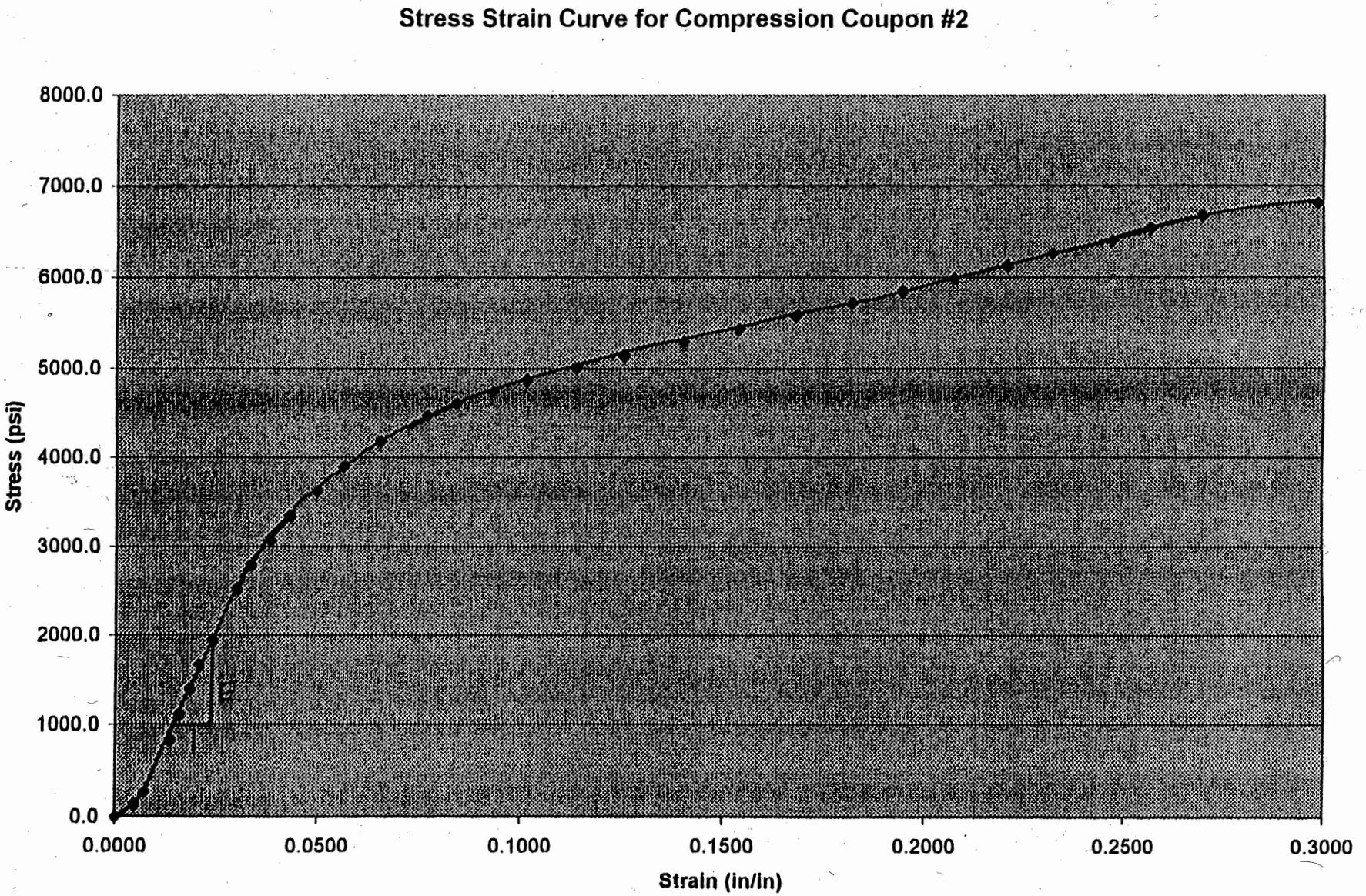
Stress Strain Curve for Compression Coupon #2
8000.0
7000.0
6000.0
5000.0
4000.0
3000.0
2000.0
1000.0
0.0
Stress (psi)
0.0000
0.0500
0.1000
0.1500
0.2000
0.2500
0.3000
Strain (in/in)

Table E.3

Determining of Compressive MOE

Coupon #3			
Width =	1.574 in		
Thickness =	0.456 in		
Area =	0.7177 in2		
Original Length =	0.787 in		
Load (#)	Extension (in)	Stress (psi)	Strain (in/in)
0	0.0000	0.0	0.0000
200	0.0045	278.7	0.0057
400	0.0072	557.3	0.0091
600	0.0093	836.0	0.0118
800	0.0125	1114.6	0.0159
1000	0.0142	1393.3	0.0180
1200	0.0165	1671.9	0.0210
1400	0.0189	1950.6	0.0240
1600	0.0217	2229.2	0.0276
1800	0.0247	2507.9	0.0314
2000	0.0278	2786.5	0.0353
2200	0.0319	3065.2	0.0405
2400	0.0363	3343.8	0.0461
2600	0.0417	3622.5	0.0530
2800	0.0483	3901.1	0.0614
3000	0.0563	4179.8	0.0715
3200	0.0673	4458.4	0.0855
3300	0.0739	4597.7	0.0939
3400	0.0813	4737.1	0.1033
3500	0.0902	4876.4	0.1146
3600	0.0998	5015.7	0.1268
3700	0.1093	5155.0	0.1389
3900	0.1287	5433.7	0.1635
4000	0.1387	5573.0	0.1762
4100	0.1483	5712.3	0.1884
4200	0.1574	5851.7	0.2000
4300	0.1667	5991.0	0.2118
4400	0.1753	6130.3	0.2227
4500	0.1837	6269.6	0.2334
4600	0.1924	6409.0	0.2445
4700	0.2013	6548.3	0.2558
4800	0.2100	6687.6	0.2668
4900	0.2183	6826.9	0.2774
5000	0.2269	6966.3	0.2883
5100	0.2357	7105.6	0.2995
5200	0.2448	7244.9	0.3111

Compressive Modulus of Elasticity was determined to be
67427 psi using stresses from 0 to 1114.6 psi.
with a R^2 = 0.9763

Figure E.3

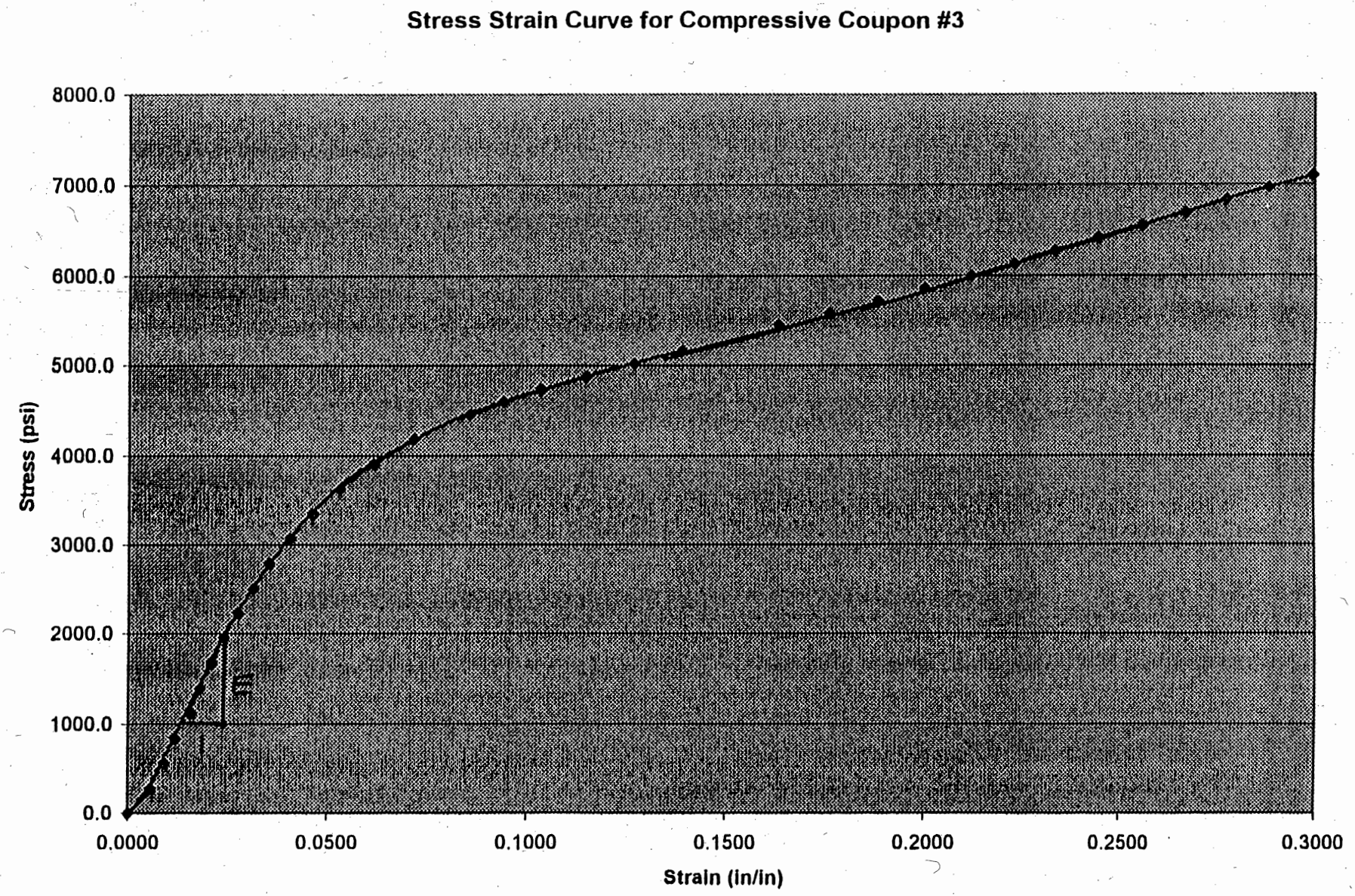
Stress Strain Curve for Compressive Coupon #3
8000.0
7000.0
6000.0
5000.0
4000.0
3000.0
2000.0
1000.0
0.0
Stress (psi)
0.0000
0.0500
0.1000
0.1500
0.2000
0.2500
0.3000
Strain (in/in)

Figure E.4 Original and Tested Compression Coupons

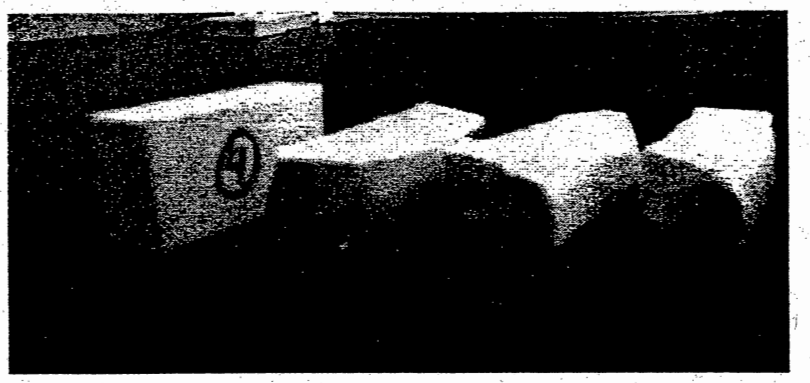

APPENDIX F

OBSERVATIONS

Figure F.1 Screws Protruding from Sides of Beam

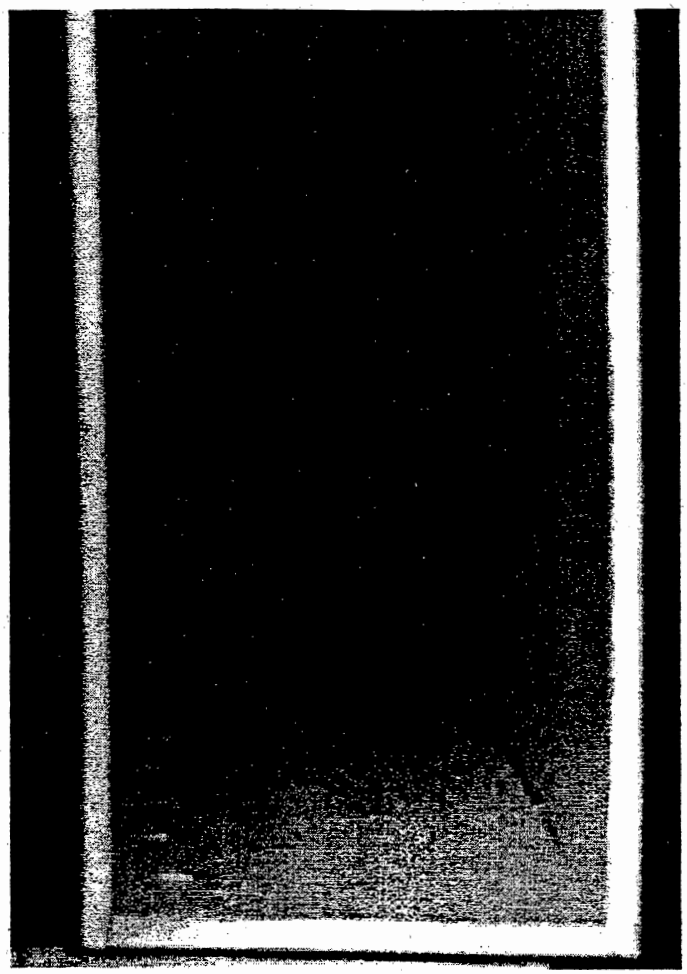

Figure F.2

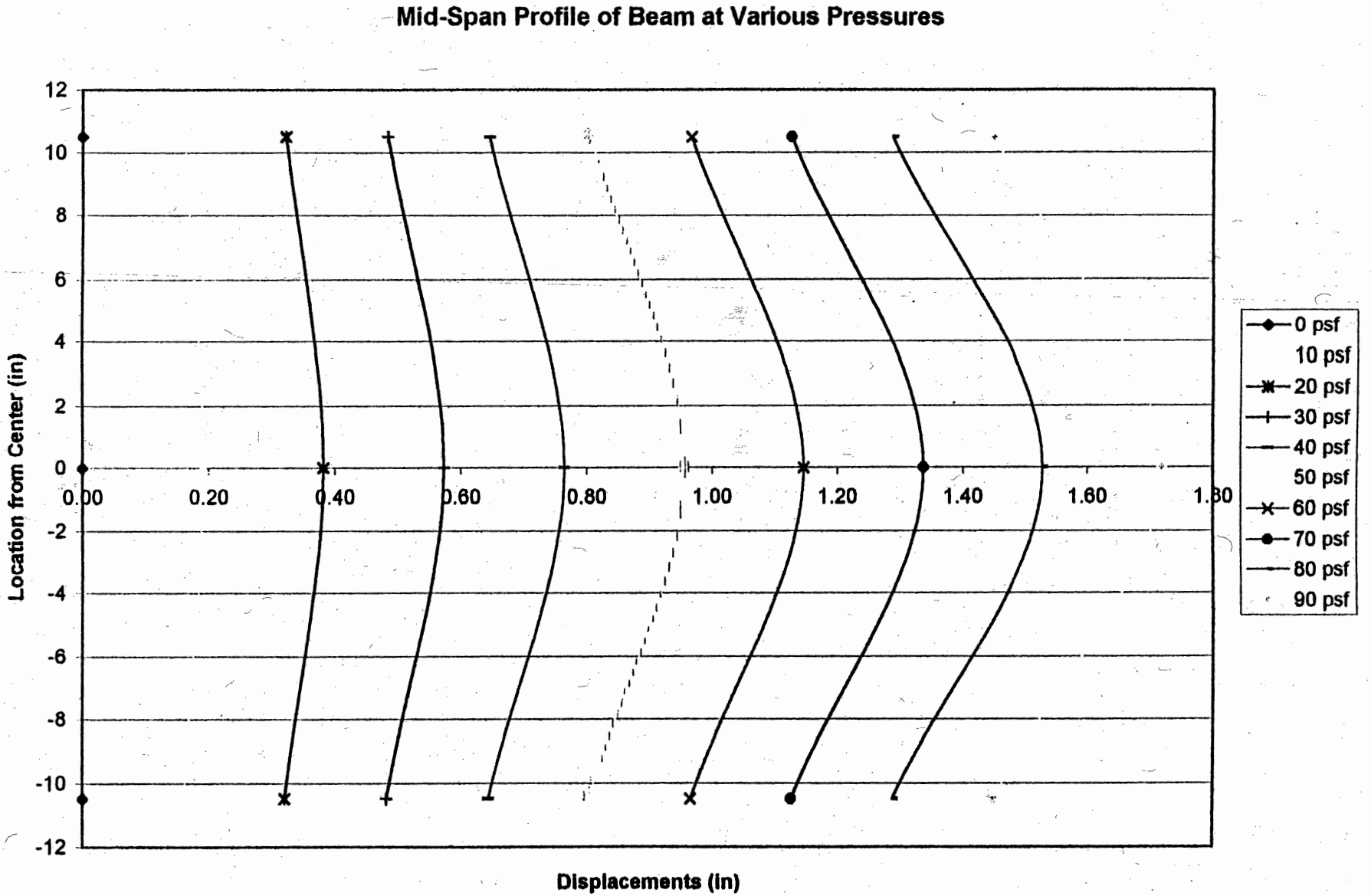
Mid-Span Profile of Beam at Various Pressures
Location from Center (in)
12
10
8
6
4
2
0
-2
-4
-6
-8
-10
-12
0.00
0.20
0.40
0.60
0.80
1.00
1.20
1.40
1.60
1.80
Displacements (in)
0 psf
10 psf
20 psf
30 psf
40 psf
50 psf
60 psf
70 psf
80 psf
90 psf

APPENDIX G

DEFLECTION COMPARISONS

Figure G.1 Deflected Shape of Beam During Test

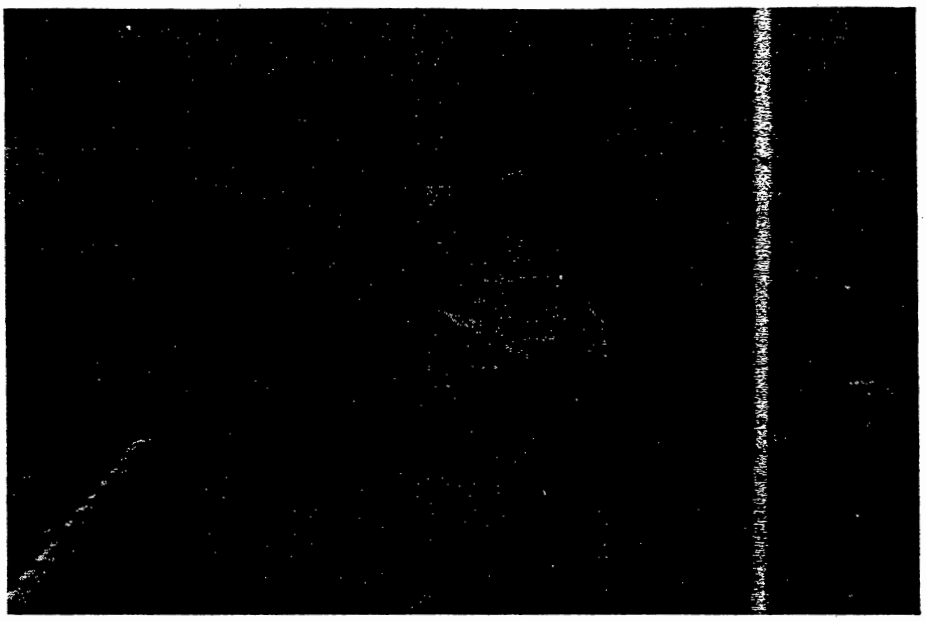

Table G.1 Mid-Span Deflections For All Sub-Tests of Both Beams A and B

			Deflection (in)	
Beam	Sub-Test #	Pressure (psf)	Top Center	Middle Center
A	1	5.2	-0.09	-0.10
		10.4	-0.15	-0.19
		7.28	-0.13	-0.13
		10.4	-0.16	-0.19
		15.6	-0.23	-0.29
		20.8	-0.31	-0.39
		22.88	-0.34	-0.43
		31.2	-0.45	-0.55
		35.36	-0.52	-0.63
		37.44	-0.56	-0.68
		38.48	-0.59	-0.71
		45.76	-0.71	-0.83
		46.8	-0.75	-0.88
	2	52	-0.92	-1.02
		56.16	-0.97	-1.07
		57.2	-1.00	-1.11
		59.28	-1.03	-1.14
		67.6	-1.17	-1.29
		72.8	-1.27	-1.39
	3	78	-1.12	-1.25
		83.2	-1.46	-1.58
B	1	3.12	-0.06	-0.11
		6.2	-0.12	-0.15
		6.2	-0.14	-0.17
		12.5	-0.20	-0.23
		15.6	-0.29	-0.33
		16.6	-0.31	-0.36
		21.8	-0.37	-0.43
		26.0	-0.44	-0.51
		29.1	-0.50	-0.59
		32.2	-0.55	-0.64
		35.4	-0.61	-0.71
		36.4	-0.63	-0.75
		41.6	-0.80	-0.96
		46.8	-0.87	-1.04
	2	52.0	-0.74	-0.95
		59.3	-0.89	-1.14
		62.4	-0.95	-1.22
		67.6	-1.04	-1.34
		70.7	-1.11	-1.43
		81.1	-1.20	-1.54
		86.3	-1.38	-1.78
		93.6	-1.51	-1.96

Figure G.1

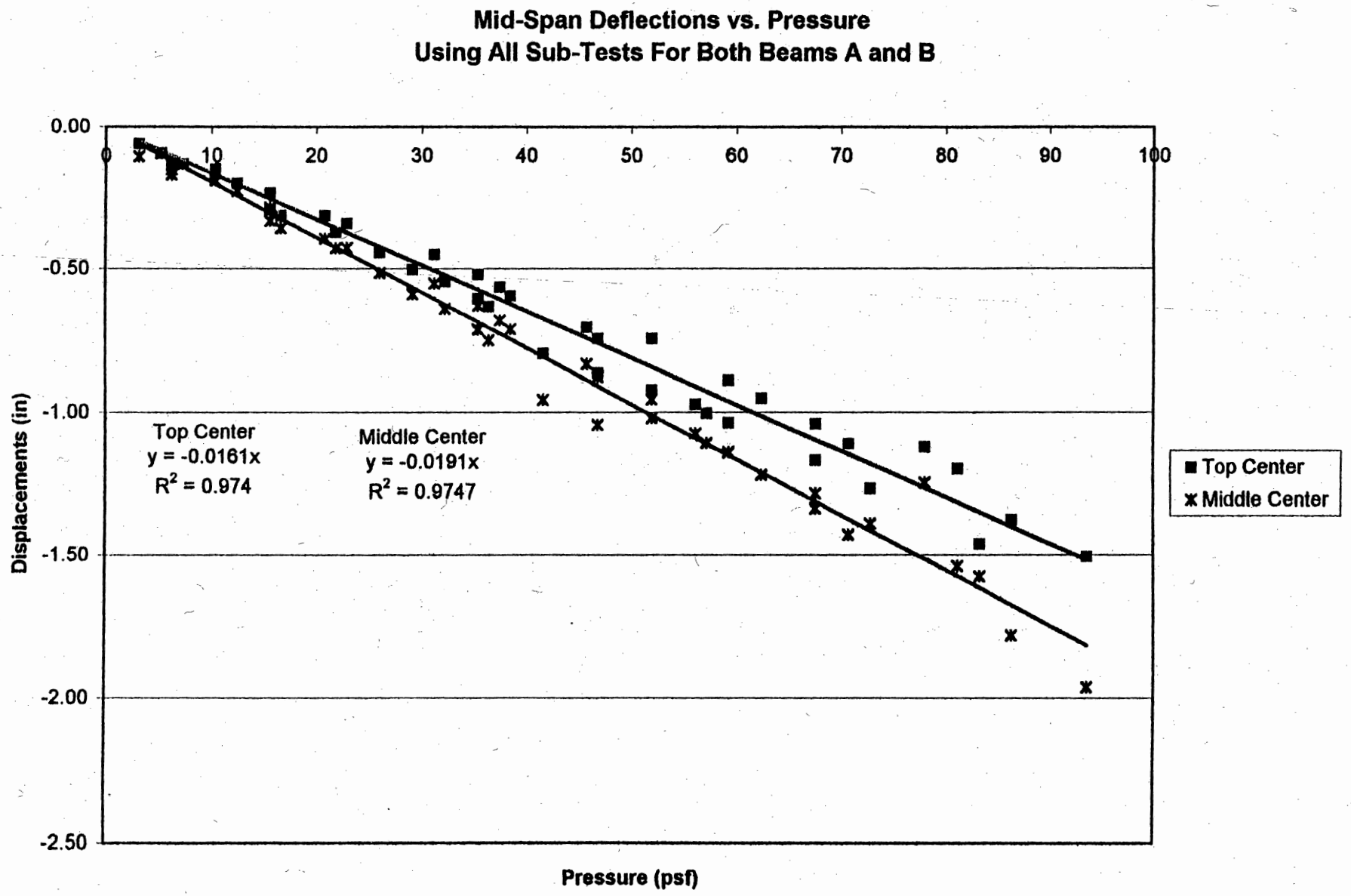
Mid-Span Deflections vs. Pressure
Using All Sub-Tests For Both Beams A and B
0.00
-0.50
-1.00
-1.50
-2.00
-2.50
0
10
20
30
40
50
60
70
80
90
100
Displacements (in)
Pressure (psf)
Top Center
y = -0.0161x
R2 = 0.974
Middle Center
y = -0.0191x
R2 = 0.9747
Top Center
Middle Center

Table G.2 Mid-Span Deflection Comparison Using Beam Theory and Section 2.4

Slopes* Using Table 2.3 of Section 2.4	
Top Center	Middle Center
0.0161	0.0191

			% Difference	
MOE Used	Value (psi)	Slope* [1]	Top Center	Middle Center
Tensile	2.15E+05	0.01184	36.0	61.3
Compressive	6.55E+04	0.03886	58.6	50.8
Average	140250	0.01815	11.3	5.2

* - Denotes the slope found in the formula: y = -mx
where: y = deflection in inches
x = pressure in psf
m = slope in inches/psf

[1] - see attached calculation

APPENDIX H

SAMPLE CALCULATIONS

THIS CALCULATION SHOWS THE ERROR ASSOCIATED USING THE OFFSET MIDDLE CENTER LVDT LOCATION AS THE ACTUAL MIDDLE CENTER.

i) SIMPLY SUPPORTED BEAM

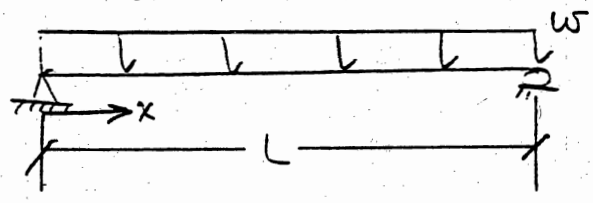

$L = 144"$ OR 12ft

Δ_{MAX} OCCURS @ THE ACTUAL CENTER $(x = 72")$

$$\Delta_{MAX} = \frac{5wL^4}{384EI}$$ [APPENDIX C - Mechanics of Materials 2ND EDITION, Hibler]

$$= 5598720 \frac{w}{EI}$$

ii) DEFLECTION @ OFFSET LVDT LOCATION

$x = 69.75$ in [FROM TABLE 2.2, SECTION 2.2]

$$\Delta_x = \frac{-wx}{24EI}(x^3 - 2Lx^2 - L^3)$$

$$= 5592160 \frac{w}{EI}$$

iii) % DIFFERENCE

$$\%\ \text{DIFF} = \%\ \text{ERROR} = \frac{\Delta_{MAX} - \Delta_x}{\Delta_{MAX}} \times 100\% = 0.117\%$$

THIS LOW % ERROR SUPPORTS THE USE OF THE OFFSET LVDT LOCATION AS THE TRUE MIDDLE CENTER LOCATION.

THIS CALCULATION SHOWS THE STRESSES INDUCED @ THE EXTREME FIBERS OF THE BEAM FROM THE PRESSURES APPLIED DURING THE TESTS

i)

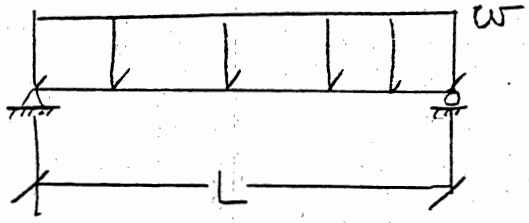

SINCE A PRESSURE WAS APPLIED, 'W' BY A TRIBUTARY WIDTH OF 2ft REDUCED THE APPLIED PRESSURE TO A DISTRIBUTED LOAD.

$$M_{MAX} = \frac{wL^2}{8} = \frac{[2 \times p]L^2}{8}$$

$$= 36p \quad \text{WHERE} \begin{cases} p = \text{PRESSURE in } [\#/ft^2] \\ M = \text{MOMENT in } [\#\text{-}ft] \end{cases}$$

ii) COMPUTING X-SECTION PROPERTIES

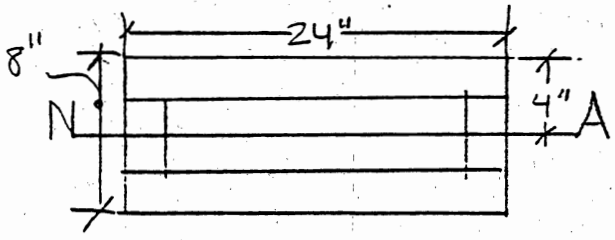

All pieces are ½" THICK

$$I_{NA} = 2\left[\left\{\frac{1}{12}(.5)[8-2(1/2)]^3\right\} + \left\{\frac{1}{12}(24)(\tfrac{1}{2})^3 + [24(1/2)]\left(4-\tfrac{.5}{2}\right)^2\right\}\right]$$

$$= 366.58\ in^4$$

iii) STRESS DISTRIBUTION

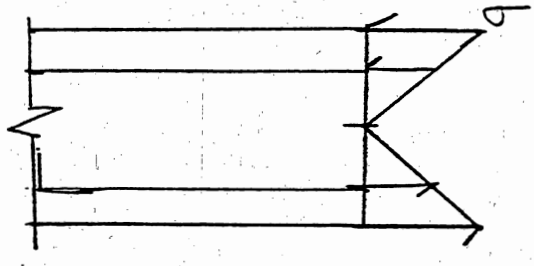

$$\sigma_{MAX} = \frac{Mc}{I}$$

$$= \frac{[(36p)(12in/ft)](8\tfrac{1}{2})}{366.58\ in^4}$$

$$= \frac{1728p}{366.58}$$

iv) WORKING RANGE OF PRESSURES

THE HIGHEST PRESSURE ACHIEVED IN THE TESTS WAS 93.6 psf

$$\sigma_{MAX} = \frac{1728\,(93.6)}{366.58} = 441.22 \text{ psi}$$

THEREFORE TAKE PROPORTIONAL LIMITS TO BE GREATER THAN THIS MAXIMUM STRESS.

i) SIMPLY SUPPORTED BEAM

$$\Delta_{MAX} = \frac{5wL^4}{384EI} = \frac{10pL^4}{384EI} \times \frac{1}{12in\,A}$$

$$= \frac{10pL^4}{4608EI}$$

WHERE p = PRESSURE in [#/ft²]

L = 144 in

I = 366.58 in⁴

E = MODULUS OF ELASTICITY. in [psi]

a.) USING E = TENSILE MODULUS OF ELASTICITY,

$$\Delta_{MAX} = \frac{2545.47}{(21SE3)}p = 0.01184\,p$$

b.) USING E = COMPRESSIVE MODULUS OF ELASTICITY,

$$\Delta_{MAX} = \frac{2545.47\,p}{65.5E3} = 0.03886\,p$$

c.) USING E = AVERAGE OF CMOE & TMOE,

$$E = \frac{21SE3 + 60.5E3}{2} = 140.25\,ksi$$

$$\Delta_{MAX} = \frac{2545.47\,p}{140.25E3} = 0.01815\,p$$

ii) EQUATIONS FROM TEST

TOP CENTER $\Delta = 0.0161\,p$

MIDDLE CENTER $\Delta = 0.0191\,p$

This calculation shows how Table 4.2, in section 9.6 of the report, was created. Three arbitrary heights & fastest mile wind speeds were chosen of ≤15', 20' & 30' and 70, 90, & 110mph, respectively. All tables & page numbers listed in the calcs. can be found in ASCE 7-93 Minimum Design Loads for Bldgs & Other Structures.

i) Velocity Pressure (q_z)

$$q_z = 0.00256\, K_z (IV)^2 \rightarrow (\text{Eqn. 3})\ \text{Sec. } 6.5.1, \text{ p. } 11$$

- Design using components & cladding as per Sec. 6.2
- Exposure category C -
- Classification category IV - Table 1, p. 2

$I = 0.95 \rightarrow$ Table 5, p. 11

$K_z = \left\{ \begin{array}{ll} 0.80 & \text{- for } h \le 15' \\ 0.87 & \text{- " } h = 20' \\ 0.98 & \text{- " } h = 30' \end{array} \right\} \rightarrow$ Table 6, p. 12

ii) Design Pressure (p)

$$p = q_z \cdot G_z \cdot C_f \rightarrow \text{Table 9, p 10}$$

$C_f = 1.2 \rightarrow$ Table 13, p. 22

w/ $M/N = 12'/2' = 6.0$

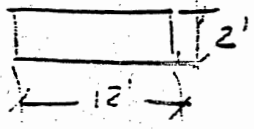

$G_z = \left\{ \begin{array}{ll} 1.32 & \text{- for } h \le 15 \\ 1.29 & h = 20' \\ 1.26 & h = 30' \end{array} \right\} \rightarrow$ Table 8, p. 15

NJIT
New Jersey Institute of Technology

PHASE-II REPORT

Recycled Plastics for Highway Appurtenances

by
M. Ala Saadeghvaziri, and
Keith M. MacBain

Research Project Supported by
NEW JERSEY DEPARTMENT OF TRANSPORTATION (NJDOT)
and
FEDERAL HIGHWAY ADMINISTRATION (FHWA)

NEW JERSEY INSTITUTE OF TECHNOLOGY
DEPARTMENT OF CIVIL AND ENVIRONMENTAL ENGINEERING
UNIVERSITY HEIGHTS
NEWARK, NJ 07102-1982
JULY 1997

OBJECTIVE

The main objectives of this study are to develop more economical traffic noise barriers and safer road barrier systems that use innovative designs and new materials such as recycled plastics.

This report presents the results of the second phase of this study. Included is a review of the key points found in Phase I of the study. Member tests and comparison of the results with the model developed in Phase I and the results of creep testing are also included. Highway applications are further developed with a prototype panel proposed in Phase I and a computer simulated crash analysis of a guardrail using steel posts is compared to that of recycled plastic posts.

RECOMMENDATIONS

Based on the research up to this point, the following interim recommendations can be made:

- Effective noise wall panels can be constructed of recycled plastics. Sound tests have shown that prototype panels are as effective as traditional designs. Furthermore, they are much lighter making them suitable for mounting on structures such as bridges.
- It is possible to predict member behavior of sections other than 4x4 (i.e., 6x6 and 6x8) for low to moderate loads using the proposed material model and the methods developed in Phase I.
- The effects of creep are significant and applications with sustained stress levels greater than 10% of ultimate should be avoided. The self weight of the proposed noise wall causes a stress level much below this limit.
- Freeze / thaw exposure indicates that recycled plastics with wood additives are not good for long term outdoor exposure.

KEY WORDS

Recycled Plastics, Material Properties, Noise Barrier, Guardrail

ACKNOWDLEGEMENT

This research and development study is sponsored by the New Jersey Department of Transportation (NJDOT) and the Federal Highway Administration (FHWA). It is coordinated by NJDOT's office of Quality Assurance, Improvements and Research. The results and conclusions are those of the authors and do not necessarily reflect the views of the sponsors.

BACKGROUND

General

Solid waste is overloading the landfills and is a major contributor to the environmental problems facing this country. Every year the U.S. alone generates 320 billion lb (145 billion kg.) of municipal solid waste. Of this waste, plastics comprise 18 percent by volume and 7 percent by weight [1]. Furthermore, plastics and paper are the fastest growing segments of solid wastes [2].

Recycling is an environmentally acceptable means of reducing solid waste and conserving resources. Reprocessing industrial plastic waste (e.g., in-house scrap) has been a common practice for as long as the plastic industry has existed. There have recently been significant developments in the recycling technology of commingled plastic waste but the key issue to be resolved is securing long-term, high-value markets for recycled polymers.

This research investigates some of the products of the recycled plastic industry to evaluate their mechanical and structural properties and to assess conformity of these properties among manufacturers. The use of recycled plastics in development of economical and environmentally acceptable highway appurtenances, such as noise and traffic barriers, is also discussed.

Mixed, or commingled, plastics once destined for the waste stream are now being recycled [3]. Collected plastic scrap is granulated, then melted and processed in an extruder. The molten plastic is then forced into a mold cavity of the shape and size of the final product. The product can be cut and shaped with the same tools and fastening devices used for wood. These molded products are resistant to attack from gas, oil, salt, sunlight, chemicals and insects and will withstand human and mechanical abuse [4]. Test results have shown mixed plastics hold nails approximately 40 percent better than wood [5]. Fiberglass and treated wood fiber, both classified as hazardous waste materials, have been successfully used to improve the mechanical properties [6] of recycled plastics.

Currently, molded shapes are used to make park benches, guardrail block outs, fences, road markers, landscape timbers and a wide variety of other non-structural applications. Although it has been highly anticipated that molded shapes "will replace wood, concrete and steel" [7], structural applications of the product are practically non-existent. This is mainly due to lack of knowledge about the mechanical and structural properties of the material, especially their relation to long term performance. Lack of testing standards and design specifications compound the problem.

Previous work [8] has revealed that the modulus of elasticity varies greatly among manufacturers. Creep effects [9] are thought to be significant and it has been noted [10] that sample size and temperature affect material properties. It has also been shown [11] that these recycled plastics are virtually non-toxic which is in sharp contrast to chemically pressure treated lumber

Phase I

The Phase I investigation included material, member, and freeze / thaw tests. A noise wall design was proposed and a material model was developed and validated. The material model was also used in a computer program to predict member behavior and compared to actual member tests. The reader is referred to the Phase I report for a more detailed discussion [12].

There is currently no industry standard for the manufacture of RP products so there is variation among the manufacturers in composition as well as the methods of acquiring materials. To represent the range of compositions available, three manufacturers referred to as A, B & C were selected for testing. Manufacturer A mixes fiberglass with the RP, B uses only RP, and C uses 50% wood fiber in addition to the RP. Material tests were performed to asses the material properties and the effects of the apparent non-homogeneity. Visually consistent sections were cut from the members and termed 'core' or 'shell' coupons based on their origin. Standard tension coupons were 1 cm x 4 cm x 20 cm nominal and compression coupons were 1 cm x 4 cm x 2 cm. The following information was revealed by the Phase I tests.

- Typical members have a visually inconsistent cross section.
- The core and shell coupons were not only visually different but also were noted to have different dry densities and greatly different material properties.
- There is a significant difference between the tension and compression material behavior as shown in Table 1.
- The material is nonlinear.
- There can be variation in material properties based on the size of the section. This is thought to be caused by the rate of cooling as larger shapes cool at a different rate.
- Freeze / thaw exposure adversely affects the material properties of products containing wood fibers but does not appear to have a significant affect on those composed entirely of RP.
- Member behavior can be predicted with reasonable accuracy for low to moderate loads using the proposed material model and considering the contributions of core and shell.

Table 1 Material Properties

	Manufacturer and type	E_t (ksi)	E_c (ksi)	max tension stress (psi)	compression stress at inflection point (psi)
A	Shell	625	125	1800	3250
	Core	NA	NA	NA	NA
B	Shell	270	100	2200	5100
	(4x4) Core	51	35	580	1000
	(6x6, 6x8) Core	150	72	750	1300
C	Shell	320	90	1000	2000
	Core	260	65	750	1900

Note: E_t represents Modulus in tension, E_c represents Modulus in compression

MATERIAL / MEMBER TESTS

Testing of 6x6 and 6x8 members in bending and 4x4 sections in axial compression was performed. The computer program developed in Phase I was used to generate theoretical load deflection data which was compared to the actual tests. The program assumes that there is a distinct division between core and shell and that the section is perfectly rectangular (i.e., roundness of the corners is ignored).

Flexure

Three point bending tests were conducted on 60" long 6x6 and 6x8 sections in accordance with ASTM D 198. One 6x6 and one 6x8 were tested from each manufacturer. Figure 1 shows typical 6x8 members in flexure.

Results

The load deformation results show non-linear behavior similar to the material and member tests of Phase I. Although all three products had good ductility for structural purposes, they all failed suddenly as reflected by the lack of a descending portion in the load-deformation curves in Figures 2 through 4. As with the 4x4 tests, the greater ductility of Manufacturer B can be attributed to the lack of reinforcement in the product.

Analytical vs. Test Results

The bending test results compared with the theoretical curve in Figures 2 through 4 show that the analytical results agree with the experimental results within 15% for loads less than 80% of

the ultimate load for all sections tested. It is suspected that stress concentrations caused by the presence of impurities discussed in Phase I effect theory to deviate from test results, particularly at larger loads. The theoretical curve is derived from the coupon tests, but the member is more able to transfer the stress concentrations to adjacent areas than the coupon due to its larger cross-sectional area (i.e., redistribution of stress).

The material properties reported by the coupon tests may not be entirely representative of the member behavior. The coupon strain was recorded over a 2" gage length and the net effect of specific, localized stress concentrations occurring in this length cannot be determined because there are several parameters that affect how stress concentrations will change the apparent material behavior. Among these are the ratio of coupon size to impurity size, the ratio of coupon size to member size, the density (frequency) of the impurity distribution and the type of strain gage and gage length. It is not the intent of this research to investigate these effects but rather to develop and investigate a method for the analysis of composite RP sections.

At larger loads when the material is yielding, the variation between coupon and member behavior will be greater because for greater loads, the coupon can rely less on the impurity bonds. This suggests that for the theoretical member, strength will be affected more than initial stiffness. The fact that the tension strain in the member at failure was greater (typically by 20%) than the maximum coupon strain supports this conclusion. Similarly, the theoretical maximum bending moment (based on maximum coupon tension strain) was less than the maximum moment experienced during testing. Because of this, the program employs a user-defined parameter, the curve fit limit (CFL) to extend the theoretical curves for the purpose of comparison with the tests. The CFL is the maximum coupon tension strain observed before failure and when the program requires the stress at a strain larger than the CFL, it uses the stress at the CFL. In other words, the theoretical curves are extrapolated by assuming pure plastic deformation to take place after the actual observed failure.

Although all of the theoretical curves predict nonlinear behavior, it can be seen that they all anticipate a more linear response than observed in the tests. It can also be seen that all but one predict a higher ultimate load than observed which is likely due to an artificial strength caused by the plastic CFL assumption noted earlier.

While it is possible to model the bending of RP sections based on the material behavior satisfactorily for low loads, this method seems to deviate more for higher loads. Because this method is based on simpler, less expensive coupon tests and does not necessitate separate tests of the entire member for each specific cross section considered, it is anticipated that it will prove useful for RP analysis. Additionally, Manufacturer B has reported to now be collecting

and sorting the scrap more carefully so the notion of stress concentrations caused by impurities may soon be irrelevant.

Compression

Axial compression tests were performed on whole 4x4 sections with an initial height of 4.5". Four samples were used for each manufacturer and testing proceeded following ASTM D 198, Static Compression of Timbers in Structural Sizes.

Results

The axial compression results showed that all manufacturers exhibited similar behavior. Near the ultimate load for the section, the stiffness dropped considerably and the shell began to buckle away from the core marking visual failure as seen in Figure 5. The ultimate compressive strength of the member, thus, is affected by not only the height of the section, but also the bond strength between core and shell materials, particularly for short columns. After visual failure, all samples sustained large plastic deformations suggesting that these materials might be well suited for one - time, large energy absorbing mechanisms such as crash cushions.

Analytical vs Test

Figures 6 through 8 show the theoretical curves plotted with the axial member compression test results. The curves can be seen to closely follow the behavior of the member before buckling of the shell occurs for all three manufacturers. The test obviously deviates from theory at this point because the possibility of shell buckling is not considered in the computer program. Note that Figure 5 suggests that Manufacturer A exhibits a local buckling failure of the shell while Manufacturer C seems to have a more general buckling failure. The agreement between the test and theory before visual failure occurs indicates that it is possible to predict axial member behavior with reasonable accuracy in this range but the model gives no prediction of when the shell buckling might occur.

A simple approximation of the shell buckling load was obtained by considering one side of the shell to be a simple column supporting a percentage of the total load based on total cross sectional area and initial E value as shown in Figure 9. The Euler buckling load was computed and the values for each manufacturer are indicated in Figures 6 through 8 which seems to give a rough indication as to when one might expect this buckling to occur. The values are not as conservative as expected, however, considering the assumptions made which suggests that the mode of failure is more of a localized buckling than a general buckling. It must be emphasized that Euler's approximation as applied here is not only approximate but very subjective and sensitive to one's interpretation of core and shell material. It is presented here

only for reference and is not viewed as a good method to predict the ultimate load for RP axial members. A more complex analysis is required if the true behavior is to be considered in detail.

Creep

Standard compression coupons were subjected to a constant dead load that produces a stress level of 10 psi. This is a typical dead load stress level at the base of a 20 ft high wall created with RP. The temperature was held constant at 95° F throughout. Figure 10 shows that after 7 months, the creep strain for all manufacturers was less than 0.15% and that no creep strain has been measured in the last 4 months for Manufacturer A. If this strain were (conservatively) considered constant throughout the height, it equates to a creep deflection of only 0.3 inch for a 20 ft high wall. Although this is acceptable for a noise wall, Table 2 shows it is extremely large when compared to the initial strain obtained from the test data. Creep deflection comprises the larger portion of the total deflection by far, even for low stress levels. Noting that 10 psi is at least 15 times less than the ultimate compressive stress found in the material tests for all manufacturers, it is apparent that creep deflection can be very significant and is discussed further in section Future Work.

Table 2 Summary of Creep Strain

Manufacturer	Initial strain (%)	Creep strain after 7 months (%)	Increase from initial strain
A	0.008	0.13	1625 %
B	0.01	0.13	1300 %
C	0.01	0.13	1300 %

NOISE WALL

Previous Work

There has been much interest in the possibility of using RP for noise walls since it is considered an environmentally sound alternative to present materials and has a low life-cycle cost [13] when compared to traditional designs. The New York Department of Transportation (NYDOT) has proposed a design that uses RP sheathing with wood or metal framework [13]. This design uses stringers oriented horizontally between the posts to support the sheathing. The Federal Highway Administration (FHWA) has reported installed RP noise walls [14]. The Oregon Department of Transportation has installed and monitored a noise wall comprised of RP from different manufacturers. Carsonite, a manufacturer that uses shredded tire pieces inside a RP shell was used as well as Trimax and Trex. The Nevada Department of

Transportation used the Carsonite product and has not reported any problems with the material. FHWA has also reported erecting test sections of noise barriers to evaluate constructability and weatherability of noise barriers using RP. One material noted to have more crumb rubber than the others began to buckle under its own weight. The other panels were not found to be damaged by the environmental loadings.

Proposed Design

As seen in Table 1, the stiffness of RP is generally low; much smaller than concrete or even wood. If current design approaches were to be used, it would be difficult to utilize RP as an economical noise barrier. An advantage of RP, however, is that it can easily be manufactured into various shapes and the cross section does not have to be solid. With this in mind, a new noise barrier design, as shown in Figure 11, is proposed. Spacing of the webs was determined through finite element (FE) analysis of a typical cell assuming the material to be linear. The proposed design uses shell thickness of 0.5" with an overall depth of 8". A 30 psf (typical AASHTO 80 to 90 mph wind load) applied to a 15' long panel resulted in a maximum deflection of 2.2" and the stresses were below 210 psi. The stress distribution from FE analysis is shown in Figure 12, which illustrates that the shear lag in the panel is not excessive. The panel length was increased to 20' resulting in a maximum deflection of 6.2" and the stresses were still below 360 psi so the linear assumption is still valid. Figure 13 shows the stress distribution in the longer panel. The shell thickness and overall depth of the cross section can also be increased to allow even greater panel length, thus, making more economical designs by further reducing the number of posts.

For typical RP material, the total density (i.e., considering both layers) of the proposed design satisfies the recommendation of 20 kg/m^2 [15] for sound attenuation. It is expected that multi-layering will significantly enhance the sound effectiveness of the wall since layering is the only way to overcome the mass requirement [15]. Prototype panels were assembled from ½" thick RP sheets by fastening them together with screws. A drawing of the prototype is shown in Figure 14 while Figure 15 shows three actual 8' long panels stacked in the proposed manner. The prototype panels were tested for sound absorption (ASTM C423-90a and E795-83) and transmission loss (ASTM E90-90 and E413-87). The full test report is included in the appendix. The noise reduction coefficient (NRC) is an average of the percent energy absorbed by the test specimen at 250, 500, 1000, and 2000 Hz frequencies. The sound transmission class (STC) of a specimen is a single number that gives an indication of the sound transmitted by fitting the test data to an ASTM defined curve. For the prototype panels, the NRC is 0.10 and the STC rating is 37. Table 3 shows these results along with some other commonly used building materials. This shows that these prototype sections are comparable by these standards even though these numbers alone do not give a full understanding of how

well a material will perform acoustically in a given situation. The STC and NRC do not reflect, for example, that the prototype panels were noted to perform better at lower frequencies (100 to 250 Hz) of the test range. Large trucks have been noted [16] to generate a majority of their noise in this frequency range.

Table 3 Acoustical Properties of Different Materials

Material	NRC	STC
Prototype Panel	0.10	37
6" concrete	0.02	54
1 ¾" wood	0.10	34
Carsonite *	0.15	36
Trimax *	0.15	25
Trex *	0.15	25

Note: * indicates materials as reported by FHWA

Ultimately, the proposed design would be extruded as a single unit rather than individual pieces as the prototype, thus, reducing assembly time and allowing for easier installation. Current design guidelines [17] do not specify a minimum STC or NRC for use as a noise wall because it is assumed that the transmission loss of the barrier is large compared to the sound that is diffracted over the barrier. The barrier attenuation is thus considered a function of the site geometry. The FHWA has however, established the Highway Innovative Technology Evaluation Center (HITEC) which evaluates products for which there are no recognized standards or specifications. They have set forth a minimum STC of 23 for noise barriers [18], which the prototype panel does satisfy.

GUARDRAIL POSTS

General

Present technology and design uses road barriers that are made of relatively rigid materials such as steel, concrete or a combination of the two. It is well known, however that flexible but strong designs can absorb more energy, reduce impact deceleration, and minimize the damage sustained by the impacting vehicle and its occupants. Previous research has resulted in designs that incorporate energy absorbing mechanisms (such as the use of rubber energy absorber) and improved the performance of bridge rails [19 - 23]. Due to high initial costs associated with these energy absorbing designs compared to conventional bridge rails, high maintenance costs, and difficulty in attachment to standard bridge decks, these energy-absorbing bridge rails have not gained wide acceptance. The proposed design for road

barriers combines the flexibility of plastics (used as posts) with the stiffness of steel rails. Thus, the final product is expected to be functionally superior to current designs.

Analysis of a typical guardrail system was performed using frame models and a linear approximation of 6x8 RP posts. A steel 6x6 box section was used for the rail at a 27" height. With the typical post spacing of 6', it was not possible to satisfy AASHTO's allowable stress requirements. Only when reducing the post spacing to 2' could the 10 kip lateral load be sustained without exceeding the allowable stress of 0.6 times the yield stress ($0.6f_y$). To meet the more demanding AASHTO bridge rail requirements of performance level one (PL-1) or greater, it would likely be cost prohibitive to use RP in a post and rail design. It should be mentioned, however, that PL-1 through PL-4 anticipate relatively rigid barriers, and can not be directly used for evaluation of the proposed design which is a flexible one.

Further investigation of RP for use as guardrail posts should include specific design guidelines to be used for RP. An equivalent replacement of steel posts is not possible because the modulus of elasticity multiplied by the area second moment of inertia (EI) varies by as much as 70 times for the sections discussed. AASHTO suggests an allowable stress design based on an equivalent static loading. Using an allowable stress method implies that the rail and posts should sustain no damage under mild events but numerous tests of steel post guardrails [24 - 26] have shown damage to posts in the zone of impact evidencing that the stresses were far beyond allowable. To effectively use RP for posts and capture the high energy absorption potential, the design must be based on recognizing the full strength of the posts in the zone of impact.

Crash Analysis

Barrier VII was used to model a vehicle impacting a guardrail. It is a two dimensional, dynamic vehicle/ barrier simulation program that uses a simple vehicle model with omni-directional springs [27] . It incorporates an elastic - purely plastic material model that is well suited for steel but not capable of fully representing a plastic nonlinear material such as RP. Because the program works in two dimensional space, events such as vehicle vaulting are not considered. Additionally, the program does not directly indicate if the barrier deflections are large enough to allow the vehicle to contact the post but this can be interpreted by examining the output file and checking if the vehicle's wheel path crosses a post.

Validation with Actual Crashes

Although Barrier VII has been successfully validated for a wide range of flexible barriers [28], sample runs were performed and then compared to actual crash tests to establish a reference point. PL-1 crash test requirements are commonly used to evaluate barrier performance.

These stipulate that a barrier successfully contain a vehicle for two different events. The first is a 1,800 lb vehicle moving at 50 mph at an angle of 20 degrees and the second is a 5,400 lb vehicle moving at 45 mph and 20 degrees. Two PL-1 small vehicle and two PL-1 large vehicle tests were selected to compare and verify with the Barrier VII output. Posts were assumed to be rigidly fixed at the base. The four tests listed below were all noted to satisfy PL-1 requirements.

Test 1: A 10 gauge thrie-beam guardrail supported by W6x15 steel posts spaced at 6.25' contained an 1,800 lb Honda Civic [25].

Test 2: Two Honda Civics. The vehicles were approximately 1900 lbs and struck a W-beam barrier at 60 mph and 15 degrees. The rail was supported by S3x5.7 steel spaced at 12.5'. Other computer models [29] have also been able to model this event with reasonable accuracy

Test 3: A 5,500 lb pickup truck impacted a W-beam guardrail at 41.6 mph and 20.9 degrees. The rail was supported by steel W6x15 posts spaced at 6.25' [25].

Test 4: A 5,600 lb pickup truck impacted a W-beam guardrail at 44.2 mph and 19.1 degrees. The rail was supported by steel W6x15 posts spaced at 6.25' [24].

Containing the vehicle is not the only PL-1 requirement, but requirements such as integrity of the passenger compartment cannot be verified with Barrier VII. Because of this, only barrier deflection, vehicle accelerations, and exit velocity were considered although these are not the only measure of a barrier's performance. Predicted barrier deflections and exit velocities were found to be similar to the test data but the predicted vehicle accelerations were larger than tests showed. This is thought to be due to the assumption of a rigid post base and to the data acquisition methods of the tests. It is difficult to obtain the absolute maximum of an impact event and typically, actual tests report maximum accelerations as a 0.05 second average. The program operates with a much smaller time interval and gives values at discrete time intervals rather than averages. Table 4 lists a summary of the four crash tests compared with the program output.

Table 4 Crash Test Data and Barrier VII Output

	Actual Crash Data		**Barrier VII Results**	
Test	dynamic deflection (in)	exit velocity (mph)	dynamic deflection (in)	exit velocity (mph)
1	0.5	42.7	3.2	39.0
2	16.0	50.4	17.5	51.5
3	13.0	35.9	13.9	28.0
4	13.8	35.6	14.6	30.2

Comparison Using RP Posts

In a crash test of a guardrail system, the use of RP posts has been reported as inadequate [30] based on a one-to-one deflection comparison with wood posts. Obviously, RP is much more flexible than wood and if deflection is used as the only parameter to determine appropriateness of the design, then it will be very difficult or uneconomical to design a guardrail post using RP.

After changing the post material properties to represent RP, tests 1 and 4 were recreated with Barrier VII to investigate both small and large vehicle response. The properties of typical 6x8 RP members from the member tests were used in the analysis. Results showed that RP posts allow for greater deflection but reduce the associated vehicle impact accelerations. The barrier deflections were about three times as large, a point where vehicle-post snagging is possible. The output showed that several posts had broken however, and assuming that the posts failed at the base, no indication of snagging was found. The vehicles were assumed to pass over the broken post base. The exit velocities reduced slightly but the maximum accelerations were reduced by about one-third. The barrier was able to contain and redirect both vehicles.

By reducing the post spacing to 4', the maximum lateral deflection was roughly two times that of steel posts at 6.25' but the accelerations were reduced by about two. Vehicle snagging was not noted to occur based on the assumption that the post failure occurred at the base. This barrier was also able to contain and redirect both vehicles. Figure 16 shows the deflected shape of the barrier at different time steps for the small vehicle impact while Table 5 summarizes the results for all events.

Table 5 Crash Analysis with Different Posts

	Longitudinal acceleration (g)	**Lateral acceleration (g)**	**Max Deflect. (in)**	**# posts yielded**	**# posts broken**
Small vehicle					
Steel posts @ 6.25'	-21.1	31.4	3.2	1	0
RP posts @ 6.25'	-8.4	10.7	10.5	5	4
RP posts @ 4'	-11.5	13.8	8.7	6	5
Large vehicle					
Steel posts @ 6.25'	-9.6	12.7	14.6	5	0
RP posts @ 6.25'	-4.7	5.4	42.9	16	9
RP posts @ 4'	-4.3	4.2	28.9	12	8

Based on this work, it is clear that RP posts allow for greater barrier deflections but vehicle accelerations can be reduced providing for a safer redirection. Only 6x8 members were considered but it is possible that other combinations of post size and spacing can provide a more optimum design in terms of deflection and accelerations. The key point of this design is the reduction in vehicle accelerations but it is gained at the cost of increased deflection and sacrificing more posts due to one-time usage. It is suggested that to effectively use RP posts for guardrails, the design should contain more posts than traditional guardrails so that they may absorb all of the energy possible and then fail, thus avoiding snagging and vehicle intrusion. This is obviously not suggested for bridge railings or terminals where limiting deflections is of great importance to contain the vehicle and avoid snagging with other objects. It must be mentioned that computer analysis such as Barrier VII is only a design tool and cannot replace full-scale crash tests. Crash tests should be of designs based on this methodology rather than a direct replacement of wood or steel as the latter has already been deemed unacceptable.

CONCLUSIONS

Experimental and analytical investigation of RP indicates that it is a viable material that could have structural applications. Material tests revealed that RP is a nonlinear material and the presence of additives such as glass and wood fibers can increase stiffness and reduce ductility. Creep deflection of RP can be very large and freeze / thaw exposure adversely affects materials with wood fibers. It is possible to predict the behavior of RP members with reasonable accuracy for low to moderate load levels based on the material properties. RP is suitable for noise walls but to be efficiently used for guardrail posts, a design methodology based around capturing the large energy absorption capabilities of RP should be considered.

Problems that need to be addressed to ensure the use of RP among structural engineers include quality control, development of standards for testing, design specifications, and long term performance evaluation. Over the last two years, manufacturers have also taken major steps in improving quality and initiating efforts to develop design standards that can be used by structural engineers. Of course, proper dissemination of this work and research as well as developments made at various universities is essential to advancing the state of knowledge.

FUTURE WORK

To further investigate the appropriateness of the RP for highway appurtenances and advance the general state of knowledge about RP, the following tests and analytical studies should be pursued:

- Wind test of full scale panels of the proposed model should be conducted. The wind tests should focus on whether the design loads obtained from current standards are a reasonable predictor of the actual wind loads, and if the flow of wind over the top of the wall causes vortex shedding that might excite the wall and cause it to vibrate.
- Crash worthiness analyses using realistic analytical models by incorporating the proposed material model into an existing program such as BARRIER VII.
- A more detailed study of the creep behavior which includes longer test duration, different stress levels and different temperatures. It has been seen that creep deflection can be far greater than initial deflection and should be investigated more thoroughly.
- The material model should be verified more exhaustively by comparing the theoretical results with more test results including different materials and cross sections.
- Impact tests and verification with analytical procedures.

It is the objective of the final phase of this study to address the first two items.

REFERENCES

1. "Furthering The Possibilities," Plastics World, April, 1990.
2. "Solid Waste Concerns Spur Plastic Recycling Efforts," Chemical & Engr. News, Jan., 1989.
3. Maczko, J., "An Alternative to Landfills for Mixed Plastic Waste," Plastics Engineering, April, 1990.
4. "Recycling Mixed Plastics: New Markets," The Council for Solid Waste Solutions, The Plastic Recycling Foundation, Washington, D.C., 1992.
5. Bennett, R. A., "Market Research on Plastics Recycling," Technical Report No. 31, The Center for Plastic Recycling Research, Rutgers-The State Univ. of New Jersey, 1989.
6. Applebaum, M. D. et. al., "The Properties and Morphology of Fiber Reinforced Refined Post-Consumer Plastics Compounded on a Non-intermeshing Twin Screw Extruder," The Society of Plastics Engineering, The 1991 ANTEC Conf., Montreal, 1991.
7. Pearson, W., "Plastics Recycling: The Business," Plastics Recycling Foundation, PA, July, 1989.
8. Coomarasamy, A. and Boyd, S. J., "Development of Specifications for Plastic Lumber for use in Highway Applications - Part II," May 1995.
9. Butler, S., Cao, L., and Beatty, C. L., "Engineering Properties of Recycled Plastic Lumber Materials," Polymer Material Science Engineering, 1992.
10. McDevitt, C. F. and Dutta, P. K., "New Materials for Roadside Safety Hardware," 1992.
11. Nosker, T. J., Weiss, J. S., Weiss, P., and Greenberg, A., "Toxicity of Construction Materials in the Marine Environment: A Comparison of Chromated-Copper-Arsenate-Treated Wood and Recycled Plastic," Arch. Environ. Contam. Toxicol., 1992.
12. Saadeghvaziri, M. A., and MacBain, K., "Recycled Plastics for Highway Appurtenances," Phase I Report, NJIT, August, 1996
13. Hag-Elsafi, O., Elwell, D. J., Glath, G. A., and Hiris, M., "Noise Barriers Using Recycled Plastic Lumber," 1997.
14. Evaluation of Recycled Materials for roadside Safety Devices, U.S. Department of Transportation, No FHWA-RD-97-XXX, March 1997.
15. Beranek, L. L., Noise and Vibration Control Engineering, John Wiley & Sons Inc., New York, 1992.
16. "Fundamentals and Abatement of Highway Traffic Noise," U. S. Department of Transportation, FHWA, National Highway Institute, Report No. FHWA-HHI-HEV-73-7976-1, June, 1973.
17. "Noise Barrier Design Handbook," FHWA Report No. FHWA-RD-76-58.
18. Guidelines for Evaluating the Performance of Highway Sound Barriers, Highway Innovative Technology Evaluation Center

19. Hirsch, T. J., and C. E. Buth, "Testing and Evaluation of Bridge Rail Concept," Final Report, Project RF 3053, Texas Transportation Institute, Texas A&M University System, College Station, May, 1975.
20. Kimball C. E., et. al., "Development of a Collapsing Ring Bridge Rail System," Report RD-76-39, FHWA, U.S. Department of Transportation, Jan., 1976.
21. Stoughton, R.L., "Vehicle Impact Testing of a See Through, Collapsing Ring, Structural Steel Tube, Bridge Barrier Railing," Office of Transportation Laboratory, California Department of Transportation, Sacramento, June, 1983.
22. Beason, W. L., T. J. Hirsch, and J. C. Cain, "A Low-Maintenance, Energy-Absorbing Bridge Rail," Transportation Research Record No. 1065, 1986.
23. "Roadside Design Guide," AASHTO, Washington, D.C., 1989.
24. Faller, R., Ritter, M., Holloway, J., Pfeifer, B., and Rosson, B., "Performance Level 1 Bridge Railings for Timber Decks," Transportation Research Record No. 1419, Oct., 1993.
25. Alberson, D., Menges, W., and Buth, E., "Performance Level 1 Bridge Railings," Transportation Research Record No. 1500, Jul., 1995.
26. Ross, H., Menges, W., and Bullard, D., "NCHRP Report 350 Compliance Tests of the ET-2000," *Transportation Research Record* No. 1528, Sep., 1996.
27. Powell, G. H., "BARRIER VII: A Computer Program For Evaluation of Automobile Barrier Systems," FHWA Report No. FHWA-RD-73-51, April, 1973.
28. Bligh, R. P., and Sicking, D., "Applications of Barrier VII in Design of Flexible Barriers," *Transportation Research Record* No 1233
29. Hendricks, B. F., and Wekezer, J. W., "Finite Element Modeling of G2 Guardrail," *Transportation Research Record* No 1528
30. Strybos J. W. P.E. "Recycled Plastics for Roadside Safety Devices", 1995.

FIGURES

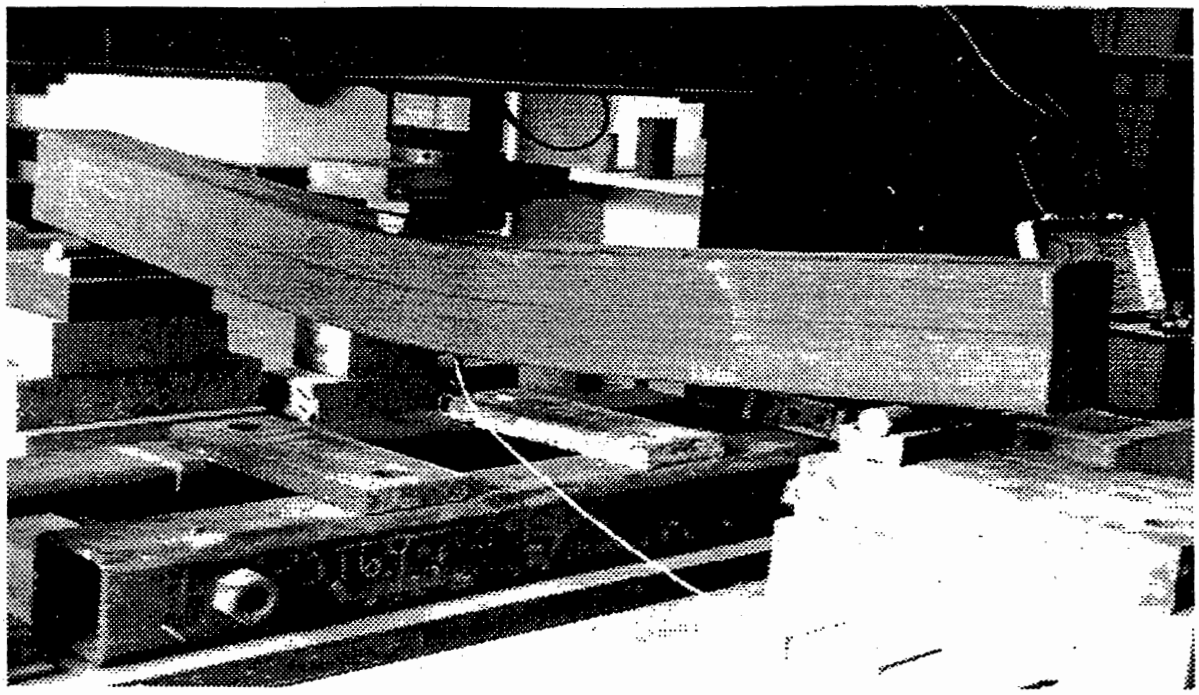

Manufacturer B

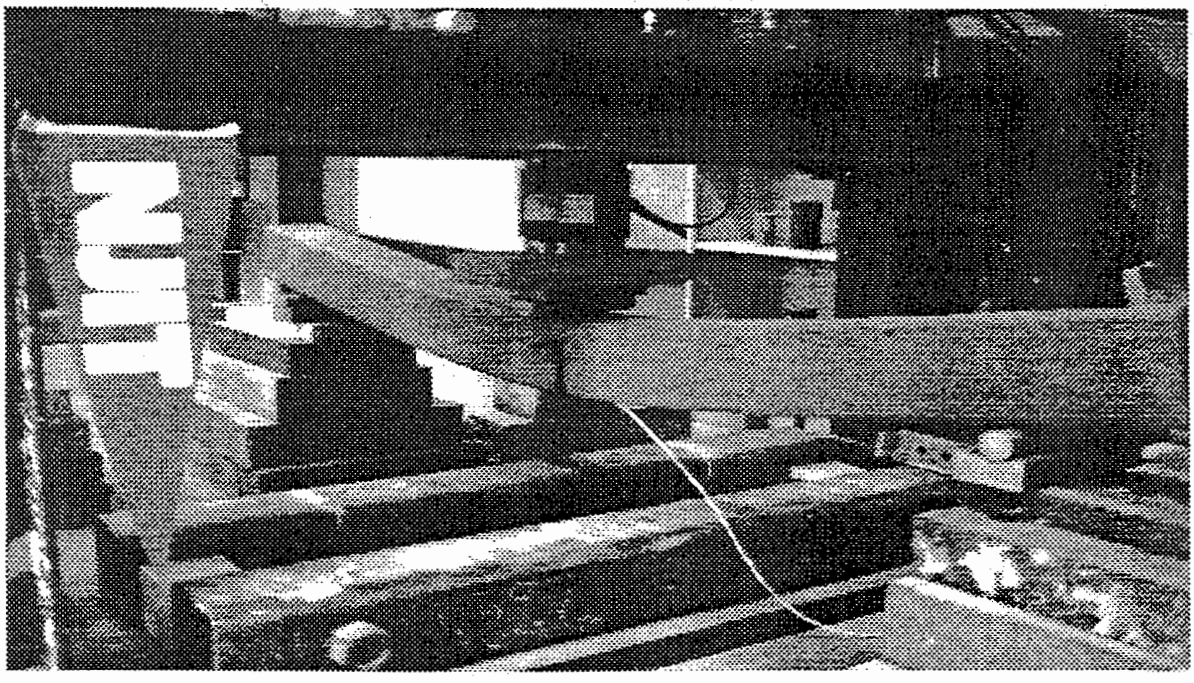

Manufacturer C

Figure 1 Bending Tests

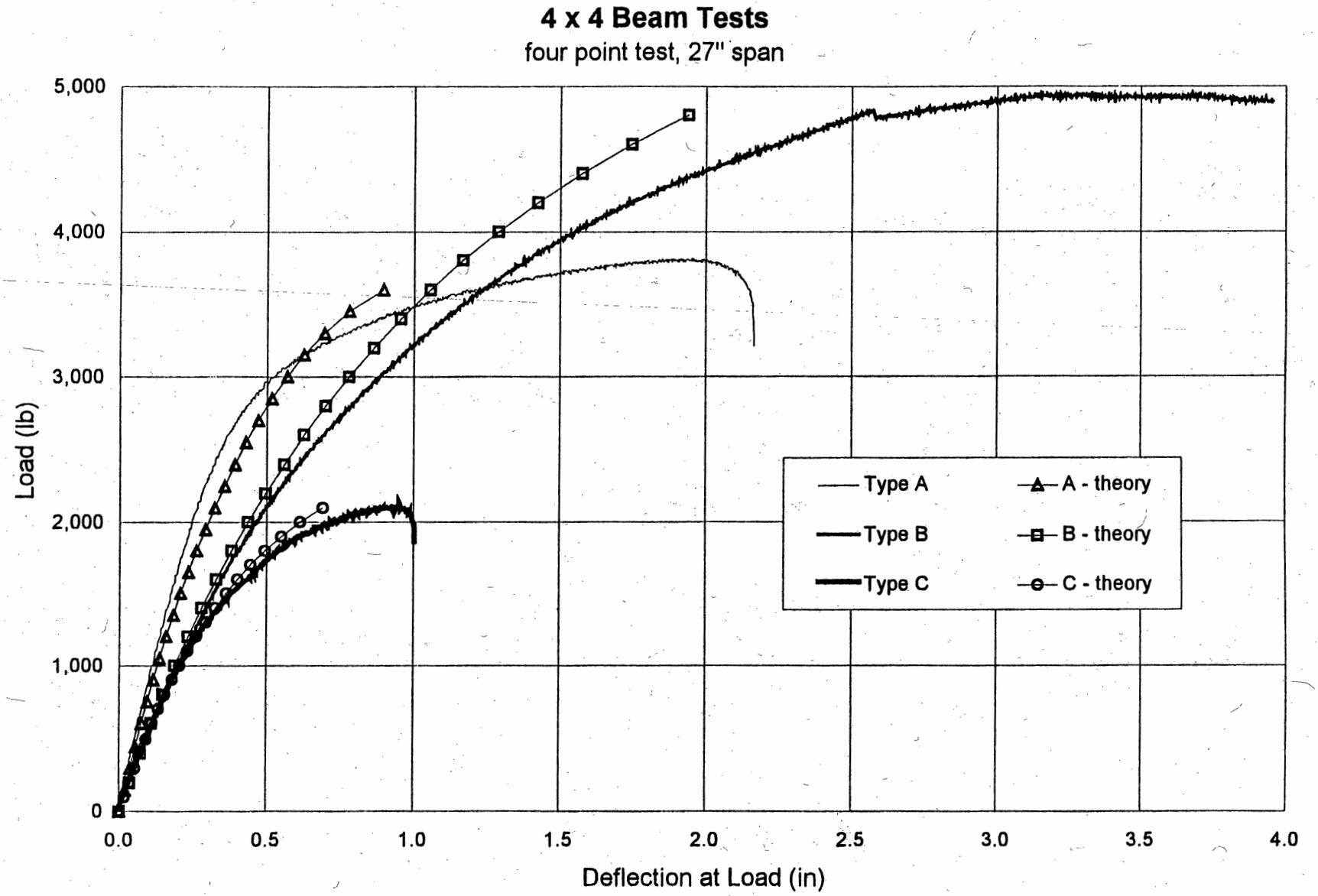
4 x 4 Beam Tests
four point test, 27" span
Load (lb)
5,000
4,000
3,000
2,000
1,000
0
0.0
0.5
1.0
1.5
2.0
2.5
3.0
3.5
4.0
Deflection at Load (in)
Type A
Type B
Type C
A - theory
B - theory
C - theory

Figure 2

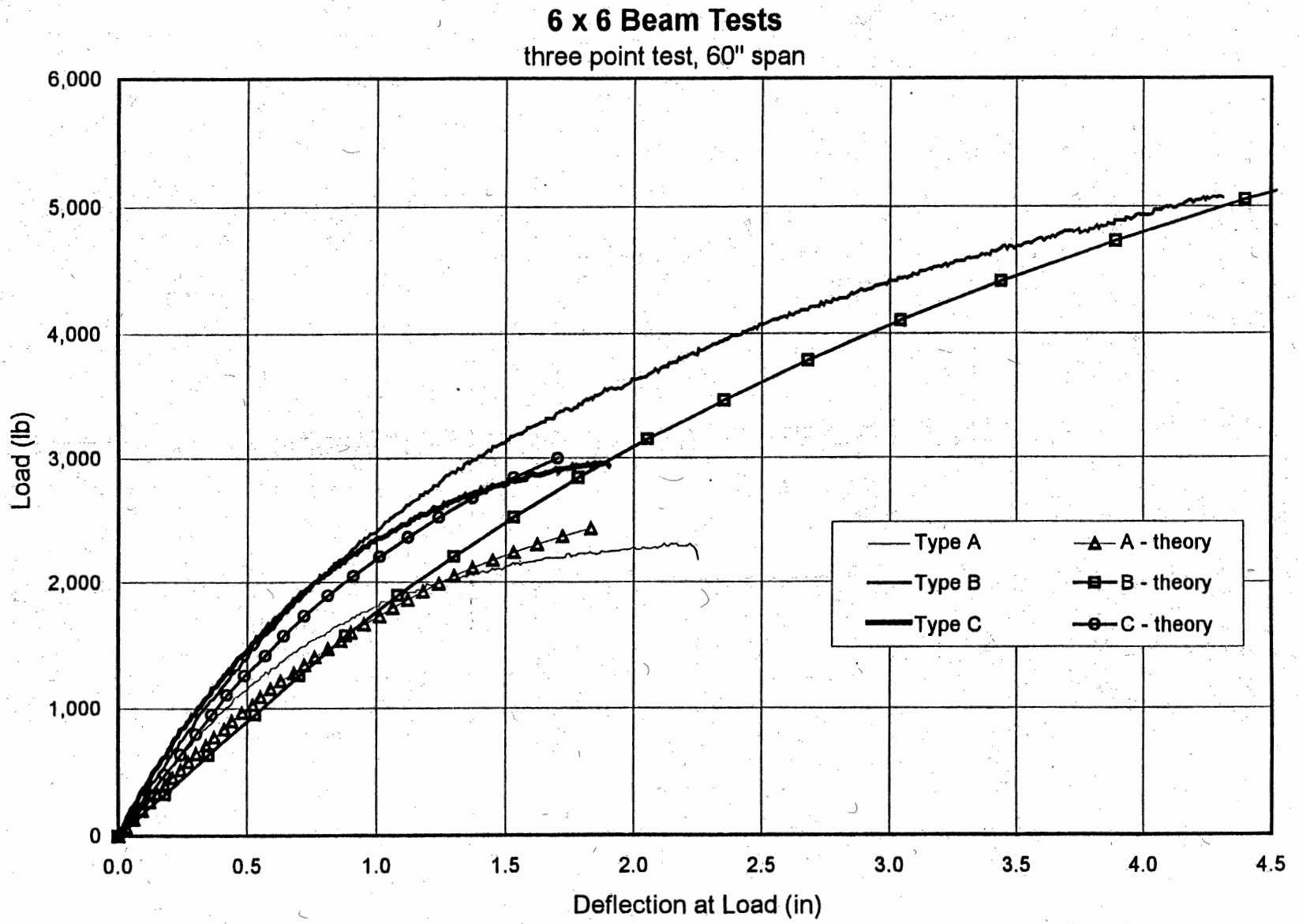
6 x 6 Beam Tests
three point test, 60" span
6,000
5,000
4,000
3,000
2,000
1,000
0
Load (lb)
0.0
0.5
1.0
1.5
2.0
2.5
3.0
3.5
4.0
4.5
Deflection at Load (in)
Type A
Type B
Type C
A - theory
B - theory
C - theory

Figure 3

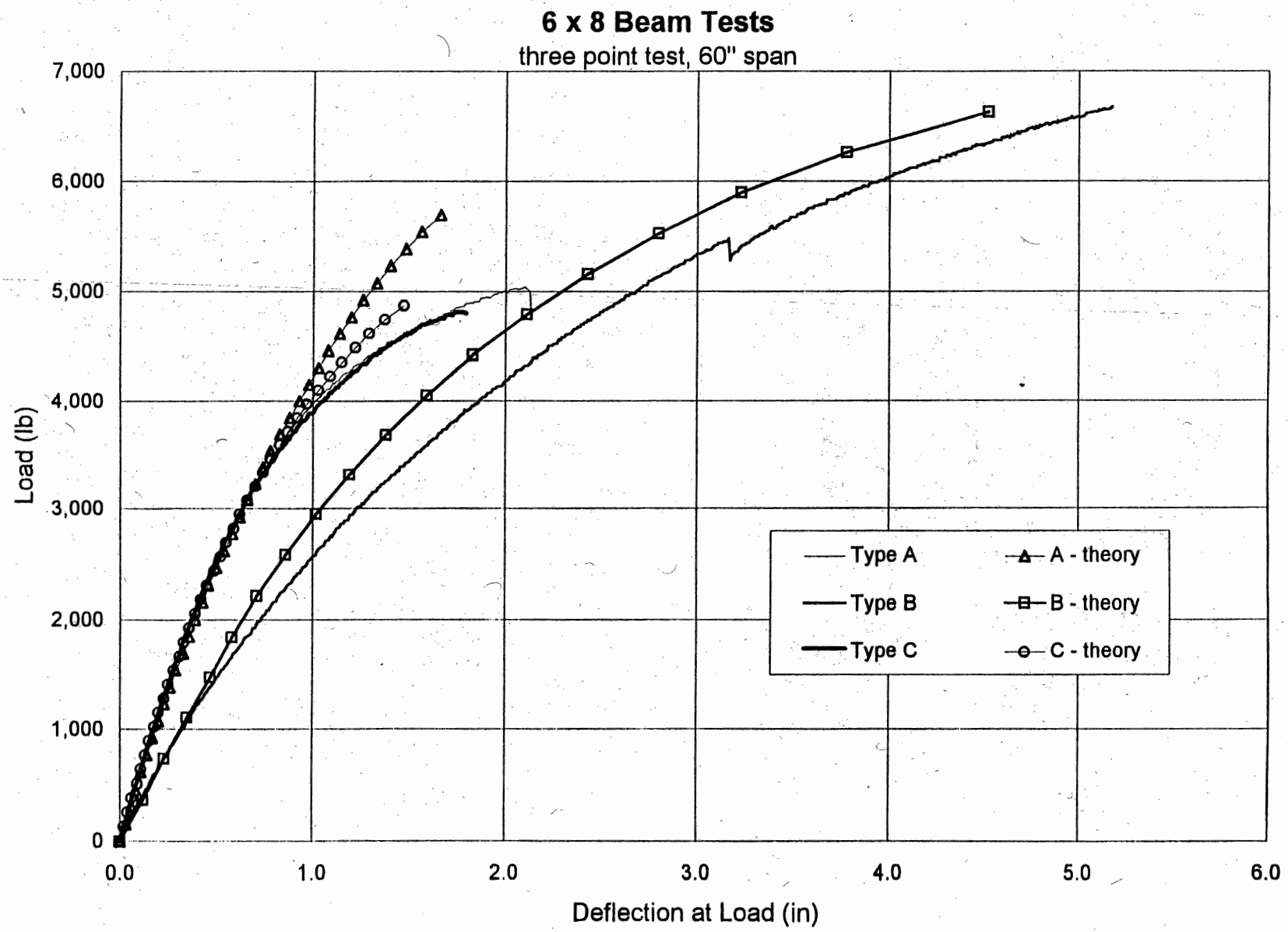
6 x 8 Beam Tests
three point test, 60" span
Load (lb)
7,000
6,000
5,000
4,000
3,000
2,000
1,000
0
0.0
1.0
2.0
3.0
4.0
5.0
6.0
Deflection at Load (in)
Type A
Type B
Type C
A - theory
B - theory
C - theory

Figure 4

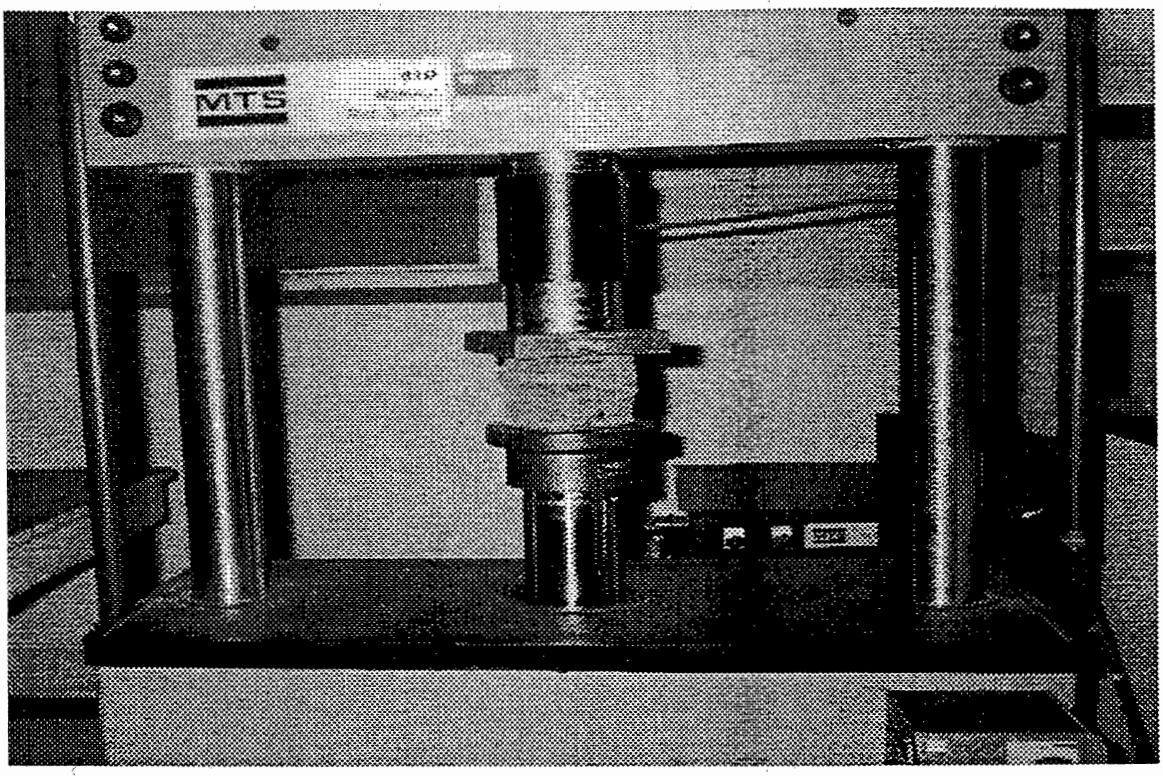

Manufacturer A

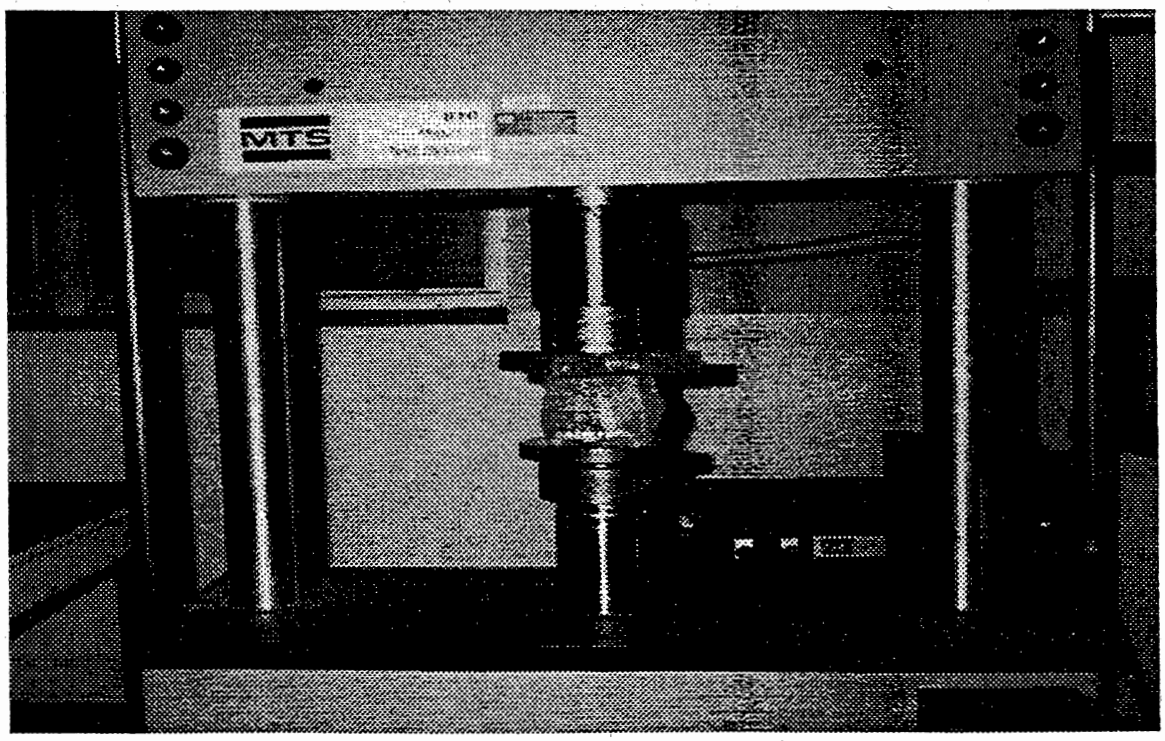

Manufacturer C

Figure 5 Axial Compression

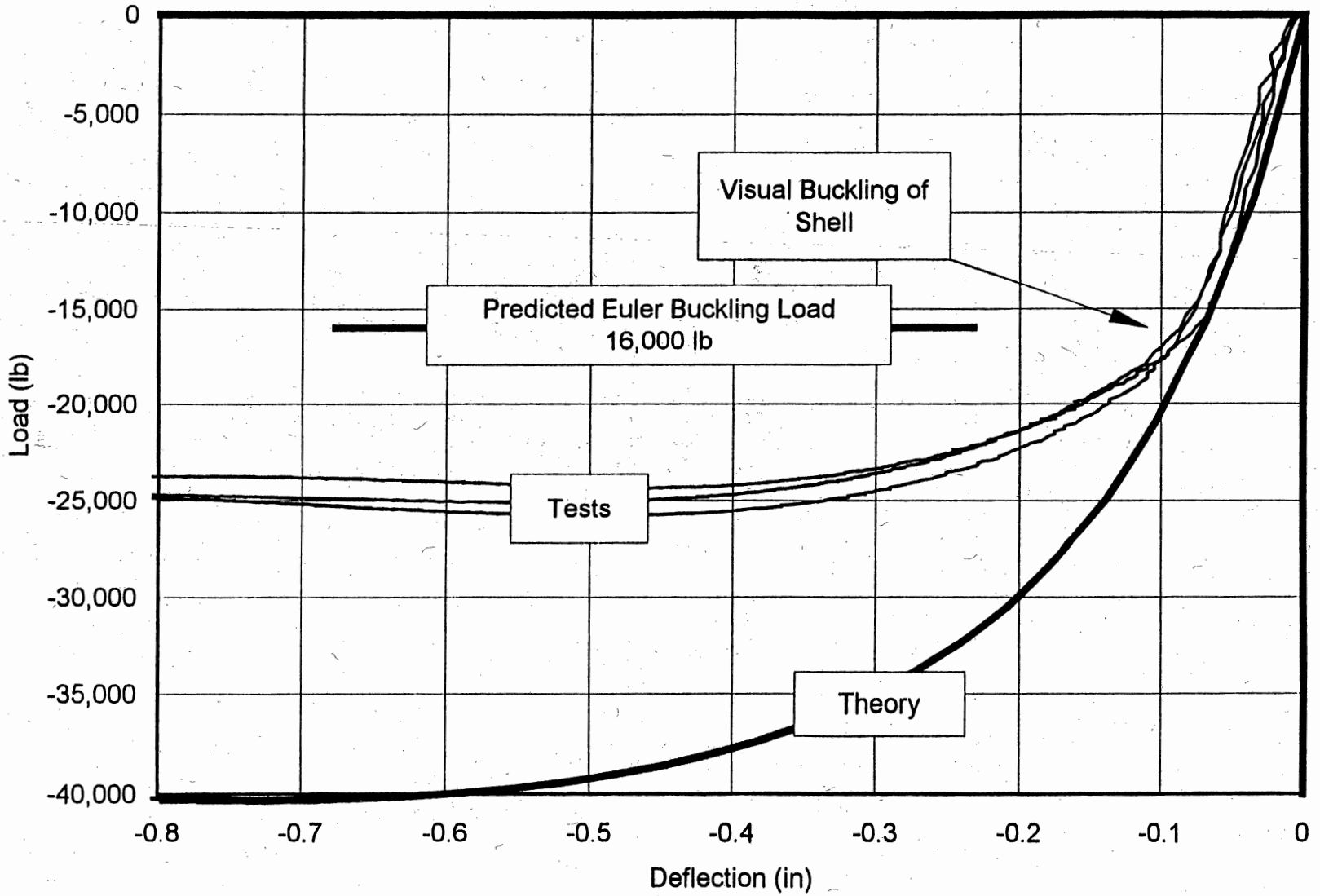

Figure 6 Axial Compression of 4x4, Manufacturer A

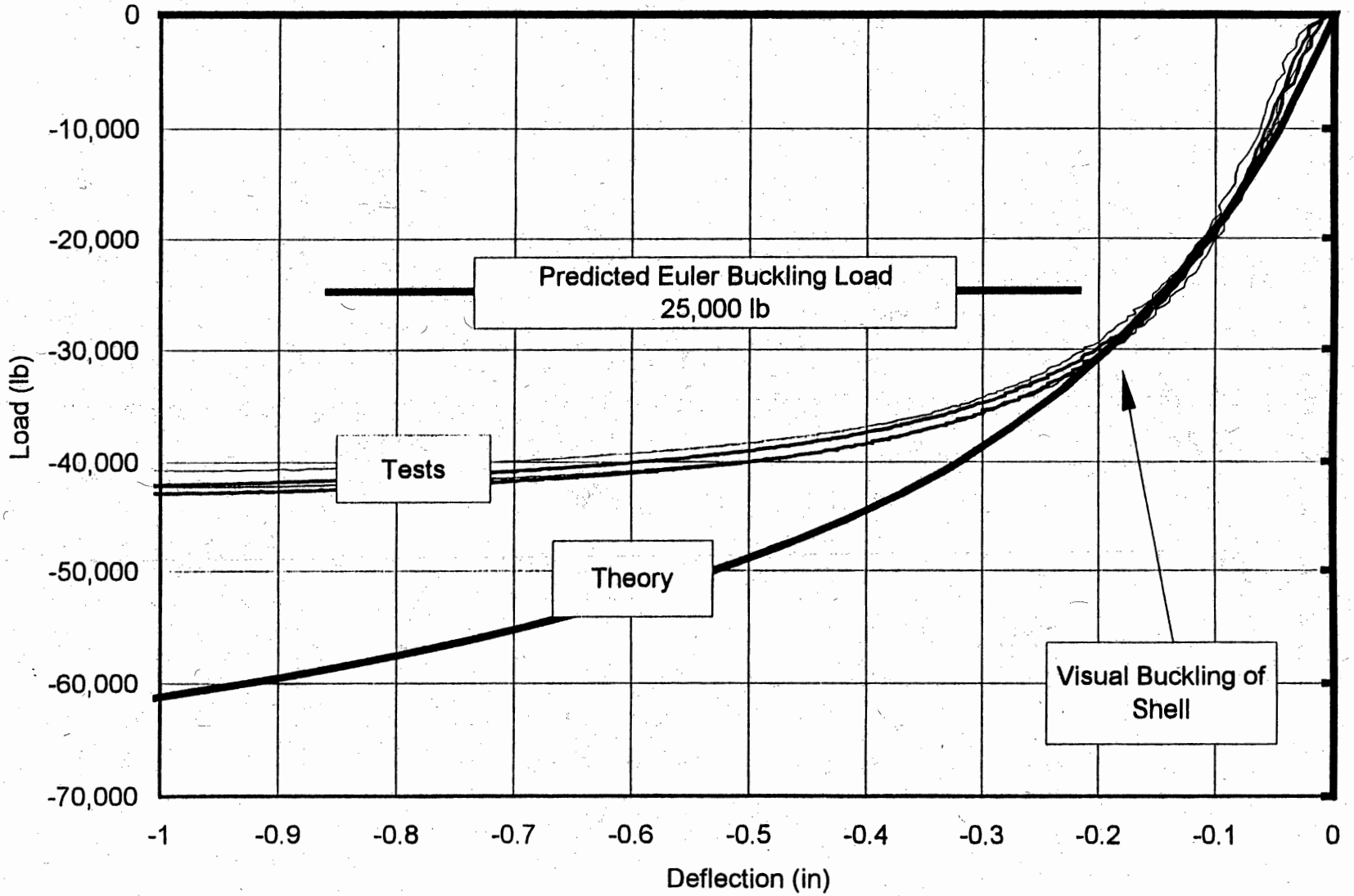

Figure 7 Axial Compression of 4x4, Manufacturer B

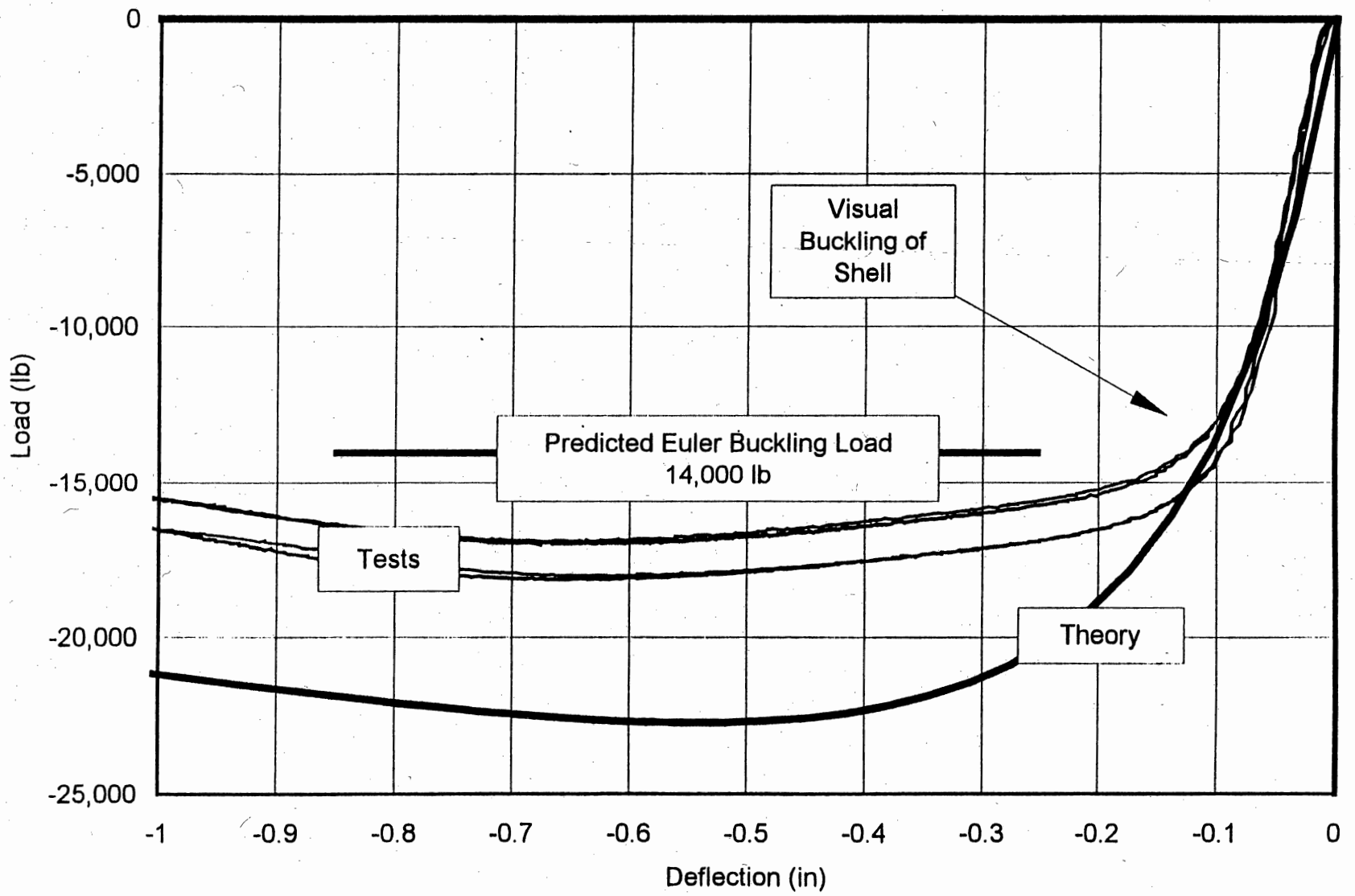

Figure 8 Axial Compression of 4x4, Manufacturer C

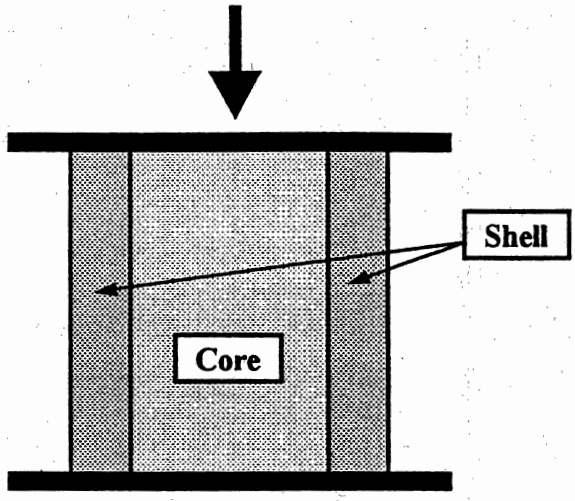

Cross Section of Actual loading

Equivalent Loading Based on Area and Initial Modulus of Elasticity

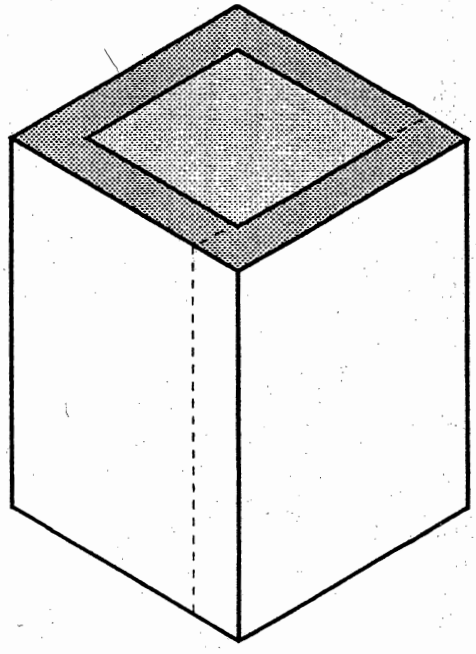

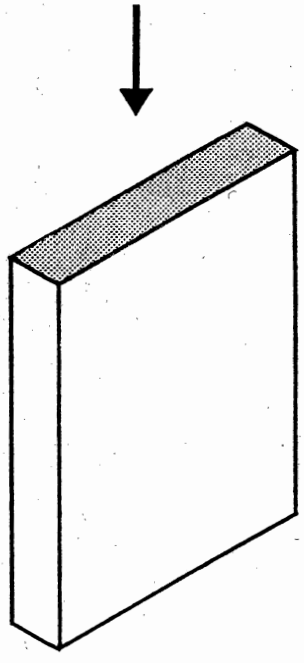

Assumed Section for Theoretical Analysis of Shell Buckling

Figure 9 Shell Buckling Analysis Approximations

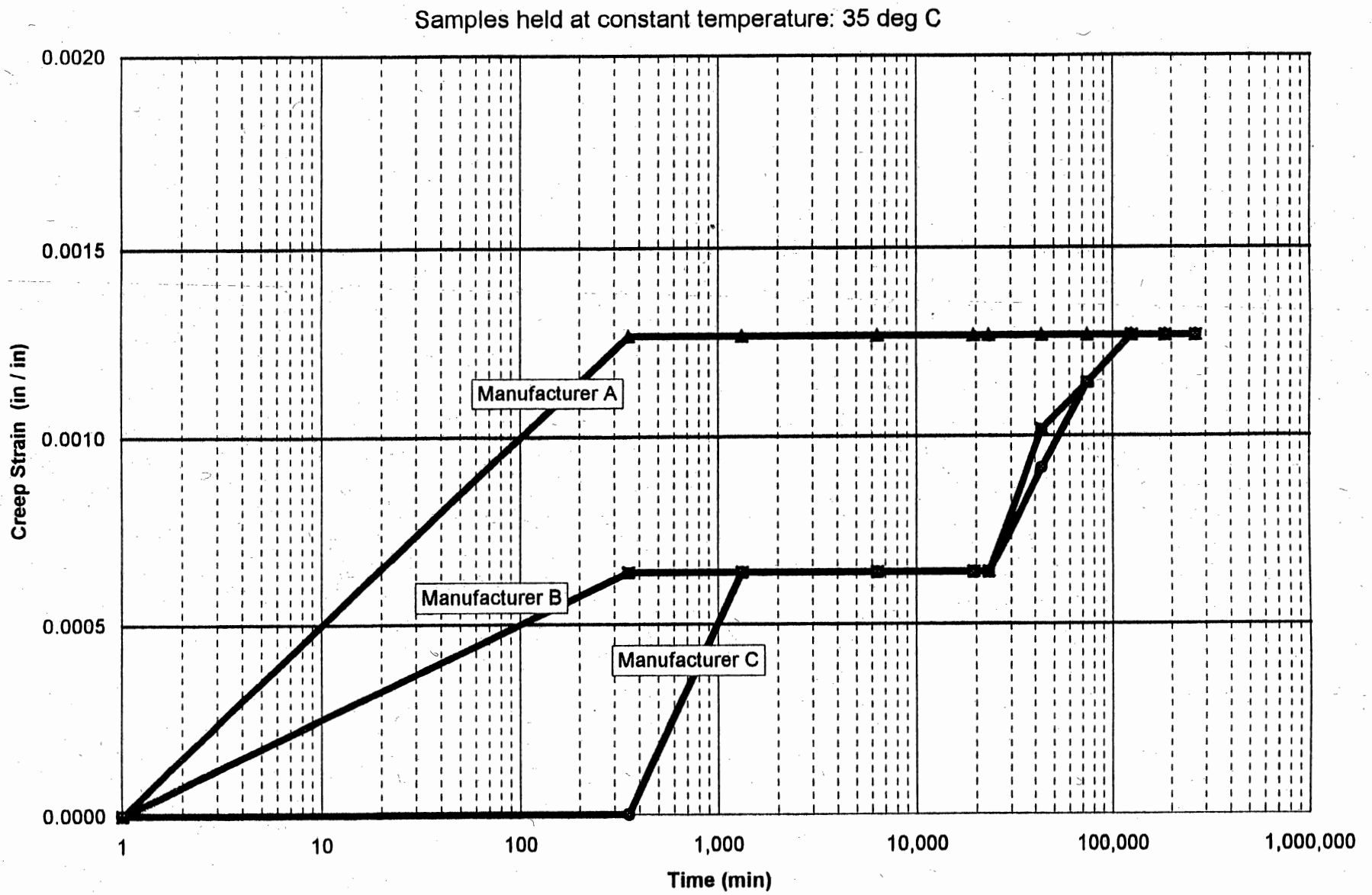

Figure 10 Creep Strain vs. Time

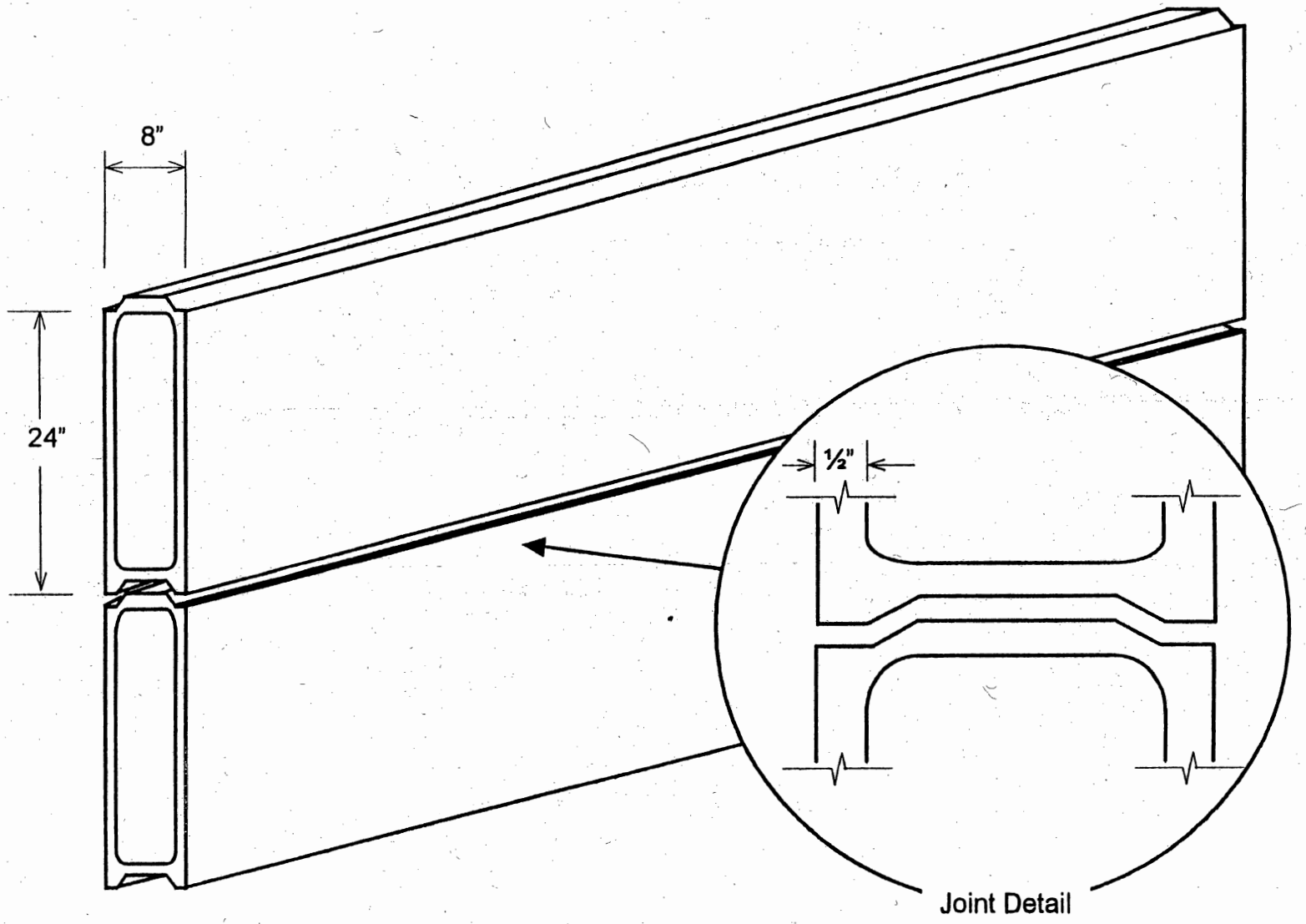

Figure 11 Proposed Noise Wall Panels

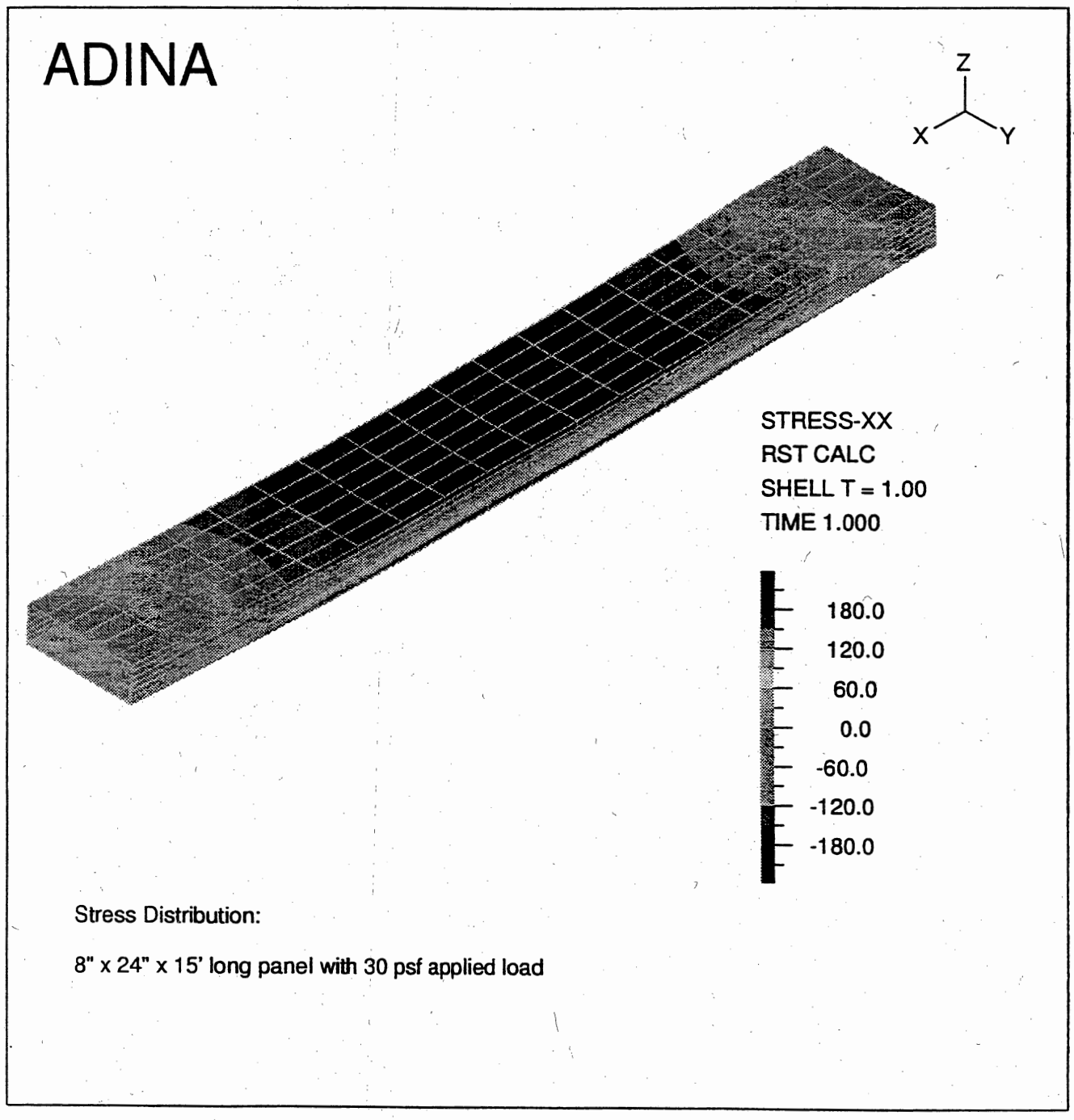

Figure 12 Stress Distribution in 15' Long Panel

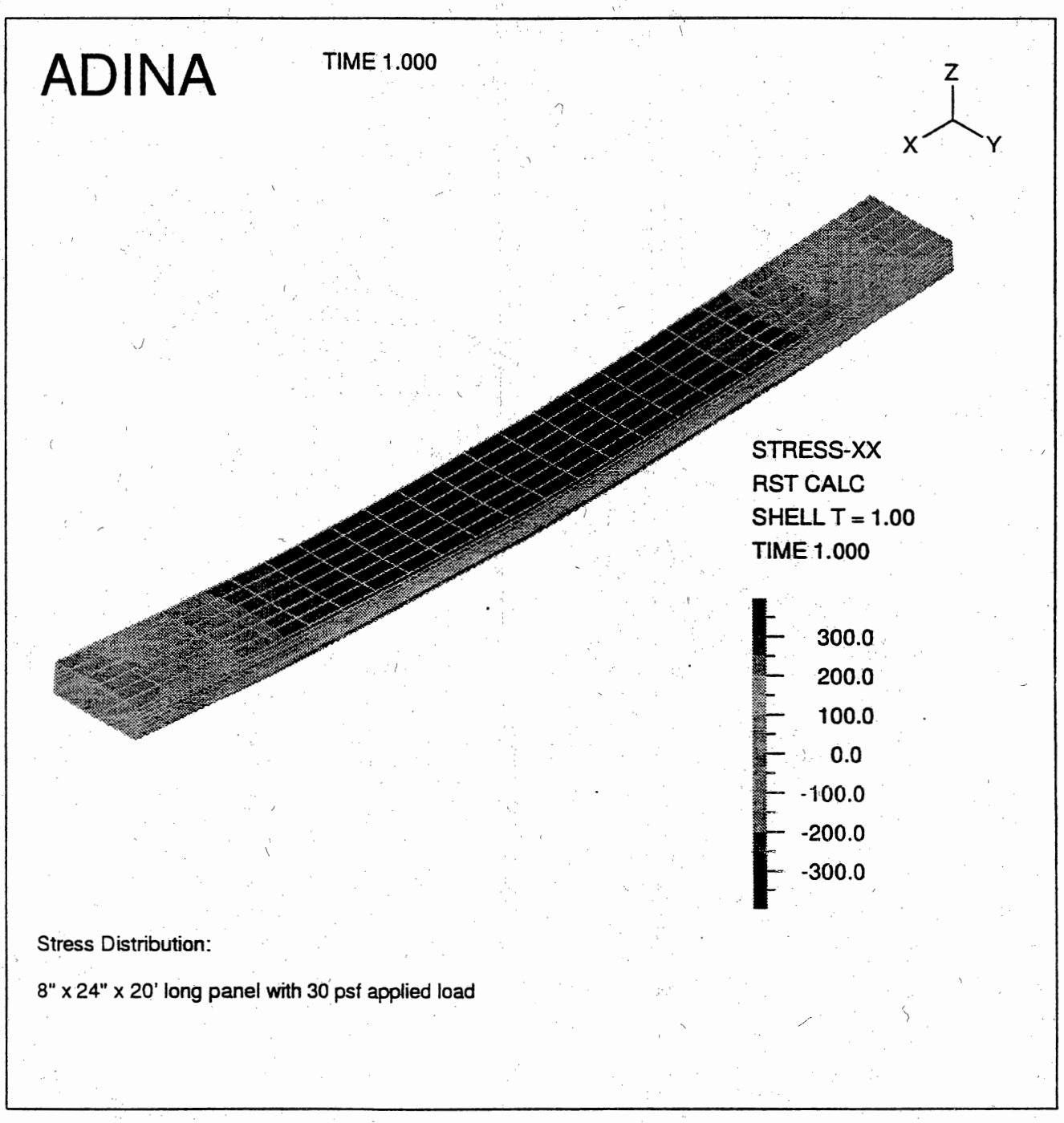

Figure 13 Stress Distribution in 20' Long Panel

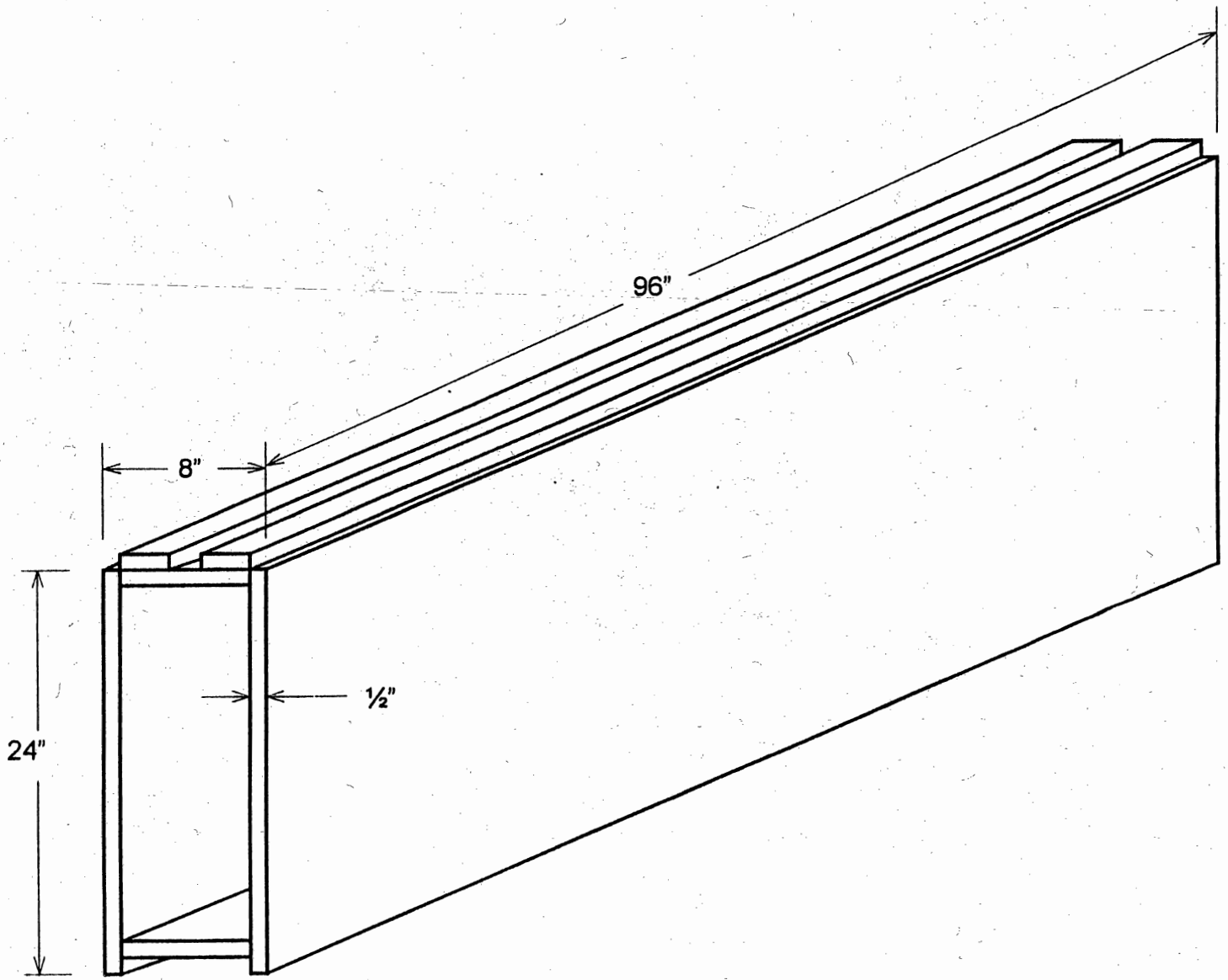

Figure 14 Prototype Panel

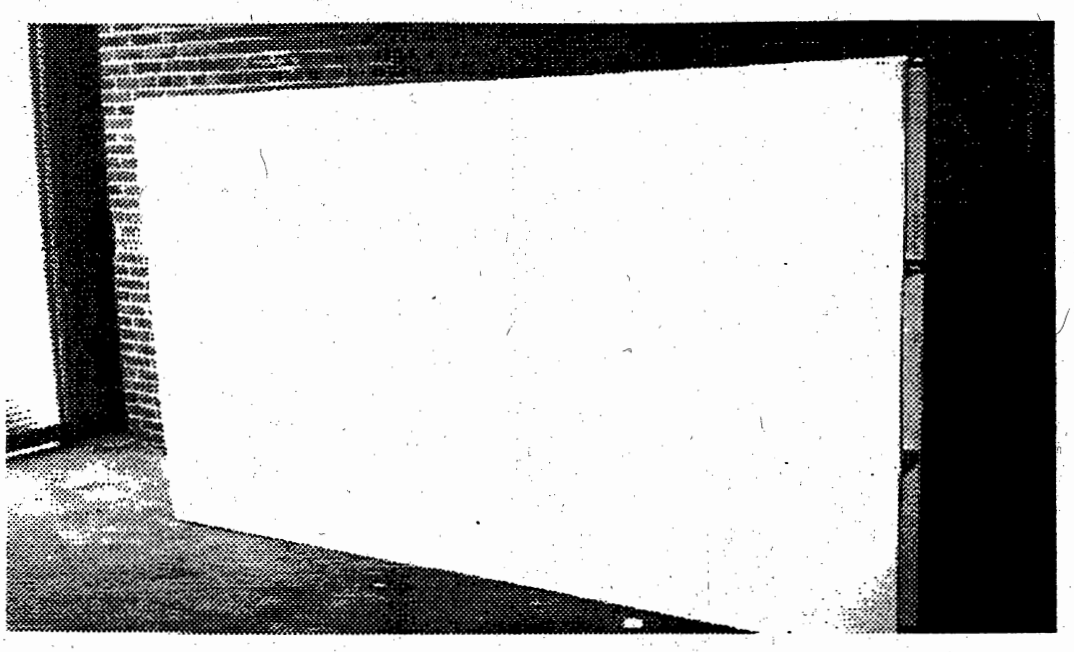

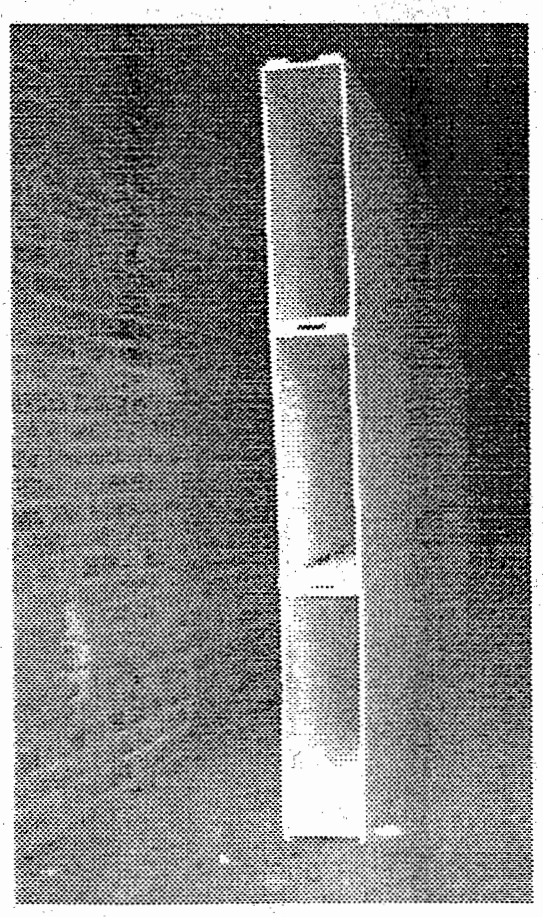

Figure 15 Three Prototype Panels Constructed of ½" Recycled Plastic Sheets

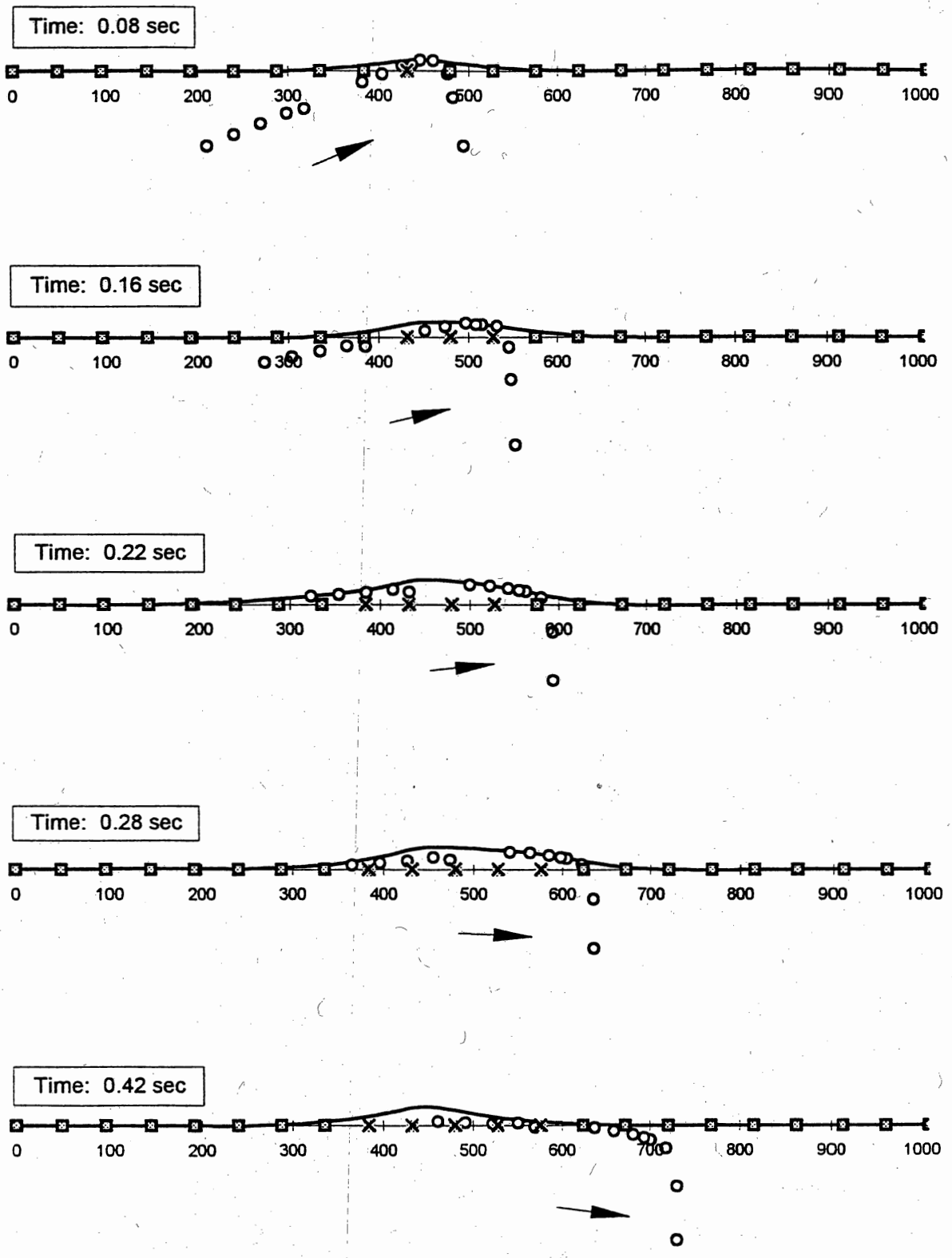

Figure 16 Deflected Barrier Shape

APPENDIX

Sound Tests for Prototype Noise Wall Panels

Test Report
for
New Jersey Institute of Technology
on
Recycled Plastic Noise Wall Panels

NOISE UNLIMITED, INC.

312 Old Allerton Road, Annandale, NJ 08801
(908)713-9300

16 May 1997

Prepared By	Checked By	Approved By
B. J. Snyder	M. K. Lowman	T. S. Bragg
30 May 1997	2 June 1997	30 May 1997

1. INTRODUCTION

The sound absorption coefficient of a surface in a specified frequency band is, aside from the effects of diffraction, the fraction of randomly incident sound energy absorbed or otherwise not reflected. The unit of measurement is sabin per square foot.

The noise reduction coefficient, NRC, is the average of the sound absorption coefficients at 250, 500, 1000, and 2000 Hz expressed to the nearest integral multiple of 0.05.

2. APPLICABLE STANDARD

Measurements were made according to:

ASTM Designation: C 423-90a, "Standard Test Method for Sound Absorption and Sound Absorption Coefficients by the Reverberation Room Method."

Standard Mountings are defined in:

ASTM Designation: E 795-91, "Standard Practices for Mounting Test Specimens During Sound Absorption Test."

3. TEST SPECIMEN

The test specimen consisted of four 24" wide by 96" long by 8" thick panels, arranged in a Type A mounting, forming a test specimen 8' wide, 8' long, and 8" thick. The specimen was submitted for testing by New Jersey Institute of Technology (NJIT) and was identified as "Recycled Plastic Noise Wall Panels." Two panels were made of 1/2" materials, and two panels were made of 1/2" and 3/8" materials mixed. The weight of the specimen was 197 lbs. The area used to calculate absorption coefficients was 64 sq. ft., the face area of the specimen.

4. TEST RESULTS

The calculated values of the sound absorption of the specimen and sound absorption coefficients together with the calculated measurement uncertainty for each are tabulated and shown graphically in Figure 1.

5. DISPOSITION OF TEST SPECIMEN

The test specimen was returned to NJIT by Keith MacBain who witnessed the test for NJIT.

NRC=.10

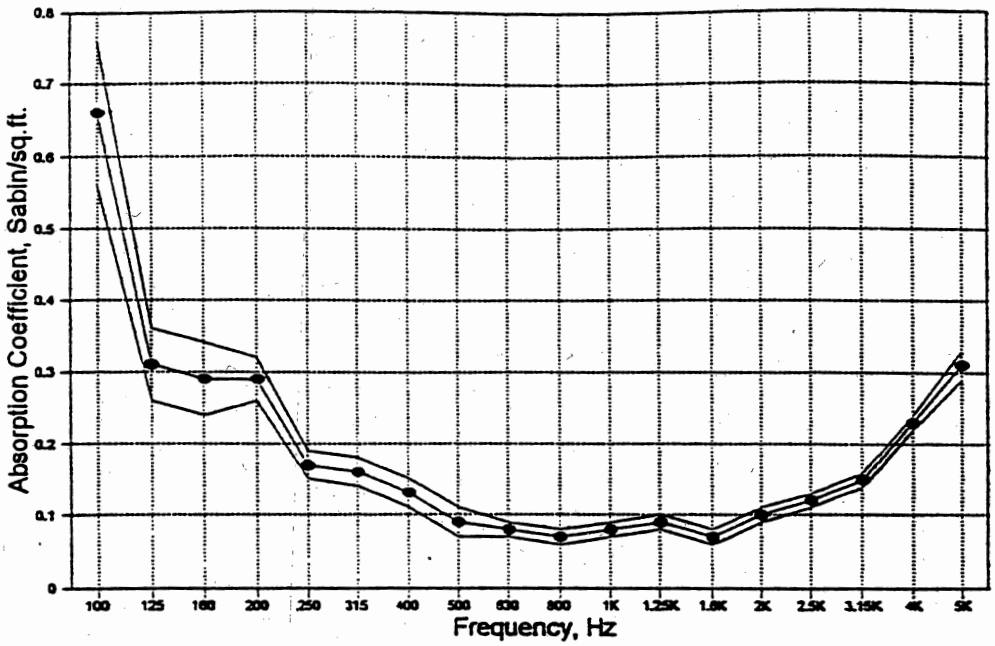

= Test Levels — Deviation

Frequency (Hz)	Absorption (Sabin)		Deviation	Coefficient (Sabin/ft²)		Deviation
100	42.3	±	6.2	0.66	±	0.1
125	19.6	±	3	0.31	±	0.05
160	18.6	±	3.3	0.29	±	0.05
200	18.9	±	1.9	0.29	±	0.03
250	10.7	±	1.5	0.17	±	0.02
315	10.3	±	1.3	0.16	±	0.02
400	8.5	±	1.2	0.13	±	0.02
500	5.5	±	1.2	0.09	±	0.02
630	4.9	±	0.8	0.08	±	0.01
800	4.3	±	0.6	0.07	±	0.01
1K	4.9	±	0.6	0.08	±	0.01
1.25K	5.9	±	0.8	0.09	±	0.01
1.6K	4.6	±	0.6	0.07	±	0.01
2K	6.6	±	0.7	0.1	±	0.01
2.5K	7.7	±	0.8	0.12	±	0.01
3.15K	9.6	±	0.7	0.15	±	0.01
4K	14.9	±	0.9	0.23	±	0.01
5K	19.6	±	1.3	0.31	±	0.02
Noise Reduction Coefficient,				0.10		

Recycled Plastic Noise Wall Panel
for
New Jersey Institute of Technology
Figure 1

Test Report No. 8645.2 No. of Pages 3

STC Test Report
for
New Jersey Institute of Technology
on
Recycled Plastic Noise Wall Panels
Constructed with ½" Thick Material

NOISE UNLIMITED, INC.

312 Old Allerton Road, Annandale, NJ 08801

16 May 1997

Prepared By	Checked By	Approved By
B. J. Snyder	M. Lowman	T. S. Bragg
B. J. Snyder 30 May 1997	M. Lowman 3 June 1997	T. S. Bragg 30 May 1997

1. INTRODUCTION

The sound transmission loss of a partition in a specified frequency band is the ratio, expressed on the decibel scale, of the airborne sound power incident on the partition to the sound power transmitted by the partition and radiated on the other side. The ratio of two like quantities proportional to power of energy is expressed on the decibel (dB) scale by multiplying its common logarithm by ten.

2. APPLICABLE STANDARD "

Measurements were made according to:

ASTM Designation: E 90-90, "Standard Method for Laboratory Measurement of Airborne Sound Transmission Loss of Building Partitions."

Sound Transmission Class, STC, was determined according to:

ASTM Designation: E 413-87, "Standard Classification for Determination of Sound Transmission Class."

3. TEST SPECIMEN

The test specimen was a wall system 48" wide by 96" high by 8" thick. The specimen was installed in the 4' by 8' test opening in the Cedar Knolls Acoustical Laboratory steel test wall under the supervision of, and with the assistance of, Keith MacBain of New Jersey Institute of Technology (NJIT). After the wall was installed, the crack around the perimeter of the test specimen was sealed with "Duxseal" on both sides. The specimen was submitted for testing by NJIT, and was identified as "Recycled Plastic Noise Wall Panel." The panels were constructed of ½" recycled plastic. The weight of the specimen was 103 pounds. The finished test area was 32 square feet.

4. TEST RESULTS

The measured sound transmission losses of the test specimen at the preferred one-third octave band center frequencies are tabulated in Table 1 and shown graphically in Figure 1.

5. DISPOSITION OF TEST SPECIMEN

The test specimen was hand carried by Keith MacBain of NJIT.

Figure 1
Sound Transmission Loss, TL (dB), vs. Frequency (Hz) on
Recycled Plastic Noise Wall Panel with ½" Material

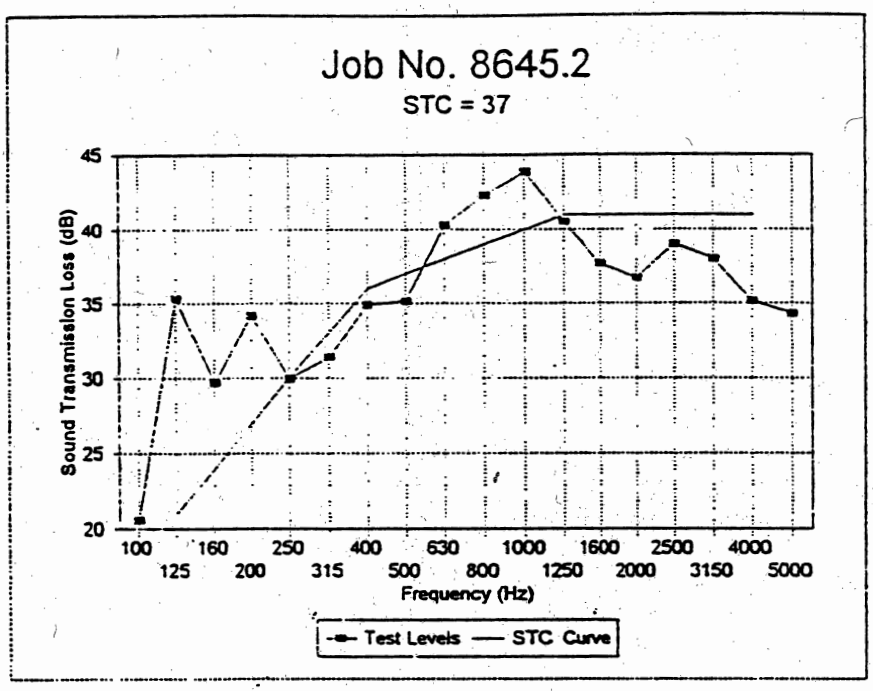

Frequency, Hz	TL	Deficiencies	Frequency, Hz	TL	Deficiencies
100	21		800	42	0
125	35	0	1000	44	0
160	30	0	1250	41	-0
200	34	0	1600	38	-3
250	30	-0	2000	37	-4
315	31	-2	2500	39	-2
400	35	-1	3150	38	-3
500	35	-2	4000	35	-6
630	40	0	5000	34	
Sound Transmission Class, STC =			37		

Sound Transmission Loss
Recycled Plastic Noise Wall Panel with ½" Material
New Jersey Institute of Technology
Table 1

Test Report No. 8645.3 No. of Pages 3

STC Test Report
for
New Jersey Institute of Technology
on
Recycled Plastic Noise Wall Panels
Constructed with 1/2"& 3/8" Thick
Materials

NOISE UNLIMITED, INC.

312 Old Allerton Road, Annandale, NJ 08801

16 May 1997

Prepared By	Checked By	Approved By
B. J. Snyder	M. Lowman	T. S. Bragg
B. J. Snyder	M. Lowman	T. S. Bragg
30 May 1997	3 June 1997	30 May 1997

1. INTRODUCTION

The sound transmission loss of a partition in a specified frequency band is the ratio, expressed on the decibel scale, of the airborne sound power incident on the partition to the sound power transmitted by the partition and radiated on the other side. The ratio of two like quantities proportional to power of energy is expressed on the decibel (dB) scale by multiplying its common logarithm by ten.

2. APPLICABLE STANDARD "

Measurements were made according to:

ASTM Designation: E 90-90, "Standard Method for Laboratory Measurement of Airborne Sound Transmission Loss of Building Partitions."

Sound Transmission Class, STC, was determined according to:

ASTM Designation: E 413-87, "Standard Classification for Determination of Sound Transmission Class."

3. TEST SPECIMEN

The test specimen was a wall system 48" wide by 96" high by 8" thick. The specimen was installed in the 4' by 8' test opening in the Cedar Knolls Acoustical Laboratory steel test wall under the supervision of, and with the assistance of, Keith MacBain of New Jersey Institute of Technology (NJIT). After the wall was installed, the crack around the perimeter of the test specimen was sealed with "Duxseal" on both sides. The specimen was submitted for testing by NJIT, and was identified as "Recycled Plastic Noise Wall Panel." The panels were constructed of 1/2" and 3/8" recycled plastic. The weight of the specimen was 94 pounds. The finished test area was 32 square feet.

4. TEST RESULTS

The measured sound transmission losses of the test specimen at the preferred one-third octave band center frequencies are tabulated in Table 1 and shown graphically in Figure 1.

5. DISPOSITION OF TEST SPECIMEN

The test specimen was hand carried by Keith MacBain of NJIT.

Figure 1
Sound Transmission Loss, TL (dB), vs. Frequency (Hz) on
Recycled Plastic Noise Wall Panel with 1/2" & 3/8" Materials

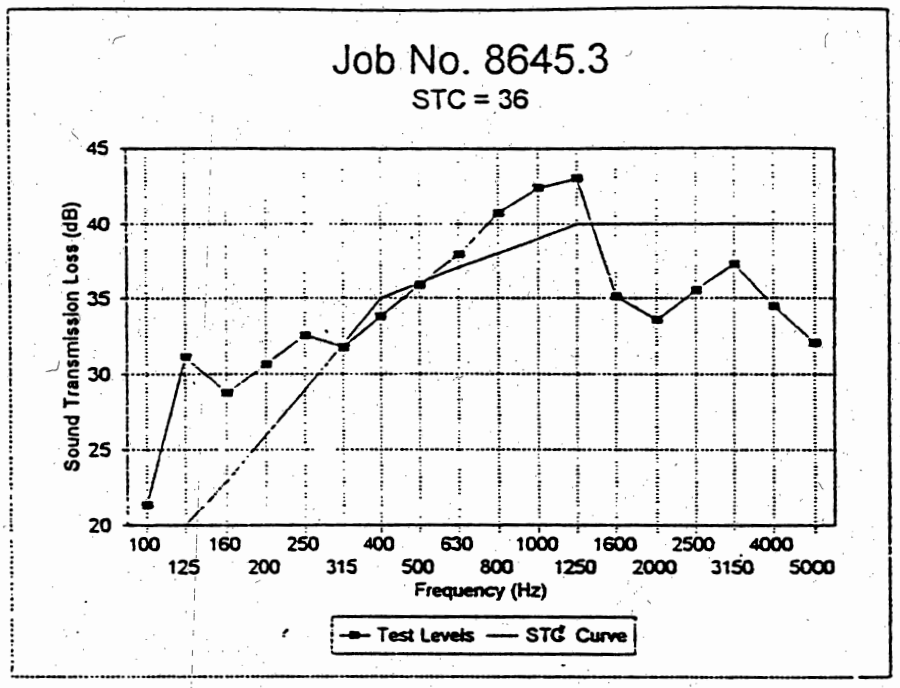

Frequency, Hz	TL	Deficiencies	Frequency, Hz	TL	Deficiencies
100	21		800	41	0
125	31	0	1000	42	0
160	29	0	1250	43	0
200	31	0	1600	35	-5
250	33	0	2000	34	-6
315	32	-0	2500	36	-4
400	34	-1	3150	37	-3
500	36	-0	4000	34	-6
630	38	0	5000	32	
Sound Transmission Class, STC =			36		

Sound Transmission Loss
Recycled Plastic Noise Wall Panel with 1/2" & 3/8" Materials
New Jersey Institute of Technology
Table 1

NJIT
New Jersey Institute of Technology

PHASE-I REPORT

Recycled Plastics for Highway Appurtenances

by
M. Ala Saadeghvaziri, and
Keith M. MacBain

Research Project Supported by
NEW JERSEY DEPARTMENT OF TRANSPORTATION (NJDOT)
and
FEDERAL HIGHWAY ADMINISTRATION (FHWA)

NEW JERSEY INSTITUTE OF TECHNOLOGY
DEPARTMENT OF CIVIL AND ENVIRONMENTAL ENGINEERING
UNIVERSITY HEIGHTS
NEWARK, NJ 07102-1982
AUGUST 1996

OBJECTIVE

The main objectives of this study are to develop more economical traffic noise barriers and safer road barrier systems that use innovative designs and new materials such as recycled plastics, thus, contributing to the management of solid waste too. The work will be conducted in three phases with the duration of three years, and will include the following tasks: material tests to evaluate mechanical and structural properties; development of a constitutive model for recycled plastics; feasibility analysis of proposed designs for sound and road barriers; freeze-thaw tests; creep and impact tests, detailed analytical evaluation using nonlinear finite element models; wind and acoustic tests; and development of design specifications and CAD programs for design of highway appurtenances using recycled plastics.

This report presents the results of the first phase of this study which includes both experimental and analytical investigations. The experimental part includes material tests to determine mechanical properties of various recycled plastics as they vary significantly among different manufacturers. Furthermore, a unified four-parameter constitutive model is proposed and verified that can be used in characterization of recycled plastics. Four-point flexural tests of recycled plastic beams were performed to assess strength, stiffness and mode of failure. Analytical results using the proposed constitutive model are in good agreement with the experimental results. An innovative noise wall design that takes advantage of multi-layering to increase stiffness and sound effectiveness is discussed. Other possible uses and research plans for Phases II and III of this study are also discussed.

KEY WORDS

Recycled Plastics, Noise Barrier, Material Properties, Material Model, Road Barrier.

INTERIM RECOMMENDATIONS

Recycled plastics is a fairly new material and presently there are no test methods or design specifications for use by structural engineers. However, in the last three years ASTM through *D20.20.01 Section on Plastic Lumber and Shapes (Chairman R. Lampo, USACERL, P.O. Box 9005, Champaign, IL 61826)* has worked on development of test methods. The following test methods are being balloted and should be available in a near future:

1) Project X-202001-1, Density and Specific Gravity,
2) Project X-202001-2, Compressive Properties,
3) Project X-202001-3, Flexural Properties,

4) Project X-202001-4, Creep Properties, and
5) Project X-202001-5, Mechanical Fasteners.

However, due to non-homogeneity of recycled plastic lumber, these test methods are for evaluating the properties of plastic lumber or shapes as a product. That is, they are not material property test methods that can be used in evaluating stress-strain relationships that can be used in analysis and design of structural systems under more complex loading.

Until the development of material property test methods, based on this study the following interim recommendations can be made:

1) The material model proposed in this report can be used in analysis of structural systems under short term general loading. The four-constant for the model can be determined using coupons as discussed.
2) Recycled products with reinforcing fibers have more stiffness but they are less ductile and variation in their mechanical characteristics is more pronounced.
3) Mechanical property of recycled plastic lumber with wood fibers appears to be significantly affected by freeze-thaw cycles. Effect of freeze-thaw cycles, at constant humidity of about 70%, on recycled plastic products with no fibers or with fiberglass appears to be minimal.
4) Recycled plastic lumber is a thermoplastic material and highly susceptible to temperature and creep. Structural use under large sustained load must be avoided until the state-of-the-knowledge on long term performance improves.

ACKNOWLEDGMENT

This research and development study is sponsored by the New Jersey Department of Transportation (NJDOT) and the Federal Highway Administration (FHWA). It is coordinated by the NJDOT's Bureau of Research and Mr. Robert Baker acts as the Project Manager. The results and conclusions are those of the authors and do not necessarily reflect the views of the sponsors.

BACKGROUND

Solid waste is overloading the landfills and is a major contributor to the environmental problems facing this country. Every year the U.S. alone generates 320 billion lb. (145 billion kg) of municipal solid waste. Of this waste, plastics comprise 18 percent by volume and 7 percent by weight (1). Furthermore, plastics and paper are the fastest growing segments of solid wastes (2).

Recycling is an environmentally acceptable means of reducing solid waste and conserving resources. Reprocessing industrial plastic waste (e.g., in-house scrap) has been a common practice for as long as the plastic industry has existed. There have recently been significant developments in the recycling technology of commingled plastic waste but the key issue to be resolved is securing long-term, high-value markets for recycled polymers.

GENERAL PROPERTIES OF RECYCLED PLASTICS

Mixed, or commingled, plastics once destined for the waste stream are now being recycled (3). Collected plastic scrap is granulated, then melted and processed in an extruder. The molten plastic is then injection molded into the shape and size of the final product. The product can be cut and shaped with the same tools and fastening devices used for wood. These molded products are resistant to attack from gas, oil, salt, sunlight, chemicals and insects and will withstand human and mechanical abuse (4). Test results have shown mixed plastics hold nails approximately 40 percent better than wood (5). Fiberglass and treated wood fiber, both classified as hazardous waste materials and costly to landfill, have been successfully used to improve the mechanical properties (6).

Currently, molded profiles are used to make park benches, guardrail block outs, fences, road markers, landscape timbers and a wide variety of other non-structural applications. Although it has been highly anticipated that molded profiles "will replace wood, concrete and steel" (7), structural applications of the product are practically non-existent. This is mainly due to lack of knowledge about the mechanical and structural properties of the material, especially their relation to long term performance. Lack of testing standards and design specifications compound the problem.

EXPERIMENTAL TESTS

The cross section of the extruded product can have any shape but only standard lumber shapes (2X10, 4X4 & 6X6) were used in testing because these are commonly produced. The

actual dimensions of the 2X10, 4X4, and 6X6 are approximately 1.5"X9.5" (3.8 cm X 24 cm), 3.5"X3.5" (8.9 cm X 8.9 cm), and 5.5"X5.5" (14 cm X 14 cm), respectively but they are generally referred to by their nominal size. The cross-section of the standard recycled plastic (RP) lumber shape is visually non-homogeneous, suggesting that the material properties also vary. Non-homogeneity of the material is attributed to the cooling process during extrusion; the section normally cools from the outside causing the periphery to solidify before the center. Shrinkage of the center as it cools can also distort the final form of the section causing rounded corners and uneven surfaces. Although the degree of variation is different for various manufacturers and shapes, all products evaluated depict this phenomenon. Material tests (tension and compression) were conducted to investigate this difference and the results were used to formulate a constitutive model for RP that can be employed in analytical studies. To validate the constitutive model and to assess global behavior of structural components (such as stiffness, strength, and ductility) flexural member tests were also performed.

There is variation among the manufacturers in composition as well as the methods of acquiring materials. To represent a range of compositions available, three manufacturers (to be called **A, B & C**) were selected for testing. Manufacturer **A** mixes fiberglass with the RP, **B** uses only RP, and **C** uses 50% wood fiber in addition to the RP.

Material Tests

Selection of Coupons

To investigate the apparent non-homogeneity, visually consistent sections were cut from both 4X4 and 6X6 shapes and termed 'core' or 'shell' coupons. Coupons were also cut from 2X10 shapes but the visually consistent shell section was too thin (typically less than 1 cm) to be used for standard coupons. The core and shell coupons were not only visually different but also were noted to have different dry densities after they were weighed and measured. Depending on manufacturer (and lumber size for Manufacturer B), the core coupons typically had 50% of the density of the shell.

Specimen Dimensions and Test Set Up

Core and shell coupons for tension tests were 1 cm x 4 cm x 20 cm nominal and the compression coupons were 1 cm x 4 cm x 2 cm nominal. Since ASTM is still developing RP test standards, procedures for wood and plastic were used. Ten tension tests were conducted similar to ASTM D 638 and ten compression tests were conducted observing ASTM D 695 for each manufacturer. Tension strain was measured with an extensometer over a 2" (5 cm) initial gage length. Figure 1 shows some tension test coupons and the test apparatus.

Results

Figures 2 through 4 show tension and compression stress-strain diagrams for both core and shell coupons for all three manufacturers. Figure 5 shows that at large strain, a typical compression test resembles hyper-elastic behavior; there was no point of maximum stress but rather the stress continued to increase after the material visually failed. Visual failure occurred near the point of inflection in the stress-strain diagram of Figure 5.

The stress-strain diagrams show that the material behavior is highly nonlinear and that there is a significant difference in both tension and compression behavior as well as the core and shell materials. For all manufacturers tested, the core was found to have lower initial modulus of elasticity *(E)* and lower ultimate strength (Manufacturer **A** foam-fills the core for aesthetic purposes). Table 1 shows differences between the properties of shell and core coupons in tension and compression for the three manufacturers tested. For Manufacturer B, the core coupons from 4X4 sizes had a smaller *E* than that of the 6X6 (E_t = 1,030 MPa, E_c = 500 MPa) and the average density of the 4X4 core (0.37 g/cc) was nearly half of that of the 6X6 (0.67 g/cc). There appears to be a correlation between density and strength in a larger scale; higher density corresponds to a higher strength but differences of less than 5% do not seem to be significant.

Coupons from all manufacturers contain varying amounts of impurities and tension failure usually occurred at these locations. Impurities are materials such as bottle tops that are inadvertently collected and granulated with the recyclable but melt at a different (normally higher) temperature. The amount of bond adhesion for these impurities is unknown. The size of the impurities varied, but typically it was less for types **A** and **C** compared to type **B**. This is believed to be a factor in the divergence from theory mentioned in later sections.

Proposed Constitutive Model

Based on analyses of the test results under both tension and compression stresses for all manufacturers, the following equation is proposed to define stress-strain relationship for recycled plastics:

$$\sigma = \frac{A\,\varepsilon}{B\,\varepsilon^{2} + C\,\varepsilon + D}$$

As it can be seen, the model contains four constants that need to be determined for each type of material; that is, tension and compression of core and shell. This requires sixteen constants for each manufacturer to fully define the section behavior. These constants were determined using Chi-square minimization method (8) as implemented by TempleGraph package (9). The model was not fit to the compression curves beyond the point of inflection. Future work will attempt to reduce the number of material constants by defining some of them in terms of other

properties of the material, such as the maximum strength, strain corresponding to the maximum strength; and feed stock used.

For all three manufacturers the proposed model can simulate the experimental results with good accuracy. In Figure 6, a stress-strain diagram from material tests of Manufacturer B is plotted along with the proposed model, which shows a good match. Table 2 gives the material constants for all three manufacturers, which were used to compare analytical results to the experimental results as discussed in the following sections.

Member Tests

Tests set up and specimens

Four-point flexural tests were performed on 27 inch (68.6 cm) long 4X4 samples in accordance with ASTM D 198. In addition to load and deformation at the load point, rotation at the end of the beam was also recorded using dial gages as shown in Figure 7. Furthermore, strain gages were adhered to the top and bottom of the member at its center and strains at these locations were recorded up to failure. Three similar tests were performed for each manufacturer.

Results

The results show a non-linear behavior similar to the material tests. An interesting observation is that despite significant differences in material properties for tension and compression (Figure 3), the strains at the top and bottom outer fibers were within 25% of each other for all specimens tested. This is due to the fact that for stain levels close to failure, areas under both tension and compression stress-strain curves are more or less equal although the tangent module are significantly different.

Although all three products had good ductility for structural purposes, they all failed suddenly as reflected in a lack of a descending portion in the load-deformation curve. Products from Manufacturer B exhibited the largest tension strain (9%) before failure. The greater ductility can be attributed to the lack of reinforcement in the product. That is, addition of fibers (glass or wood) reduces ductility, apparently due to bond failure.

Analytical vs. Experimental Results

A computer program was developed to analyze simply supported beams using the proposed material model along with the constants given in Table 2. The program uses numerical

integration techniques to generate theoretical moment-curvature, load-deflection and load-rotation curves. The analysis assumes that there is a distinct division between core and shell. The length and width of shell and core portion are to be specified as an input parameter by the user.

Figures 8 through 10 show the test results compared with the theoretical curve for all three products. The analytical results agree with the experimental results within 15% for loads less than 80% of the ultimate load. It is suspected that stress concentrations caused by the presence of impurities (mentioned in material tests) cause the deviation between the experimental and theoretical results at larger loads. The theoretical curve is derived from the coupon tests where due to smaller area impurities have a more pronounced effect. Member tests are less affected by these impurities since due to larger cross-sectional area stresses can be redistributed. At larger loads when the material is yielding, the variation between coupon and member behavior will be greater suggesting that strength will be affected more than initial stiffness. The fact that the tension strain in the member at failure was greater (typically by 20%) than the maximum coupon strain supports this conclusion. The maximum bending moment measured was also greater than that predicted by theory using the maximum coupon tension strain as the upper limit.

HIGHWAY APPLICATIONS

An Innovative Noise Wall

As it can be seen from Table 1, the stiffness of RP is generally low; much smaller than concrete or even wood. If current design approaches were to be used, it would be difficult to utilize RP as an economical noise barrier. An advantage of RP, however, is that it can easily be manufactured into various shapes and the cross section does not have to be solid. With this in mind, a new noise barrier design, as shown in Figures 11 & 12, is proposed. Spacing of the webs was determined through finite element analysis of a typical cell as shown in Figure 13. It was determined that spacing of 24" (60 cm) is optimal in terms of local deflection and shear lag along panel length. As seen from Figure 14, the shear lag for a 48" (120 cm) panel is severe and deflections are high. Proposed design uses shell thickness of ½" (1.3 cm) with an overall depth of 6" (15 cm). With these dimensions the panel length can be as great as 20' (6.1 m) based on a wind load of 80 mph (36 m/s). The shell thickness and overall depth of the cross section can be increased to accommodate even greater panel length, thus, making more economical designs by further *reducing the number of posts.*

For typical RP material, the total density (i.e., considering both layers) of the proposed design satisfies the recommendation of 20 kg/m^2 (10). It is expected that multi-layering will also

enhance the sound effectiveness of the wall significantly since layering is the only way to overcome the mass requirement (10). Currently, acoustic tests are being planned to validate the expected performance. Acoustic tests will be performed based on ASTM and will include sound transmission test (ASTM E90-90 and E413-87) and sound absorption test (ASTM C423-90a and E795-83).

Guardrail Posts

Present technology and design use road barriers that are made of relatively rigid materials such as steel, concrete, or a combination of the two. However, it is well known that flexible but strong designs can absorb more energy and minimize the damage sustained by the impacting vehicle. Previous research has resulted in designs that incorporate energy-absorbing mechanisms (such as the use of rubber energy absorber) and improved the performance of bridge rails (11-15). Due to high initial costs associated with these energy-absorbing designs compared to conventional bridge rails, high maintenance costs and difficulty in attachment to standard bridge decks, these energy-absorbing bridge rails have not gained wide acceptance. Here, a new design is being proposed for further evaluation. The proposed design for road barriers (including its possible use as bridge rail) combines the flexibility and strength of plastics (used as posts) with the stiffness of steel rails. Thus, the final product is expected to be functionally superior to current designs.

For all levels of performance (PL-1, PL-2, and PL-3), the AASHTO's design forces anticipate rigid barriers (16), and can not be directly used for evaluation of the proposed design which is a flexible one. Therefore, verification of the proposed design requires detailed analytical and experimental study. Among parameters that need to be investigated are: level of forces and the amount of deflection in the lateral as well as longitudinal direction, redirection of the automobile, rotation of the railing and possibility of roll over, angle of impact and the nature of the force distribution in different components of the system. Based on preliminary analyses of a typical guardrail system (Colorado Type 5) using frame models, the following statements can be made:

I. Due to rigidity of steel rails and flexibility of the RP posts impact forces are distributed to a larger number of posts making relative displacement of the posts smaller. Consequently, the possibility of snagging is reduced and redirection of the automobile will be smoother.
II. Deflection of the guardrail system with RP posts, obviously, is higher than that with steel posts. However, AASHTO's guide specifications (both Roadside Design Guide and Guide Specs. for Bridge Railings) do not put any limitations on the level of deflections.
III. Due to high energy-absorption capacity of RP posts, the vehicular impact acceleration will be reduced significantly. Collision of a point mass with an initial velocity to the typical guardrail system with different posts was used to verify this point. It was observed that

for the system with RP posts, due to its flexibility, forces were only 40% of the forces generated in the rigid posts. This will mean lower injuries to the passengers and less damage to the car.

It should be mentioned that in a crash test of a guardrail system, the use of RP posts has been reported as inadequate (17) based on a one-to-one deflection comparison with wood posts. Obviously, RP is much more flexible than wood and if total deflection is compared to wood, and this is the only parameter to determine appropriateness of the design, then it will be very difficult or uneconomical to design a guardrail post using RP. The approach that is being pursued in the current study is to evaluate the proposed design in terms of functionality, geometric considerations and strength requirement.

FREEZE-THAW TESTS

Coupons and whole sections have been exposed to sixty (60) freeze-thaw cycles. The temperature range was from -15° C to 20° C and the average cycle was 14 hours frozen, 10 hours thawed. The humidity was roughly constant in the range of 65 to 75%. These samples are currently being tension and compression tested, and the properties will be compared with those of coupons and sections not exposed to freeze-thaw cycles. The objective is to determine the effect of freeze-thaw cycles on mechanical properties such as stiffness, strength and rupture strain under both tension and compression stresses. Some preliminary results of tension tests are shown in Figures 15 through 17 for all three manufacturers. Shown on these figures, for comparison purposes, are the curve fit results for coupons that were not subjected to freeze-thaw cycles as discussed before. The results show that the products of manufacturers A and B (i.e. recycled plastic with fiber glass and with no fiber at all) retain their mechanical properties, while the mechanical properties of product C (i.e. recycled plastic with wood fiber) decays significantly when subjected to freeze and thaw cycles.

CONCLUSIONS

Experimental and analytical investigation of Recycled Plastics presented in this interim report indicate that this is a viable material that could have structural applications. Due to differences in feed stock, manufacturing process, presence of additives such as glass and wood fibers, there are significant differences in mechanical and structural characteristics of RP products. However, this by itself will not be a limiting factor in its structural application. Concrete also has different material characteristics depending on its composition. Problems that need to be addressed to ensure its use among structural engineers are quality control, development of standards for testing, design specifications, and long term performance evaluation. Currently,

Recycled Plastics Subcommittee (D20.20) of Plastics Committee of ASTM is addressing the needs related to development of procedures for material and member testing. Over the last two years, manufacturers have also taken major steps in improving quality and initiating efforts to develop design standards that can be used by structural engineers. Efforts of manufacturers is consolidated through the Plastic Lumber Trade Association (PLTA, based in Ohio), a non-profit organization that is expected to fulfill the needs of the industry similar to what ACI and AISC do for concrete and steel. Further research and development work is essential to advancing the-state-of-knowledge on recycled plastic in order to confidently employ the material in the design of transportation systems. Completion of Phase II & III of this study, as outlined in the following section, will be a major step toward achieving this goal.

PHASES II & III TASKS

To further investigate the appropriateness of the RP for highway appurtenances the following tests and analytical studies are being pursued under this study:

I. Sound test as discussed in the previous section.
II. Wind test of full scale panels of the proposed model will be conducted. The wind tests will focus on two issues: 1) are the design loads obtained from current standards a reasonable predictor of the actual wind loads, and 2) does the flow of wind over the top of the wall shed vertices that would excite the wall and cause it to vibrate,
III. Crash worthiness analyses using realistic analytical models by incorporating the proposed material model into an existing program such as BARRIER VII (18).
IV. Further material tests including creep and impact tests.
V. Development of simplified design methods and CAD programs.

REFERENCES

1. "Furthering The Possibilities," Plastics World, April, 1990.
2. "Solid Waste Concerns Spur Plastic Recycling Efforts," Chemical & Engrg. News, Jan., 1989.
3. Maczko, J., "An Alternative to Landfills for Mixed Plastic Waste," Plastics Engineering, April, 1990.
4. "Recycling Mixed Plastics: New Markets," The Council for Solid Waste Solutions, The Plastic Recycling Foundation, Washington, DC, undated.
5. Bennett, R. A., "Market Research on Plastics Recycling," Technical Report # 31, The Center for Plastic Recycling Research, Rutgers-The State Univ. of New Jersey, 1989.
6. M. D. Applebaum, et. al., "The Properties and Morphology of Fiber Reinforced Refined Post-Consumer Plastics Compounded on a Non-intermeshing Twin Screw Extruder," The Society of Plastics Engineering, The 1991 ANTEC Conf., Montreal, 1991.
7. Pearson, W., "Plastics Recycling: The Business," Plastics Recycling Foundation, PA, July, 1989.
8. Press W. H., *"Numerical Recipes,"* Cambridge, 1988.
9. "TempleGraphs 2.4," Michalisin Assoc., Inc., Ambler, PA, 1922.
10. Beranek, Leo L., and Istvan L. Ver, *"Noise and Vibration Control Engineering: Principles and Applications,"* John Wiley & Sons Inc., NY, 1992.
11. T. J. Hirsch, et. al., "Energy Absorbing Bridge Rail (Fragmenting Tube)," Technical Memorandum 505-8, Texas Transportation Institute, Texas A&M University System, College Station, Feb., 1970.
12. Hirsch, T. J., and C. E. Buth, "Testing and Evaluation of Bridge Rail Concept," Final Report, Project RF 3053, Texas Transportation Institute, Texas A&M University System, College Station, May, 1975.
13. Kimball C. E., et. al., "Development of a Collapsing Ring Bridge Rail System," Report RD-76-39, FHWA, U.S. Department of Transportation, Jan., 1976.
14. Stoughton, R.L., "Vehicle Impact Testing of a See-Through, Collapsing Ring, Structural Steel Tube, Bridge Barrier Railing," Office of Transportation Laboratory, California Department of Transportation, Sacramento, June, 1983.
15. Beason, W. L., T. J. Hirsch, and J. C. Cain, "A Low-Maintenance, Energy-Absorbing Bridge Rail," Transportation Research Record 1065, pp. -61, 1986.
16. "Roadside Design Guide," AASHTO, Washington, DC, 1989.
17. Strybos John. W., "Recycled Plastics for Roadside Safety Devices," Proceedings of Structures Congress, ASCE, Boston, April, 1995.
18. Powell, G. H., "BARRIER VII: A Computer Program For Evaluation of Automobile Barrier Systems," FHWA Report No. FHWA-RD-73-51, April,

TABLES

FIGURES

Manufacturer		E_t *(MPa)*	E_c *(MPa)*	σ_t^{max} *(MPa)*	σ_c^{max} *(MPa)*	σ_c *@ inflection point (MPa)*
A						
	Shell	4,300	860	12.5	(3)	22.5
	Core	(1)	(1)	(1)	(1),(3)	(1)
B						
	Shell	1,860	690	15.2	(3)	35.0
	Core	350 (2)	240 (2)	4.0	(3)	9.0
C						
	Shell	2,210	620	6.9	(3)	14.0
	Core	1,790	450	4.8	(3)	13.0

E_t = initial tangent Young's Modulus in tension

E_c = initial tangent Young's Modulus in compression

σ_t^{max} = maximum tension stress

σ_c^{max} = maximum c ompression stress

Notes:

1. The core of this manufacturer is foam-filled for astetic purposes
2. Values for the 6x6 were as much as 3 times larger
3. The material did not reach a maximum value in compression

Table 1

Manufacturer & coupon		$\sigma = \frac{A\varepsilon}{B\varepsilon^2 + C\varepsilon + D}$ (MPa)			
		Equation Coefficients			
		A	B	C	D
A	Shell - tension	1.76E+05	168,500	8,490	40
	Shell - compression	1.69E+06	72,400	-43,280	1,940
	Core - tension	0	0	0	10
	Core - compression	0	0	0	10
B	Shell - tension	1.17E+05	2,460	6,040	62
	Shell - compression	2.55E+06	-5,390	-51,870	3,700
	Core - tension (1)	9.45E+04	147,000	17,700	264
	Core - compression (1)	8.62E+04	78,050	-198,700	3,870
C	Shell - tension	1.39E+05	298,400	12,110	62
	Shell - compression	8.34E+05	115,880	-39,880	1,360
	Core - tension	1.39E+05	728,000	10,310	77
	Core - compression	9.58E+05	87,030	-46,780	2,110

Notes:

(1) values for 6 X 6 were different

Tabe 2

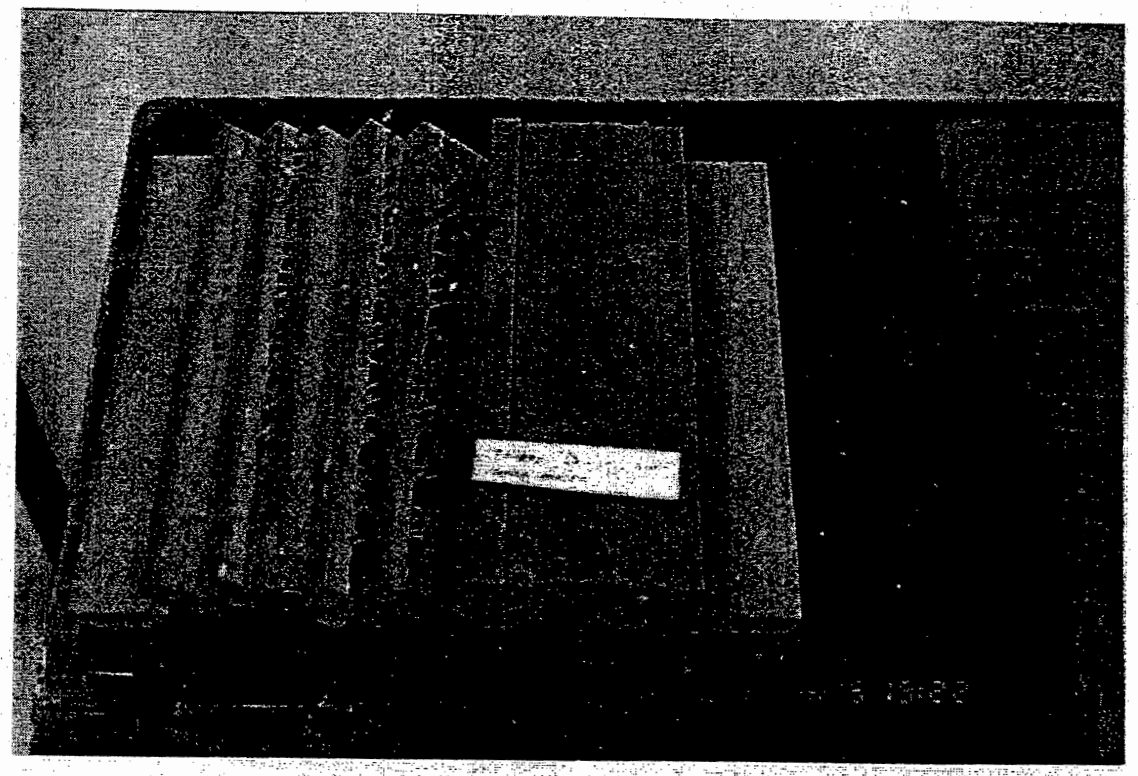

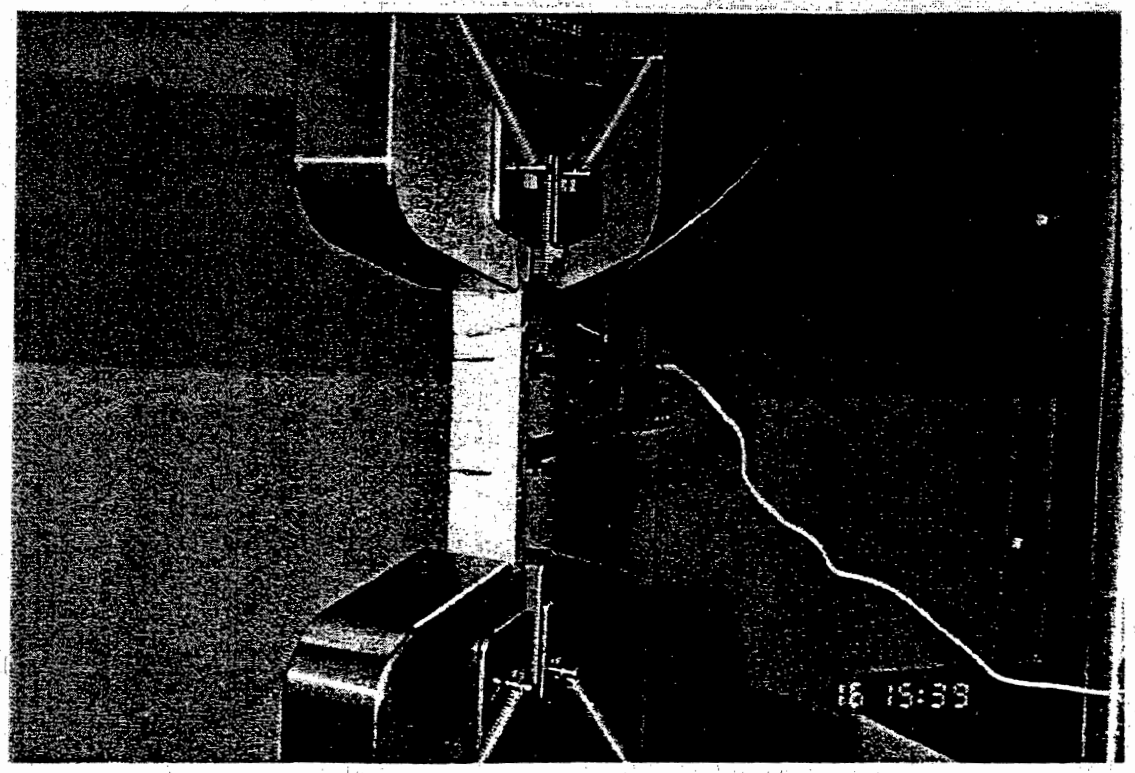

Figure 1. Some Tension Coupons and Test Apparatus

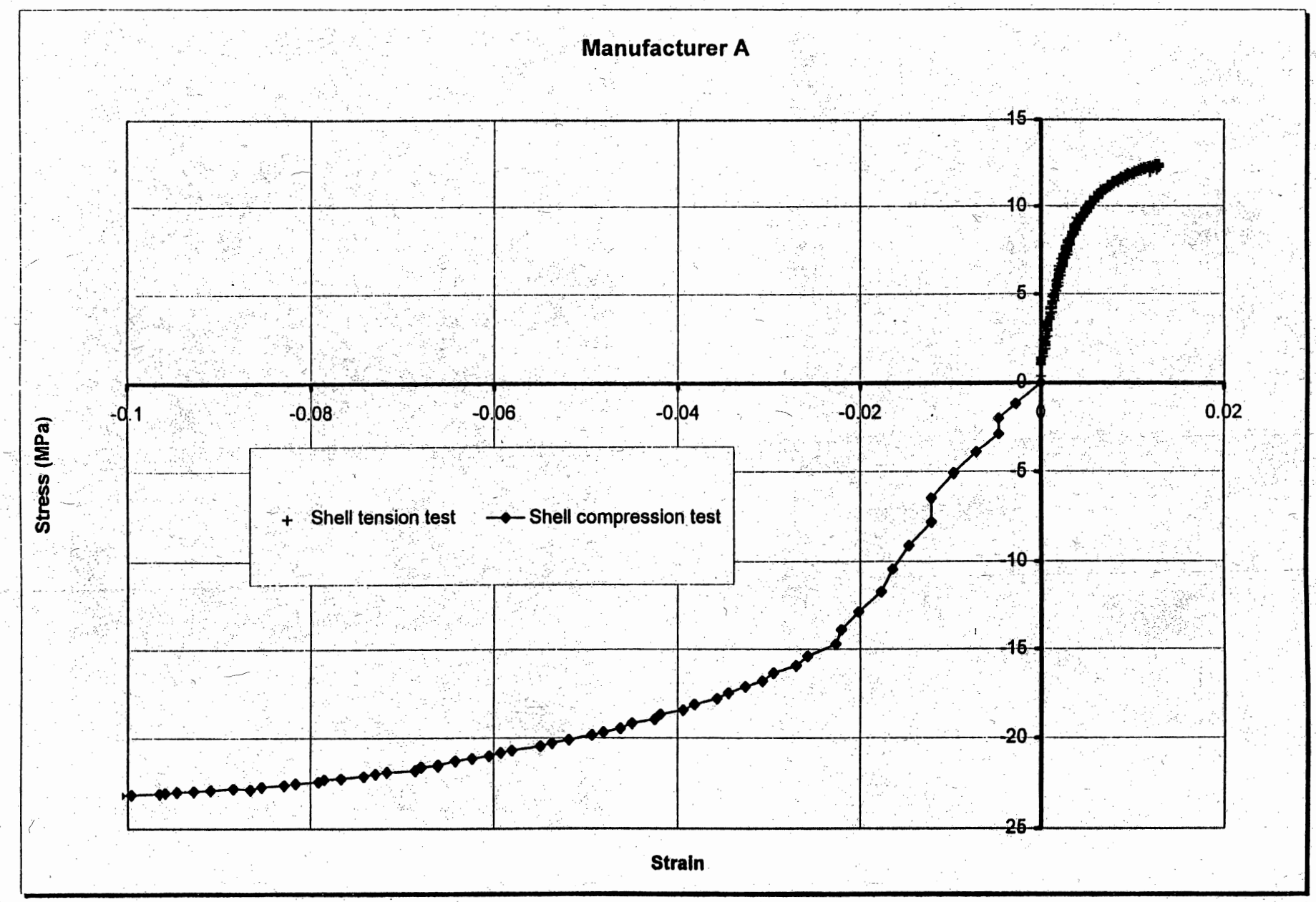

Figure 2. Stress-Strain Diagrams for Manufacturer A.

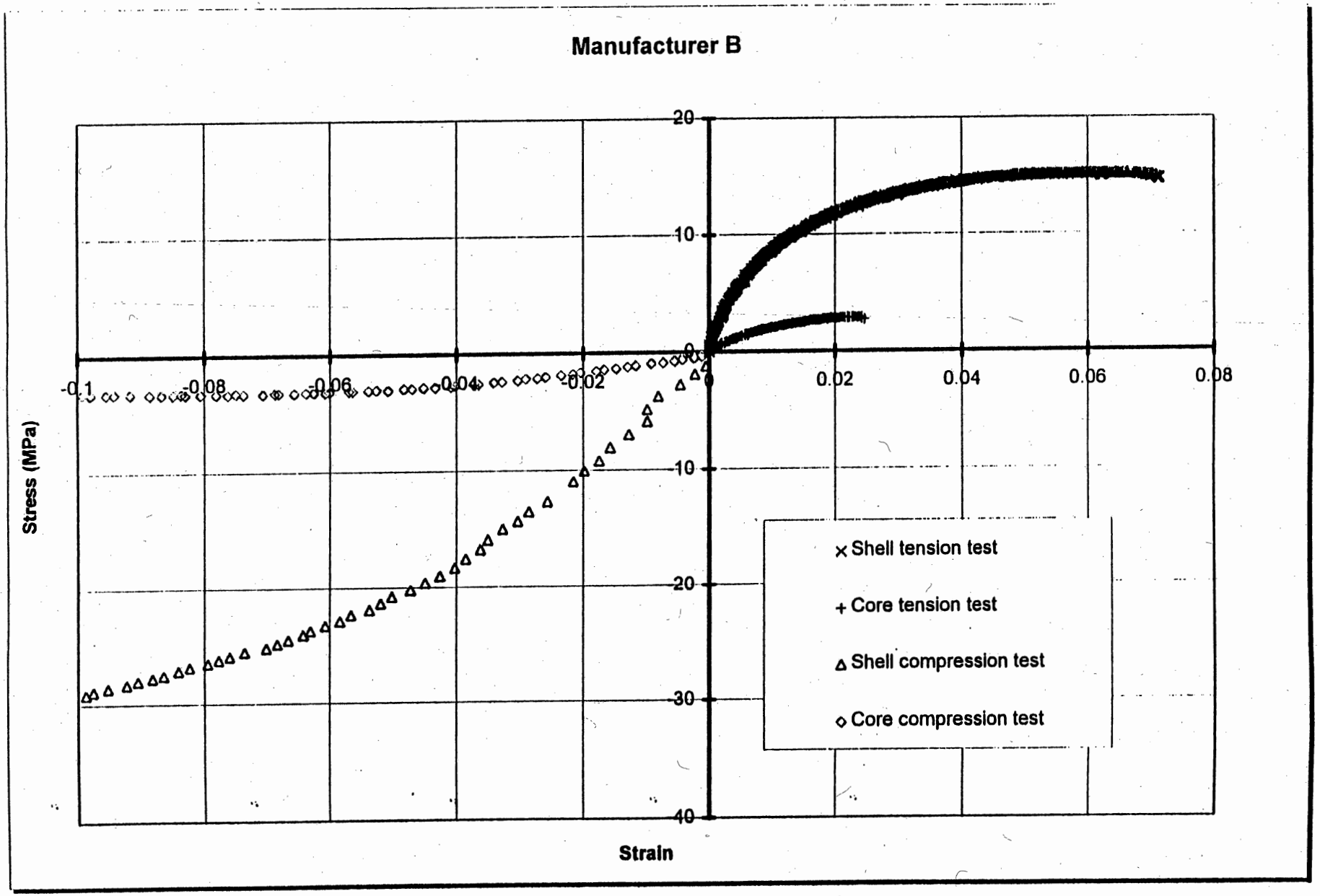

Figure 3. Stress-Strain Diagrams for Manufacturer B.

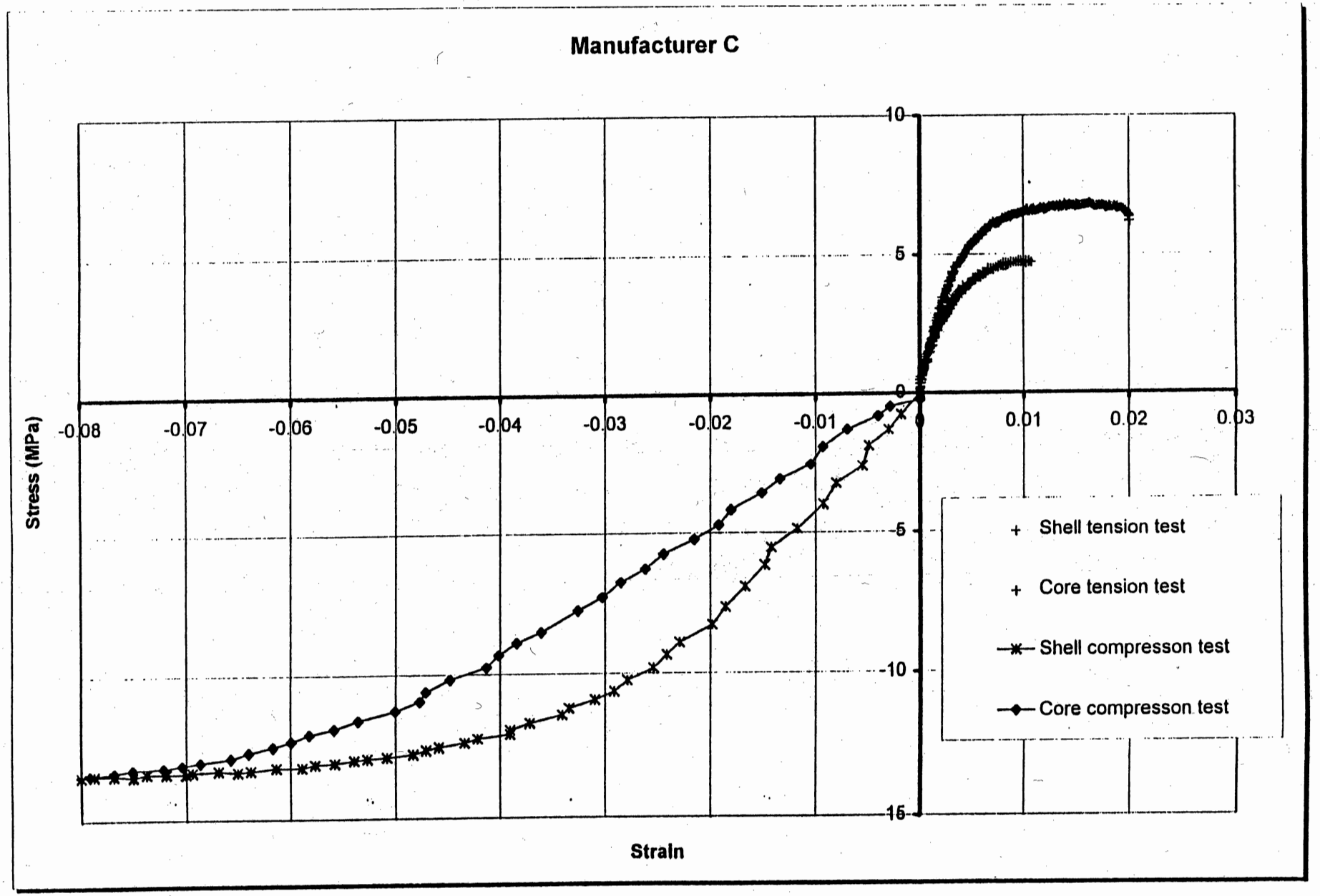

Figure 4. Stress-Strain Diagrams for Manufacturer C.

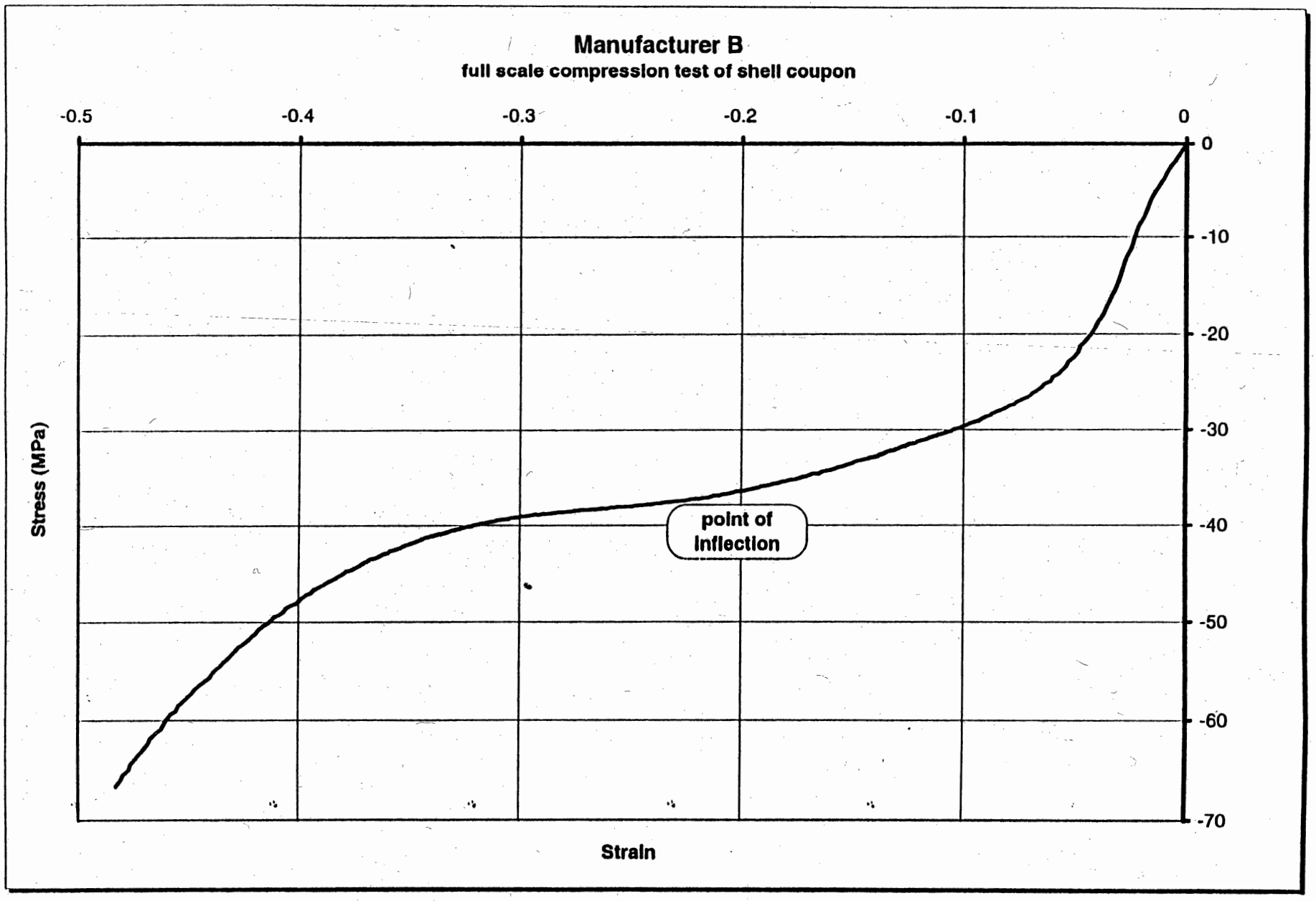

Figure 5. Compression Stress-Strain Curve for Manufacturer B.

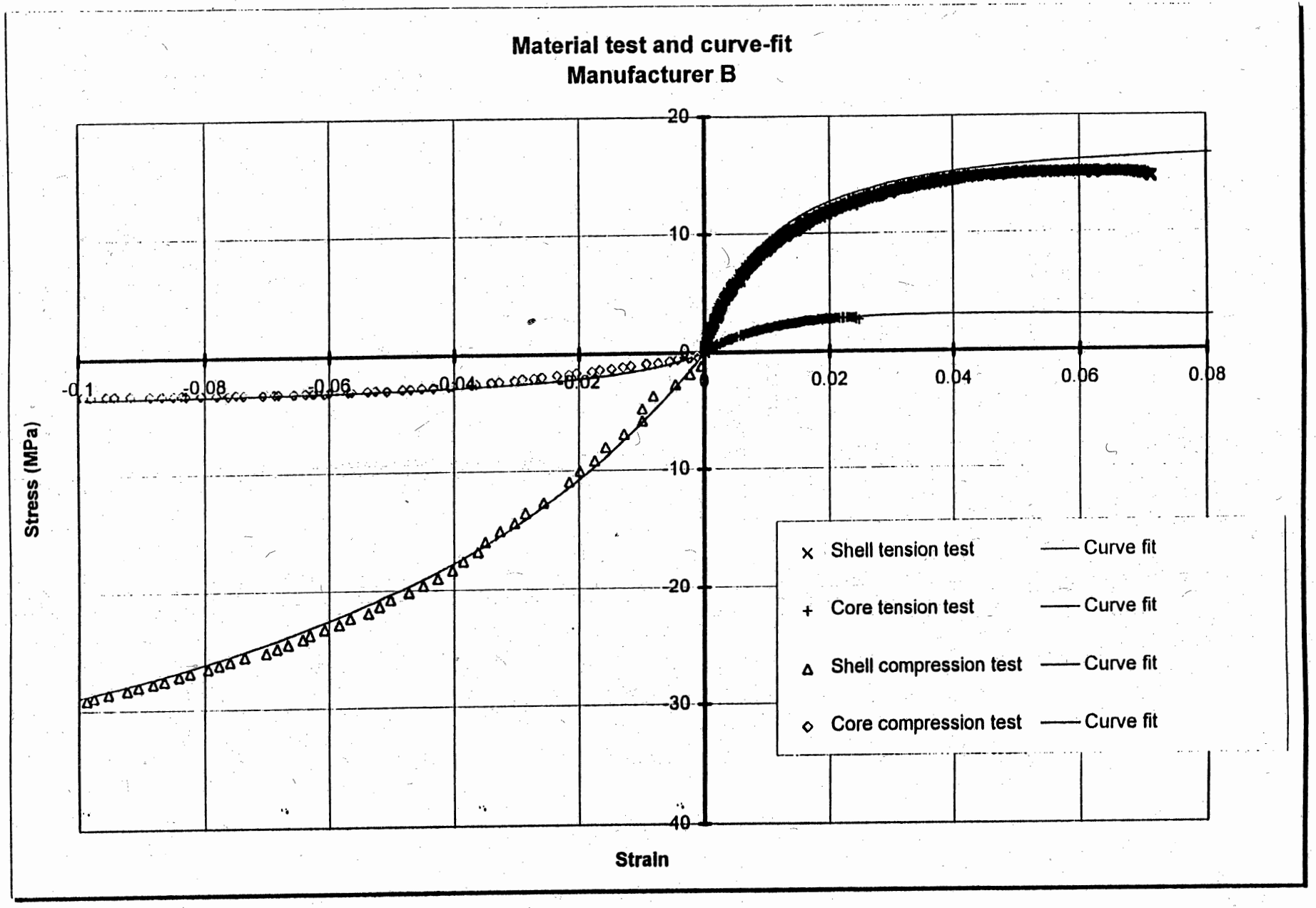

Figure 6. Material Tests and Curve Fit for Manufacturer B.

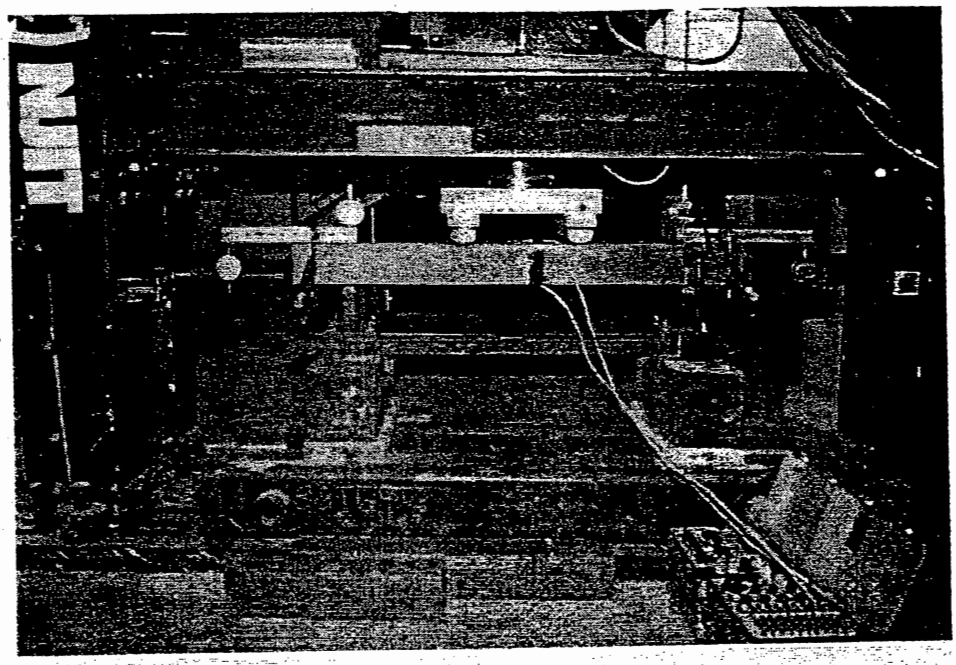

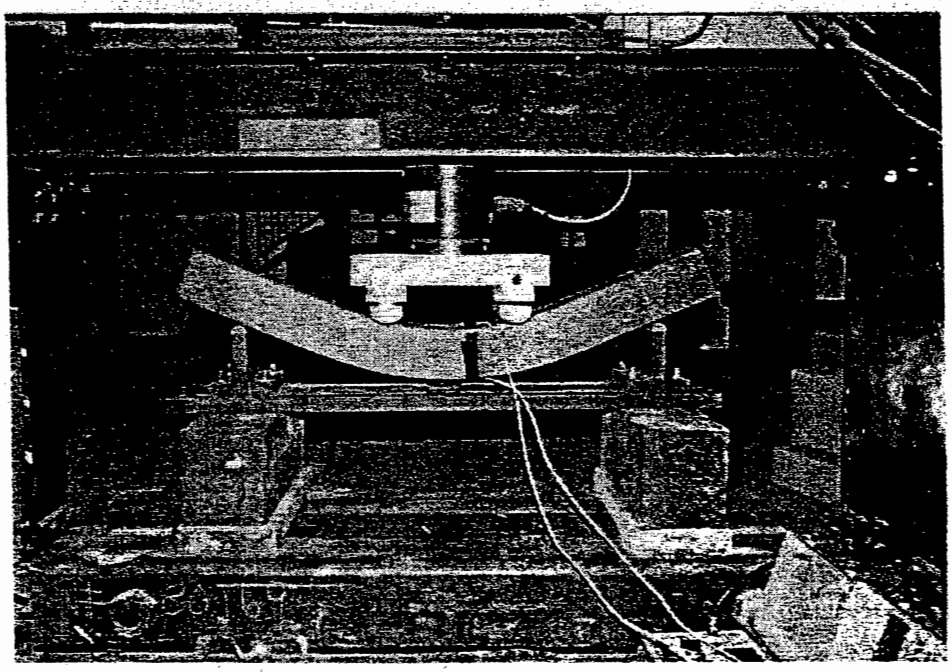

Figure 7. Typical Flexural Test Set Up and a Test Specimen during Loading.

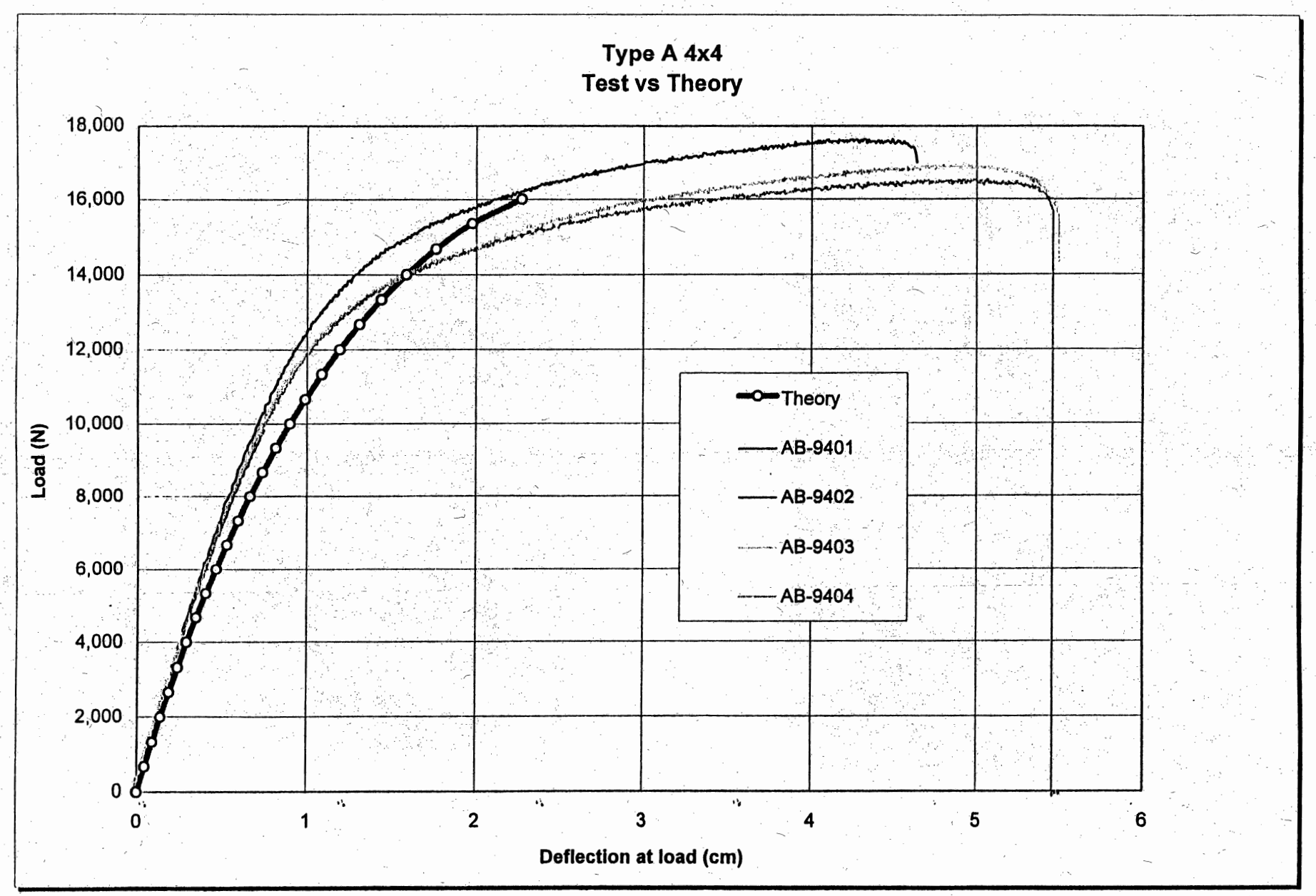

Figure 8. Load-Deformation for Manufacturer A.

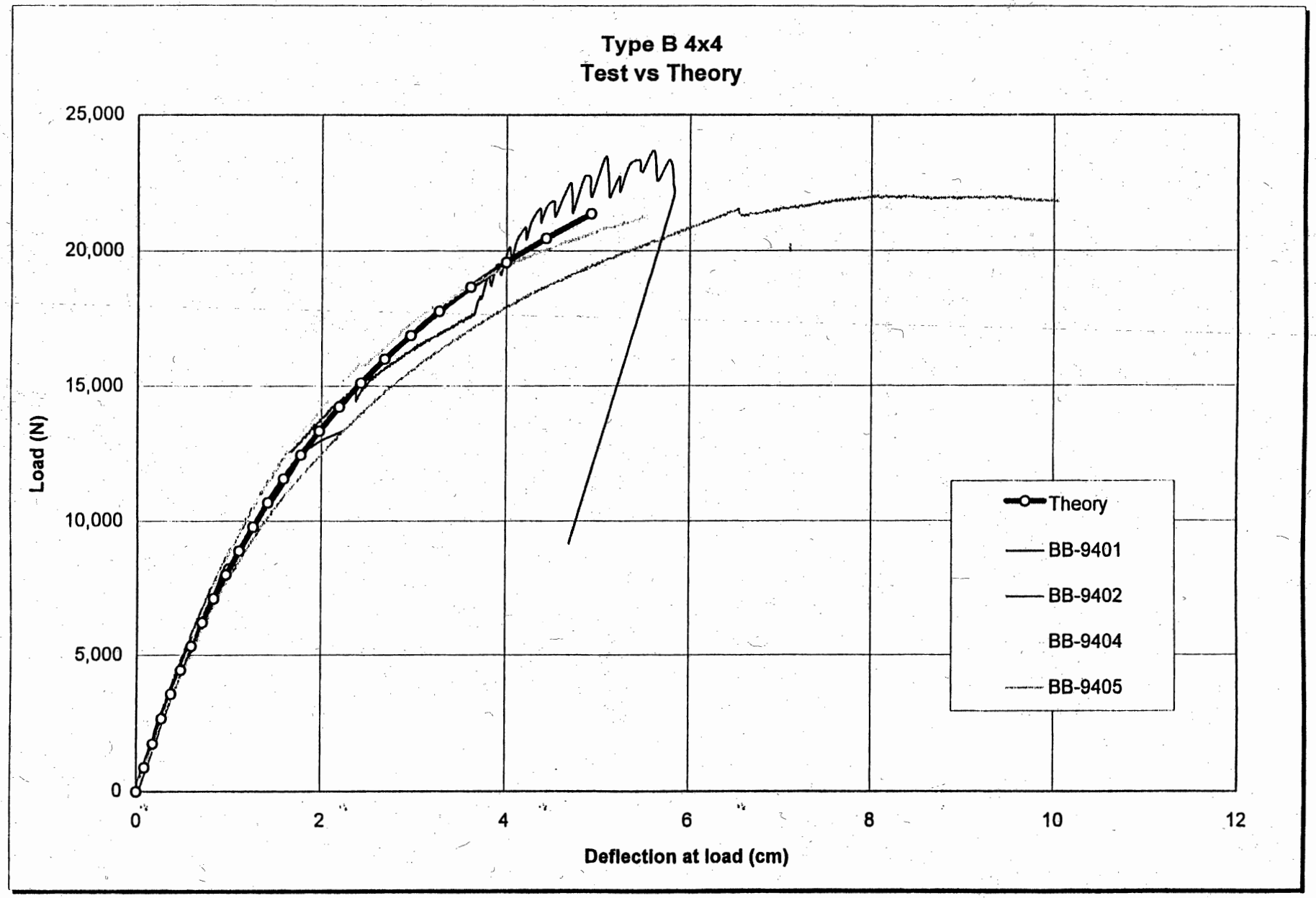

Figure 9. Load-Deformation for Manufacturer B.

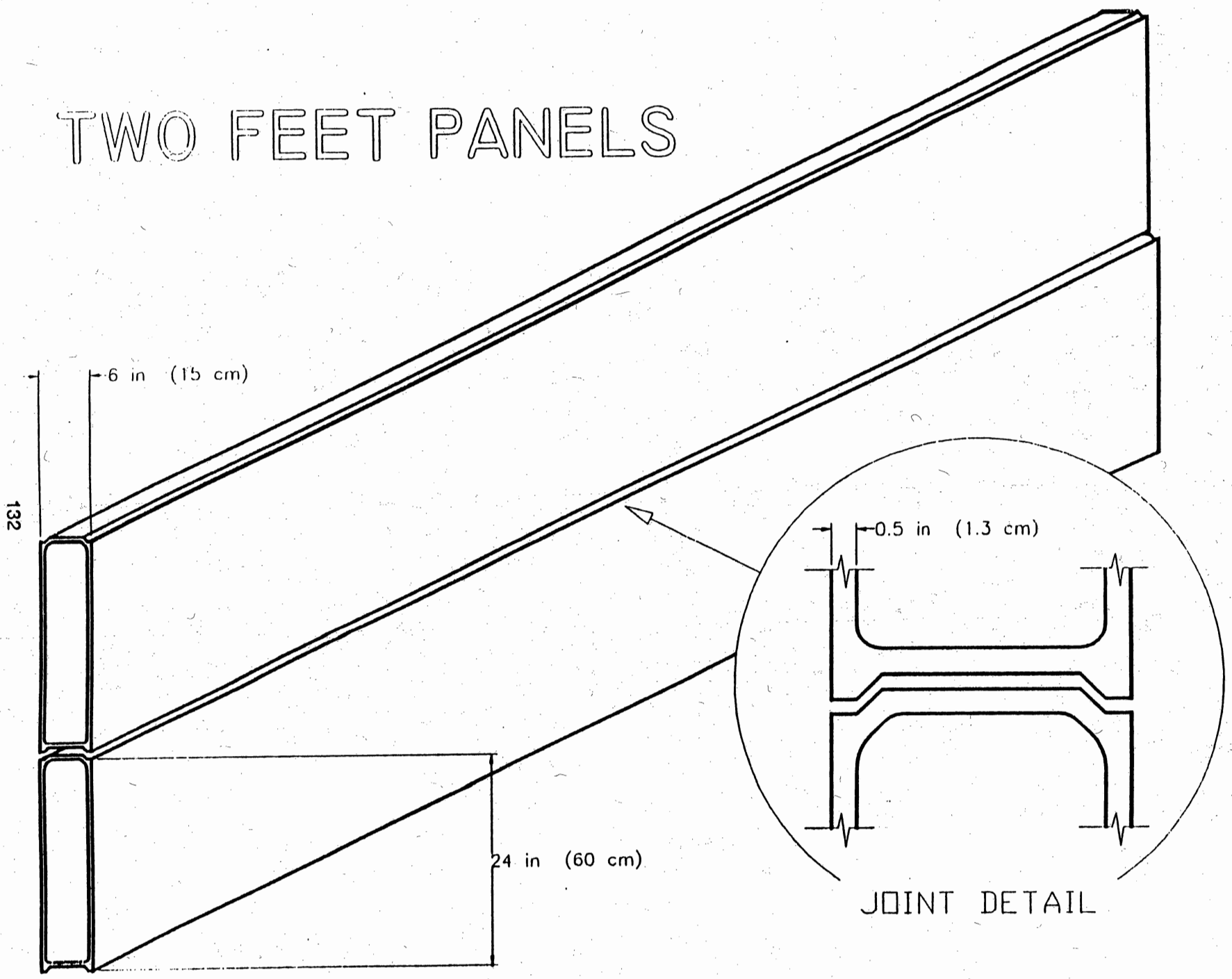

Figure 11. Schematic of the Proposed Noise Barrier Panel (two feet panel).

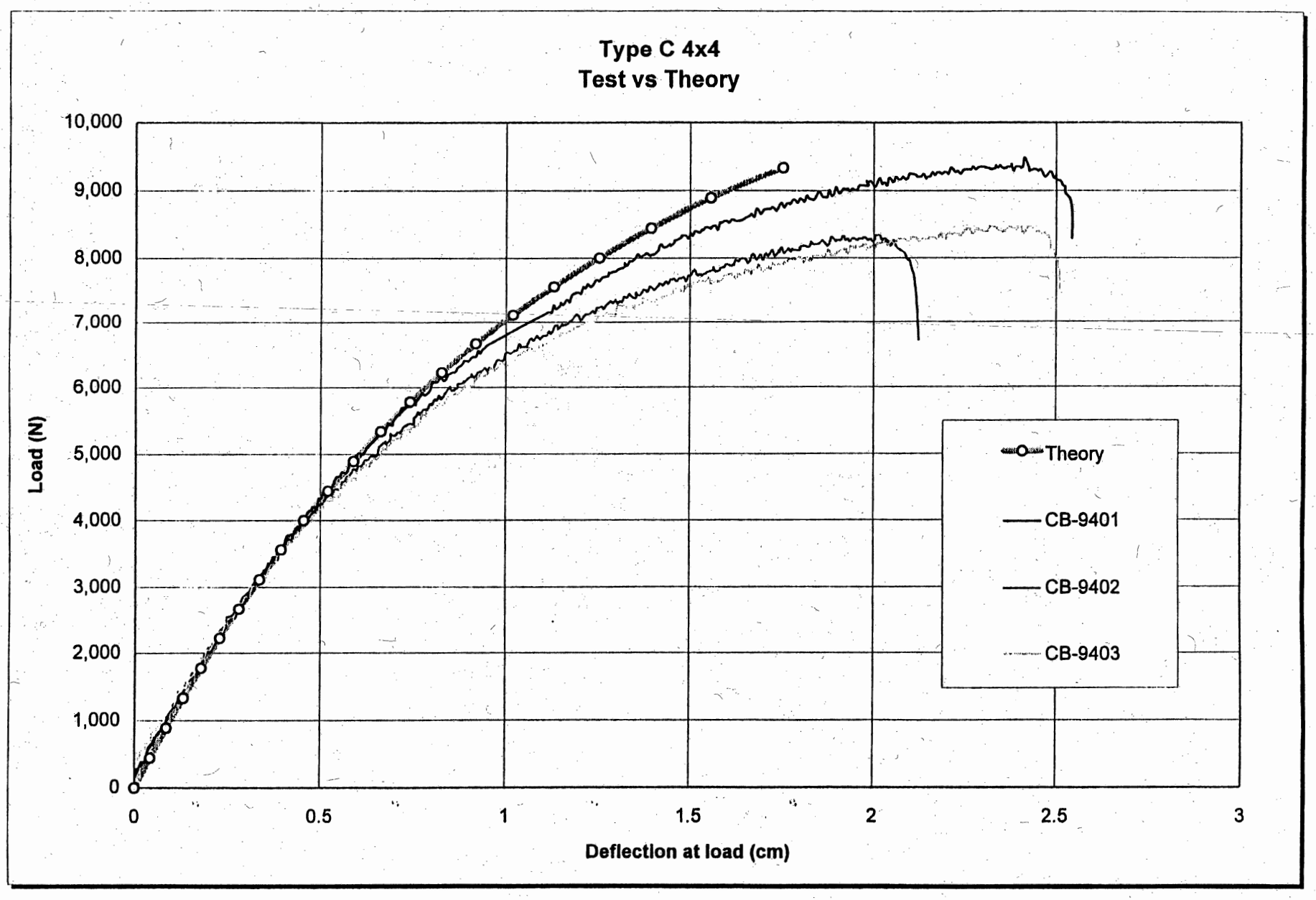

Figure 10. Load-Deformation for Manufacturer C.

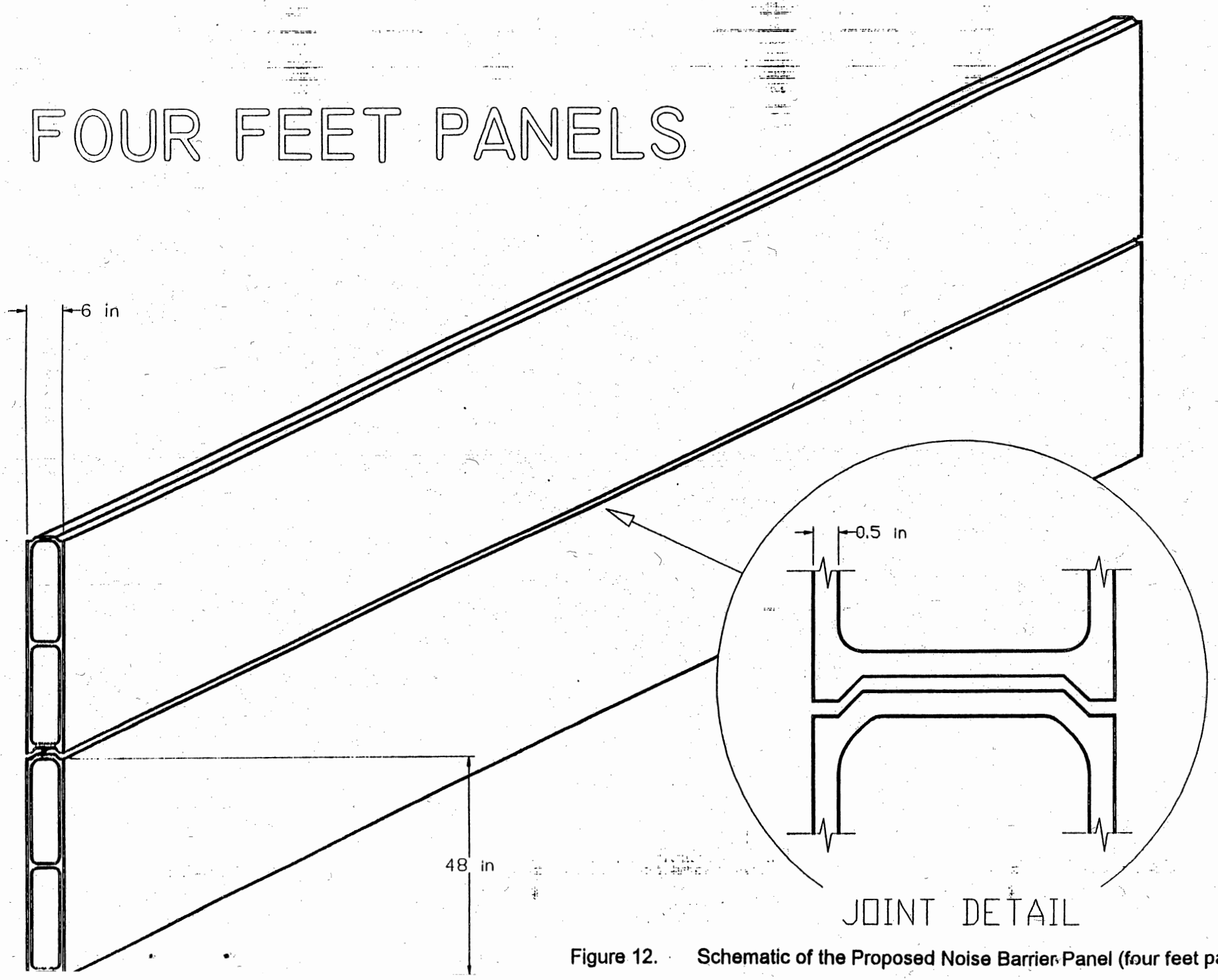

Figure 12. Schematic of the Proposed Noise Barrier Panel (four feet panel).

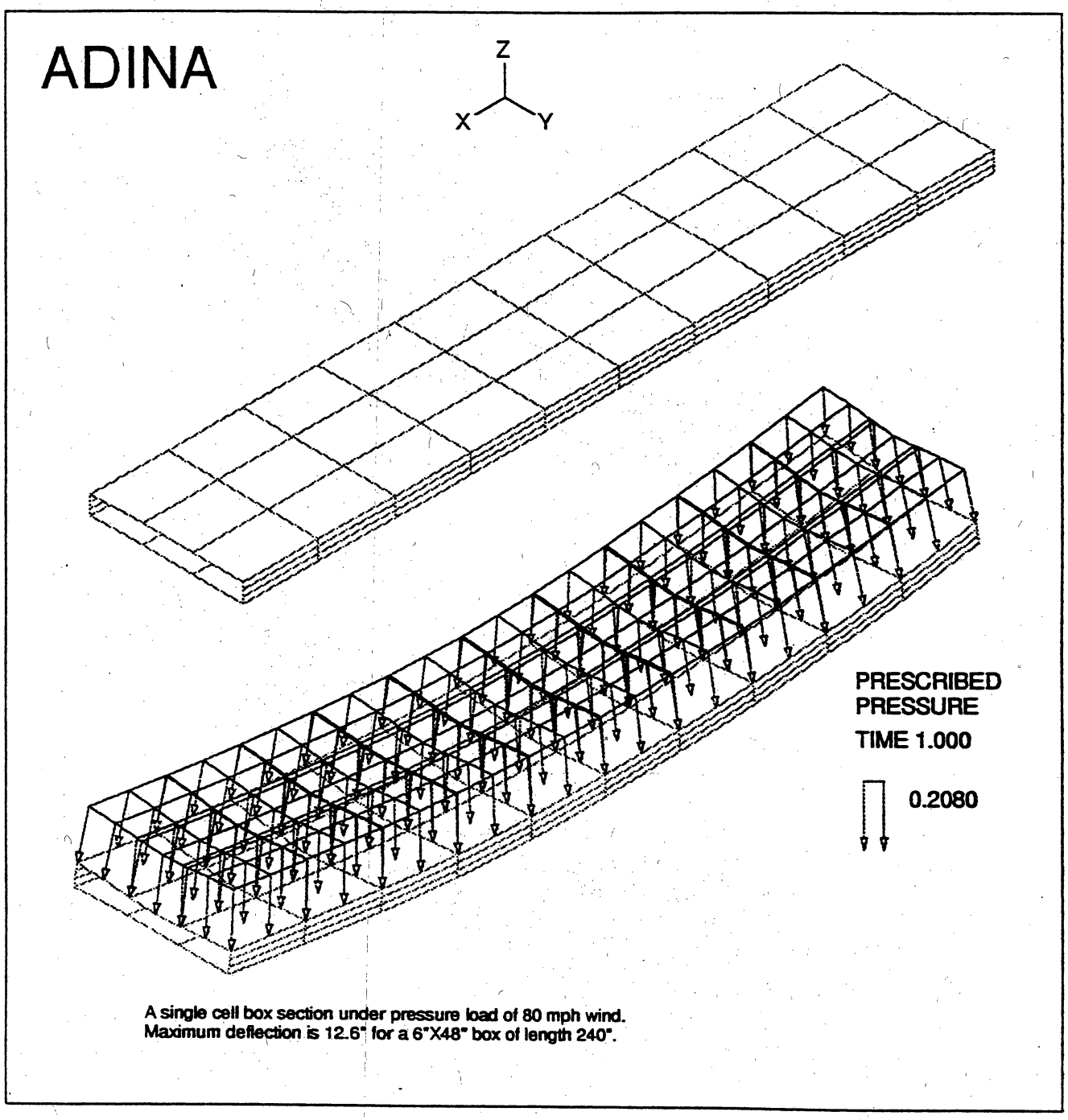

Figure 13. Finite Element Model of a Single Noise Wall Panel.

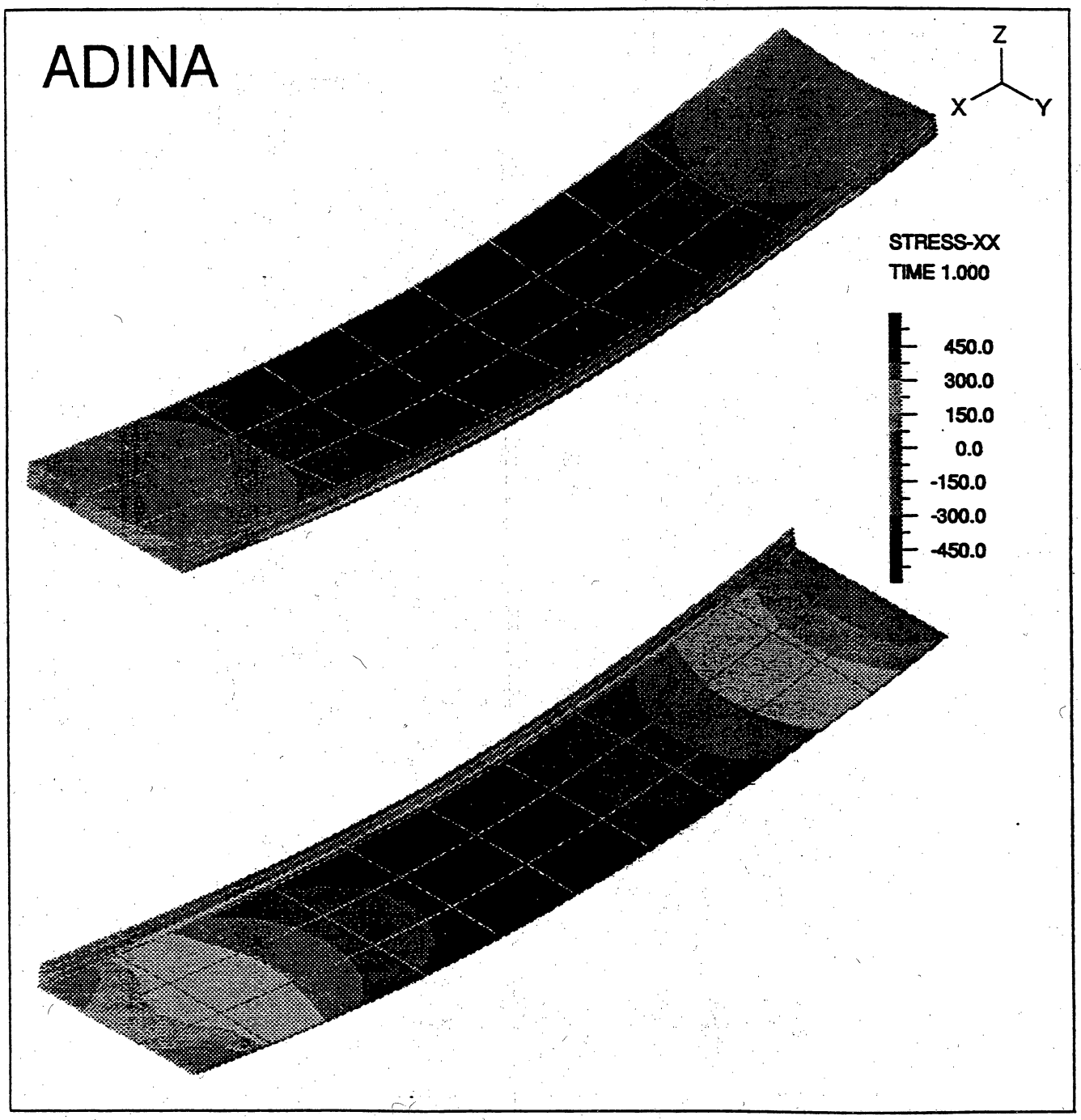

Figure 14. Contours of Flexural Stresses

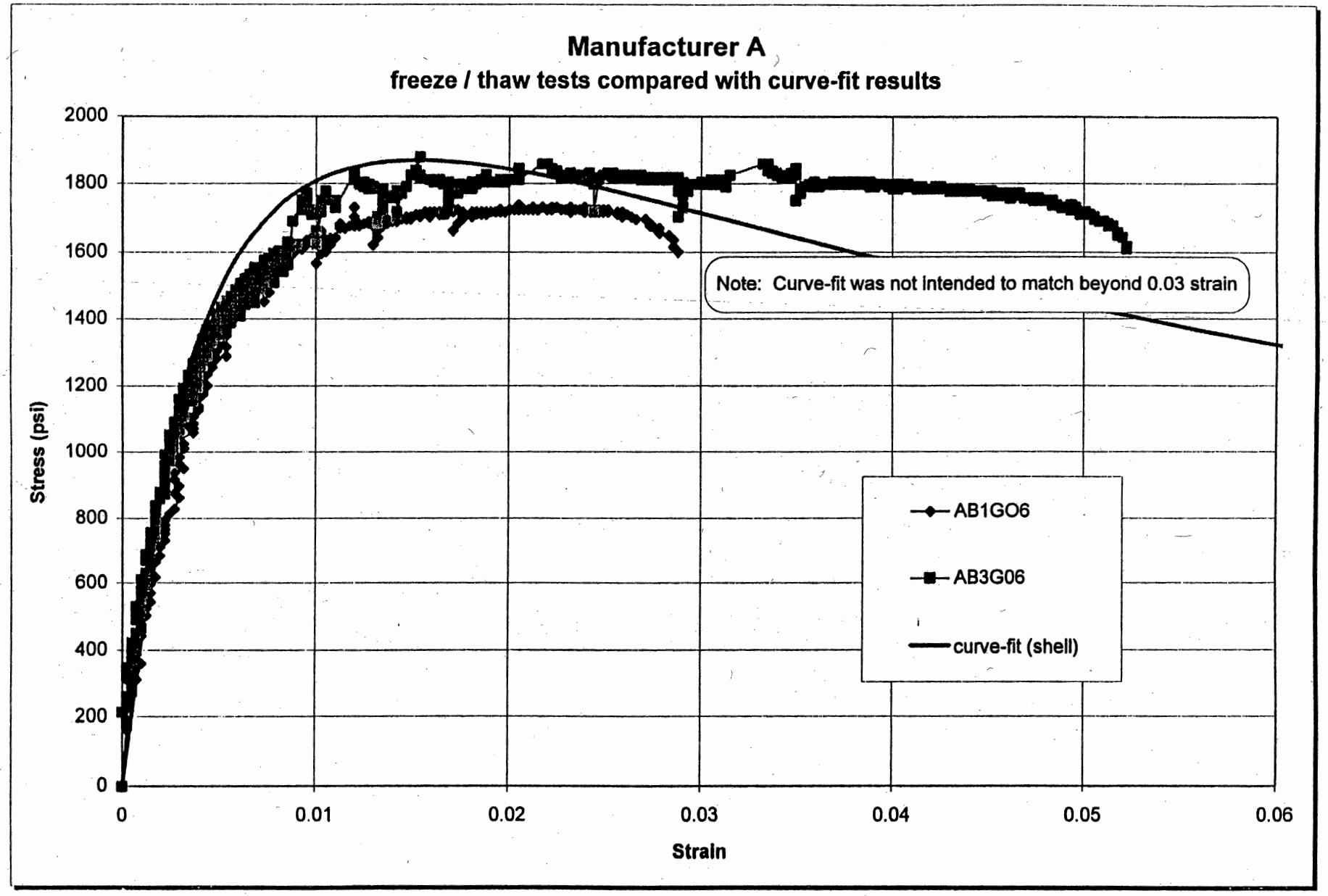

Figure 15. Freeze - Thaw results compared to Curve Fit results for Manufacturer A

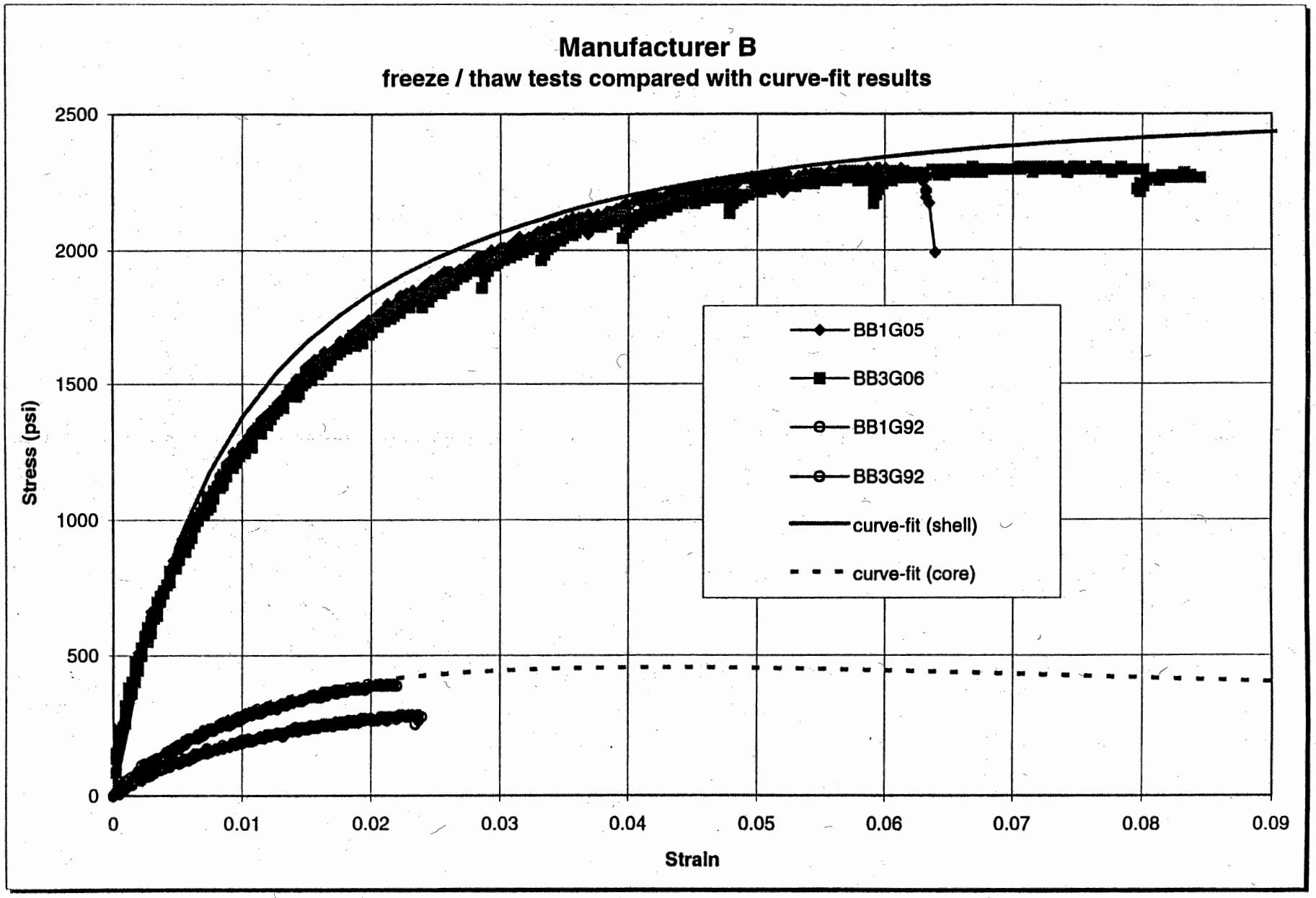

Figure 16. Freeze - Thaw results compared to Curve Fit results for Manufacturer B

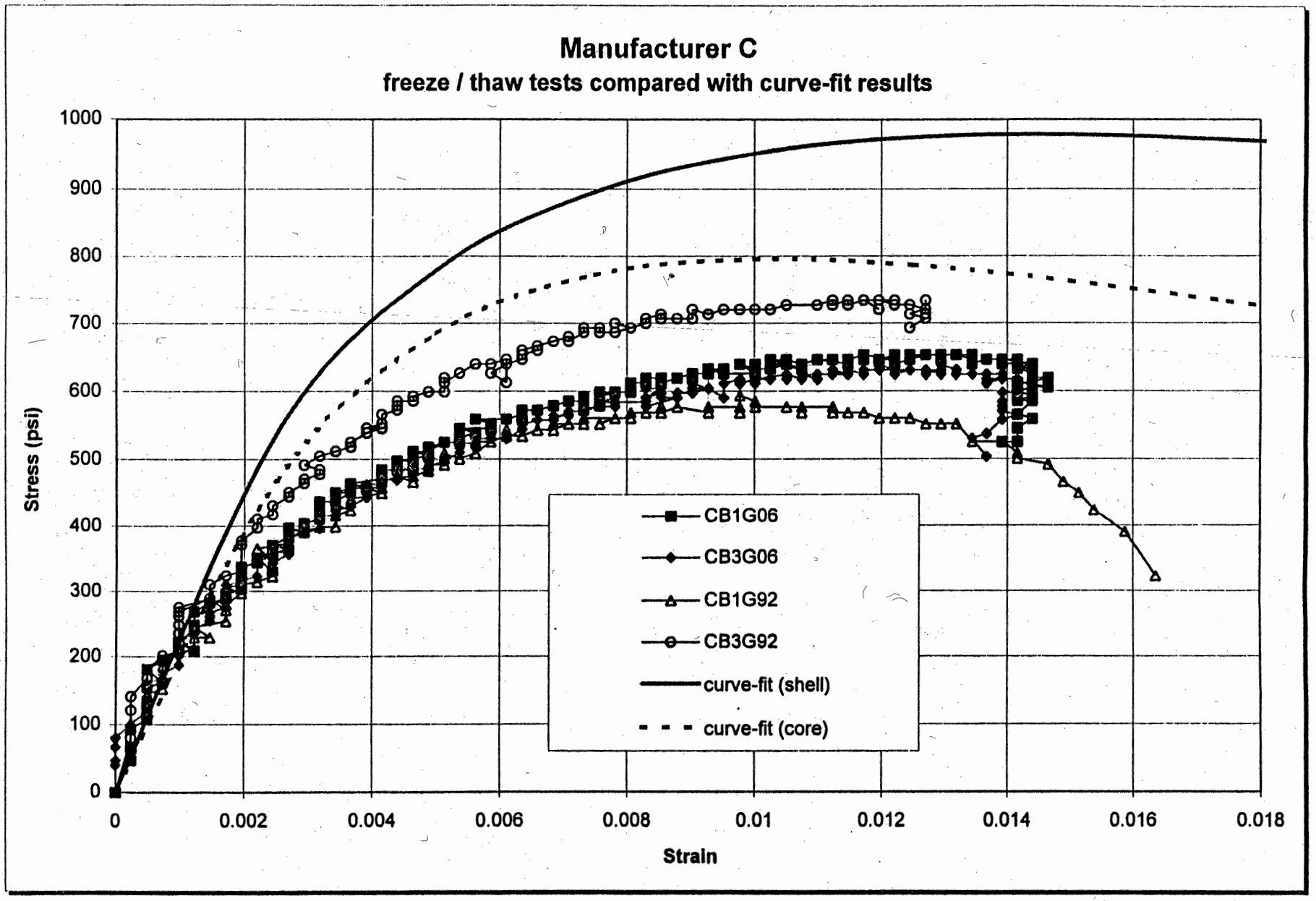

Figure 17. Freeze - Thaw results compared to Curve Fit results for Manufacturer C

APPENDIX I

⇒ Grid Layout for 4 X 4 Lumber to Cut tension Test Coupons.

⇒ Grid Layout for 6 X 6 Lumber to Cut Tension Test Coupons.

⇒ List of Tension and Compression Tests Coupons Manufacturer A.

⇒ List of Tension and Compression Tests Coupons Manufacturer B.

⇒ List of Tension and Compression Tests Coupons Manufacturer C.

Grid layout for 4 x 4 lumber

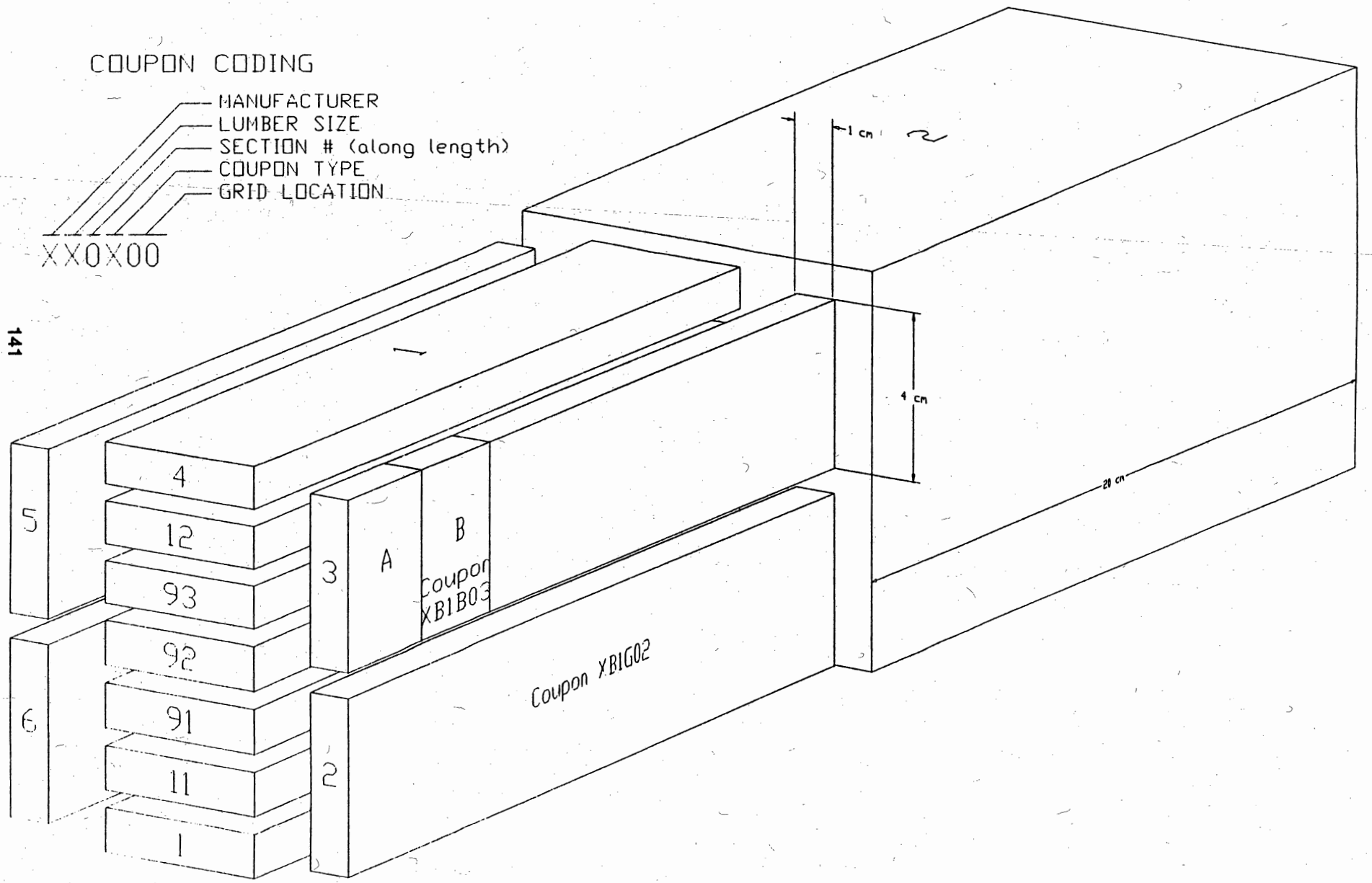

Grid layout for 6 x 6 lumber

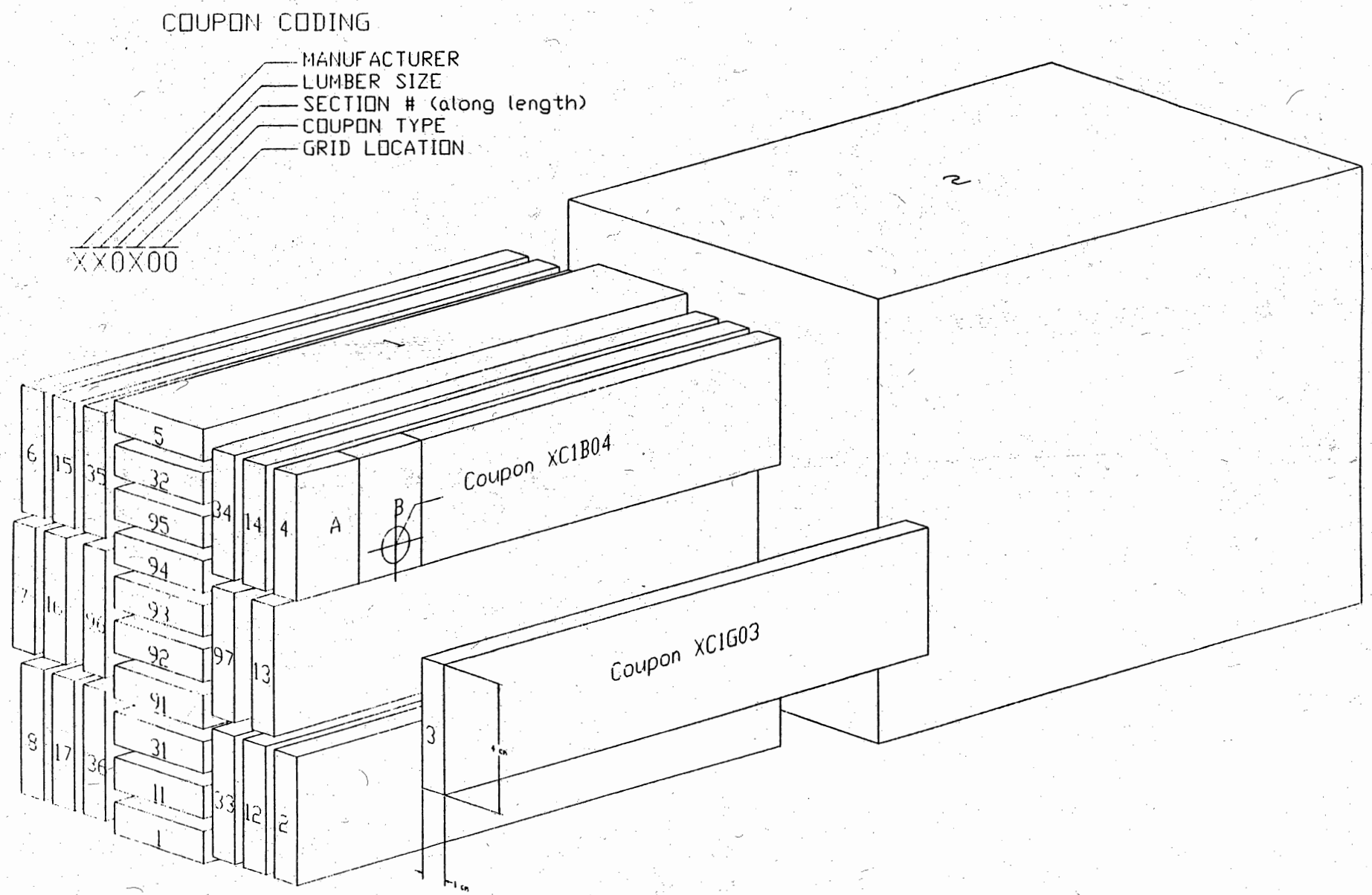

Manufacturer A

Tension

Shell		Core	
Coupon code	Density (g/cm^3)	Coupon code	Density (g/cm^3)
AC1G01	1.03	AC1G91	0.50
02	1.07	92	0.72
03	1.10	93	0.00
04	1.14	94	0.50
05	1.10	95	0.56
06	0.00	96	0.00
07	0.00	97	0.52
08	0.00	98	0.00
AC3G01	1.05	AC3G91	0.48
02	0.00	92	0.45
03	0.98	93	0.46
04	0.00	94	0.51
05	1.02	95	0.51
06	0.00	96	0.00
07	1.10	97	0.49
08	1.11	98	0.00
AB1G01	0.95	AB1G91	0.56
02	0.90	92	0.56
03	0.91		0.00
04	0.93		0.00
05	0.91		0.00
06	0.93		0.00
AB3G01	0.00	AB3G91	0.60
02	0.95	92	0.57
03	0.93		0.00
04	0.00		0.00
05	0.96		0.00
06	0.94		0.00

Compression

Shell		Core	
Coupon code	Density (g/cm^3)	Coupon code	Density (g/cm^3)
AC3A08	1.11		
B08	1.11		
C08	1.1		
D08	1.09		
E08	1.09		
AB3A02			
03			
AB1A01	0.95		
02	0.94		
03	0.95		
04	0.94		
05	0.93		
AB3A02	0.94		
03	0.93		
05	0.91		

Note: Shaded block indicates coupon was tested

Manufacturer B

Tension

Shell Coupon code	Shell Density (g/cm^3)	Core Coupon code	Core Density (g/cm^3)
BC1G01	1.00	BC1G91	0.66
02	1.02	92	0.00
03	0.98	93	0.68
04	1.02	94	0.71
05	1.02	95	0.96
06	1.18	96	0.69
07	1.14	97	0.73
08	0.00	98	0.00
BC3G01	1.01	BC3G91	0.69
02	1.01	92	0.63
03	1.00	93	0.65
04	1.02	94	0.68
05	1.01	95	0.00
06	1.02	96	0.70
07	1.04	97	0.68
08	1.03	98	0.00
BB1G01	1.03	BB1G91	0.34
02	0.00	92	0.36
03	0.00		0.00
04	0.00		0.00
05	1.04		0.00
06	0.00		0.00
BB3G01	0.00	BB3G91	0.38
02	0.00	92	0.37
03	0.00		0.00
04	0.00		0.00
05	1.05		0.00
06	1.05		0.00

Compression

Shell Coupon code	Shell Density (g/cm^3)	Core Coupon code	Core Density (g/cm^3)
BC3A06	1.02	BC3A96	0.71
B06	1.01	B96	0.71
C06	1.02	C96	0.70
D06	1.02	D96	0.70
BB1A01	1.03	BB1A91	0.34
B01	1.03	B91	0.35
BB3A05	1.05	BB3A91	0.37
B05	1.05	B91	0.38
BC1A04	1.02	BC1A96	0.69
A06	1.13	B96	0.69
A07	1.11	BC3A92	0.63

Note: Shaded block indicates coupon was tested

Manufacturer C

Tension

Shell

Coupon code	Density (g/cm^3)
CC1G01	0.92
02	0.00
03	0.95
04	0.00
05	0.93
06	0.00
07	0.96
08	0.00
CC3G01	0.95
02	0.00
03	0.90
04	0.00
05	0.89
06	0.00
07	0.93
08	0.00
CB1G01	0.90
02	0.00
03	0.00
04	0.93
05	0.00
06	0.91
CB3G01	0.00
02	0.90
03	0.00
04	0.00
05	0.00
06	0.88

Core

Coupon code	Density (g/cm^3)
CC1G91	0.86
92	0.83
93	0.00
94	0.00
95	0.00
96	0.91
97	0.90
98	0.00
CC3G91	0.86
92	0.83
93	0.00
94	0.00
95	0.00
96	0.92
97	0.92
98	0.00
CB1G91	0.91
92	0.85
	0.00
	0.00
	0.00
	0.00
CB3G91	0.90
92	0.91
	0.00
	0.00
	0.00
	0.00

Compression

Shell

Coupon code	Density (g/cm^3)
CC3A03	0.90
B03	0.91
C03	0.90
D03	0.90
CB1A01	0.90
CB3A02	0.90
CC3A01	0.95
CC1A01	0.92
A03	0.95
CB1A04	0.93

Core

Coupon code	Density (g/cm^3)
CC3A97	0.92
B97	0.92
C97	0.91
D97	0.91
CB1A91	0.91
B91	0.91
CB3A91	0.90
B91	0.90
CC3A91	0.86
CC1A91	0.86
CC1A97	0.90

Note: Shaded block indicates coupon was tested